

**PHENOTYPIC CHARACTERIZATION OF VIRULENCE, EVOLUTIONARY
RELATIONSHIP AND GLOBAL EXPANSION IN *Trypanosoma evansi* ISOLATES FROM
SURRA ENDEMIC REGIONS**

BY

KAMIDI CHRISTINE MUHONJA

**A THESIS SUBMITTED IN FULFILLMENT OF THE REQUIREMENTS FOR THE
DEGREE OF DOCTOR OF PHILOSOPHY IN BIOMEDICAL SCIENCES AND
TECHNOLOGY**

DEPARTMENT OF BIOMEDICAL SCIENCES AND TECHNOLOGY

MASENO UNIVERSITY

©2018

DECLARATION

I hereby declare that this thesis is the result of my original work and its findings have not been presented for the award of a degree certificate in any institution

KAMIDI, CHRISTINE MUHONJA (B.Sc., M.Sc.)

PHD/PH/00017/2014

Signature..... Date.....

This research thesis has been submitted for examination with our approval as university

supervisors:

1. **Prof. Collins Ouma, Ph.D.**

Department of Biomedical Sciences and Technology,
School of Public Health and Community Development,
Maseno University.

Signature..... Date.....

2. **Dr. Grace Murilla, Ph.D.**

Kenya Agricultural and livestock Research Organization
Biotechnology Research Institute
Kikuyu.

Signature..... *Grace Murilla* Date.....

3. **Dr. Paul Mireji, Ph.D.**

Kenya Agricultural and Livestock Research Organization,
Biotechnology Research Institute,
Kikuyu.

Signature..... Date.....

4. **Prof. Serap Aksoy, Ph.D.**

Epidemiology of Microbial Diseases,
School of Public Health,
Yale University.
USA.

Signature... Date.....

ACKNOWLEDGEMENTS

I am very grateful to the Most High God, for His faithfulness that endures forever, who has made it possible for me to achieve all that I have in my academics and life in general. It is with humility that I recognize and appreciate his protection, guidance, care and love which has given me so much hope. My deepest and sincere gratitude goes to my mentors, Prof. Serap Aksoy, Dr. Gisella Caccone, Dr. Grace Murilla, Dr. Paul Mireji and Prof. Collins Ouma for their great moral support, tireless advice, intellectual training and guidance in the course of executing this thesis work and also allowing me to be part of an enthusiastic team of researchers. My appreciation also goes to Dr. Norah Saarman, Kirstin Dion and Joanna Auma for their assistance, professionalism not forgetting your kindness, which goes beyond what words can describe. Special thanks to my other mentors Drs. Ephraim Mukisira and Raymond Mdachi, for their support, consistent encouragement and timely advice. My sincere thanks go to the following Biochemistry and Molecular Biology laboratory staff for their support, staying long hours in the laboratory during my studies; Mr. Bernard Wanyonyi, Mr. Johnson Makau, Ms. Carol Mariani, Mr. John Ndichu, Ms. Jane Hanya, Ms. Purity and Mr. Kariuki Ndung'u. My very special thanks to my beloved parents Charles and Anne Kamidi for bringing me up as a responsible and God-fearing person, making it possible for me to understand the principles of life and instilling in me the love for schooling. I will forever be grateful. Last but not least, great thanks go to my relatives and my friends for their understanding, encouragement and support over the years of my study in Belgium, Yale University/Biotechnology Research Institute/Maseno University and life. "Psalm 1: 1-3, Blessed is the one who does not walk in step with the wicked or stand in the way that sinners take or sit in the company of mockers, but whose delight is in the law of the LORD, and who meditates on his Law Day and night. That person is like a tree planted by streams of water, which yields its fruit in season and whose leaf does not wither— whatever they do prospers.

DEDICATION

To my darling Mother Anne Kamidi, Father Charles Kamidi, and friends Winnie Mutai and Winnie Okeyo for their unceasing love, prayer, support and encouragement.

ABSTRACT

Trypanosoma evansi parasite is the causative agent of trypanosomiasis (surra) in camels and other livestock with devastating economic consequences in many parts of the world, including Kenya, Vietnam, Brazil, China, Indonesia and the Philippines. The trypanosome is mechanically transmitted by tabanids and Stomoxys biting flies. Two strains of the parasite (A and B) have been documented to date where Type A strains is established across all *T. evansi* areas whereas Type B has been reported both in Kenya and Ethiopia. *T. evansi* has been emerging in non-endemic areas and infecting new hosts. It is also thought that *T. evansi* is under-diagnosed and the level of infection is greater than frequently reported. Investigations were conducted to establish 1) levels of virulence between various strains of *T. evansi* in the mouse model, 2) evolutionary origins of *T. evansi* in Kenya and 3) spatial expansion of *T. evansi* to other endemic regions of the world, in relation to *T. brucei brucei*, *T. b. rhodesiense* and *T. equiperdum* parasites, respectively. The absence of the tools that distinguish these strains of the parasite necessitate in-depth assessment of the key virulence indicators. The phylogenetic relationship in the various parasite strains enriched the current understanding of how *T. evansi* evolved and adapted to various regions. In a laboratory-based study, groups of male Swiss white mice were each inoculated with 17 isolates of *T. evansi* (Types A and B) collected from surra endemic countries (10 isolates from Kenya and 7 from South America and Asia). Following infection, the infected animals were monitored for parasitaemia, however, all groups of mice were monitored for live body weight, packed cell volume (PCV) and survivorship over the experimental period of 60 days (endpoint, above which all remaining animals were euthanized). In addition, DNA was isolated from 107 (41 *T. evansi*, 51 *T. b. brucei* and 15 *T. b. rhodesiense*) isolates, most of which were collected from Kenya and stored at the KETRI Cryobank. Individual DNA samples were genotyped with 15 polymorphic microsatellite markers to quantify levels and patterns of genetic diversity. Using the same microsatellite for the spatial expansion study, DNA was further extracted from an additional 11 isolates classified as *T. equiperdum* and 8 *T. evansi* were added to the already generated data (107 isolates) making a total of 132 isolates genotyped. Data was analyzed using one-way ANOVA in comparison of means of individual isolates from parameters recorded while for the genetic studies, distinct genetic clusters were identified using structure and Principal Component Analysis (PCA). Results of survivorship demonstrated three virulence categories; high virulence (0-10 days), moderate (11-30 days) and low virulence (31-60 days). Only one isolate was identified as Type B, depicting high virulence in mice. Differences in survivorship, PCV and bodyweights between isolates were significant and correlated with $P < 0.05$. The genotyping placed *T. evansi* isolates into at least two distinct *T. brucei* genetic units. Allelic richness within clusters of all isolates ranged from 2.10 to 3.86 indicating the lowest genetic diversity in cluster that contains both *T. b. brucei* and *T. b. rhodesiense*, but not *T. evansi* and the highest genetic diversity in cluster that contains *T. b. brucei*, *T. b. rhodesiense*, and *T. evansi* spanning a wide range of heterozygosity. The data also demonstrated that the origin of *T. evansi* isolates was from multiple *T. brucei* strains of different genetic backgrounds, implying 1) independent origins of *T. evansi* from *T. brucei* strains and 2) repeated events of acquisition of mechanical transmission of *T. evansi*, hence escape from obligate link with tsetse fly vectors. For spatial expansion the mean allelic richness was highest at 7.58 in *T. b. brucei*, lowest at 4.63 in *T. evansi*, and intermediate at 7.35 and 6.19 in *T. b. rhodesiense* and *T. equiperdum*, respectively. The study suggests that one isolate of *T. equiperdum* is genetically distinct from other *T. evansi* and *T. equiperdum* isolates; it thus represents an important addition to the emerging panel of new isolates. Overall, these findings suggest 1) region-specific differential virulence between *T. evansi* isolates, and 2) potential epidemiological implications of the genotyping results underpinned by probability of *T. brucei* strains from different genetic backgrounds becoming causative agent's livestock disease 3) the findings also challenge the taxonomic rank of species for these parasites and have important implications in the epidemiology, diagnostics and treatment of trypanosomiasis.

TABLE OF CONTENTS

DECLARATION.....	ii
ACKNOWLEDGEMENTS.....	iii
DEDICATION.....	iv
ABSTRACT.....	v
TABLE OF CONTENTS.....	vi
LIST OF ABBREVIATIONS.....	ix
LIST OF FIGURES.....	xii
LIST OF TABLES.....	x
CHAPTER ONE: INTRODUCTION.....	1
1.1 Background information.....	1
1.2 Statement of the problem.....	3
1.3 Objectives of the Study.....	4
1.3.1 General Objective.....	4
1.3.2 Specific objectives.....	4
1.3.3 Research questions.....	4
1.4 Significance of the study.....	5
CHAPTER TWO: LITERATURE REVIEW.....	6
2.1 Geographic distribution and economic impact of surra.....	6
2.2 Morphology.....	7
2.3 Life cycle.....	9
2.4 Vectors.....	10
2.5 Host ranges of Surra.....	11
2.6 Diagnosis and Parasitological tests.....	13
2.6.1 Serological tests.....	13
2.6.2 RoTat 1.2 gene.....	13

2.7	Control of surra.....	14
2.7.1	Vector control.....	14
2.7.2	Parasite Control.....	15
2.8	Virulence.....	15
2.9	Genetic studies.....	16
CHAPTER THREE: MATERIALS AND METHODS.....		20
3.1	Study design.....	20
3.2	Determination of differential virulence of <i>T. evansi</i> isolates in mice.....	20
3.2.1	Source of <i>T. evansi</i> isolates.....	20
3.2.2	PCR-Screening of <i>T. evansi</i> isolates.....	21
3.2.3	Experimental animals.....	22
3.2.4	<i>T. evansi</i> isolates and preparation of inoculum.....	23
3.2.5	Trypanosome inoculation into experimental mice.....	24
3.2.6	Evaluation of parasitaemia in infected mice.....	24
3.2.7	Survival.....	24
3.2.8	Assessment of Packed Blood Cell Volume (PCV) in infected and uninfected mice.....	25
3.2.9	Assessment of body weights in infected and uninfected mice.....	25
3.2.10	Data analysis.....	25
3.3	Determination of multiple evolutionary origin and dynamics of global expansion of <i>T. evansi</i>	26
3.3.1	Trypanosome isolates.....	26
3.3.2	DNA extractions and PCR based diagnostic tests.....	33
3.3.3	Microsatellite genotyping.....	37
3.3.4	Identification of distinct genetic clusters.....	39
3.3.5	Estimating levels of genetic diversity and differentiation.....	40
3.4	Estimating levels of genetic diversity for spatial expansion of <i>T. evansi</i>	41
CHAPTER FOUR: RESULTS.....		42
4.1	Comparison of virulence in mice model of selected <i>T. evansi</i> isolates.....	42

4.1.1	Parasitaemia profiles and survival of infected mice	42
4.1.2	Survival.....	47
4.1.3	Packed blood cell volume	49
4.1.4	Body weight profiles.....	52
4.2	Evolutionary origin of <i>T. evansi</i> in Kenya.....	54
4.2.1	PCR-based diagnostic tests.....	54
4.2.2	Identification of distinct genetic clusters	55
4.2.3	Genetic diversity and levels of differentiation.....	64
4.2.4	Interpretation of evolutionary origins of <i>T. evansi</i>	77
4.3	To determine the origin and dynamics of the <i>T. evansi</i> spatial expansion from Africa to multiple continents.....	79
CHAPTER FIVE: DISCUSSION.....		87
5.1	Differential virulence of <i>T. evansi</i> in mice	87
5.2	Evolutionary origins of <i>T. evansi</i> in Kenya.....	91
5.3	Spatial expansion of <i>T. evansi</i>	92
CHAPTER SIX: SUMMARY OF FINDINGS, CONCLUSIONS AND RECOMMENDATIONS.....		94
6.1	Summary of findings.....	94
6.2	Conclusion	94
6.3	Recommendations from the current study	96
6.4	Recommendations for future research	96
REFERENCES.....		98
APPENDICES.....		110
Appendix 1: Ethical approval		110
Appendix 2: DNA extraction protocol.....		111
Appendix 3: Manuscripts generated from current work		114
Appendix 4: Abstracts presented in meetings from the current work.....		116

LIST OF ABBREVIATIONS AND ACRONYMS

AAT	Animal African Trypanosomiasis
ANOVA	Analysis of variance
AR	Allelic Richness
BioRI	Biotechnology Research Institute
CI	Confidence Interval
DNA	Deoxyribonucleic acid
dNTPs	Deoxyribonucleic triphosphates
DPI	Days post infection
F _{IS}	Inbreeding Coefficient
F _{ST}	Variance among subpopulations relative to the total variance
HAT	Human African Trypanosomiasis
H _e	Expected Heterozygosity
H _o	Observed Heterozygosity
HWE	Hardy Weinberg Equilibrium
IACUC	Institutional Animal care and use committee
IP	Intraperitoneal
KALRO	Kenya Agricultural and Livestock Research Organization
KETRI	Kenya Trypanosomiasis Research Institute
LD	Linkage Disequilibrium
PBS	Phosphate buffered saline
PCA	Principal Component Analysis
PCR	Polymerase chain reaction
PSG	Phosphate saline glucose
RNA	Ribonucleic acid
RNA	Ribose Nucleic Acid
<i>T. b</i>	<i>Trypanosoma brucei</i>
Tev	<i>Trypanosoma evansi</i>
Teq	<i>Trypanosoma equiperdum</i>
VSG	Variable surface glycoprotein
WHO	World Health Organization

LIST OF TABLES

Table 3. 1: Selected <i>Trypanosoma evansi</i> isolates for virulence studies.....	21
Table 3. 2: Sample details and PCR assay results of <i>T. evansi</i> genotyped for this study.....	29
Table 3. 3: Sample details of strains from previous studies showing sample ID, publication, taxon, kDNA, host of isolation, and locality of origin.....	31
Table 3. 4: Sample details and PCR assay results of <i>T. evansi</i> (Tev) and <i>T. equiperdum</i> (Teq) genotyped for this study.....	34
Table 3. 5: PCR primers used in microsatellite marker amplification.....	38
Table 4. 1: Sample details of <i>T. evansi</i> phenotyped for this study	44
Table 4. 2: Comparison of mean parasitaemia values between various <i>Trypanosoma evansi</i> isolates following infection of mice at different virulence levels.....	45
Table 4. 3: Rank tests for survival time of Swiss White mice infected with <i>Trypanosoma evansi</i> isolates of varied virulence obtained from different endemic regions of the world.....	48
Table 4. 4: Comparison of Packed Cell Volume change (%) between various <i>Trypanosoma evansi</i> isolates collected from different countries.....	51
Table 4. 5: Comparison of bodyweights change (%) between various <i>Trypanosoma evansi</i> isolates collected from different countries.....	54
Table 4. 6: Assignment scores from STRUCTURE v2.3.4 clustering analysis with K=7	59
Table 4. 7: Assignment scores from STRUCTURE v2.3.4	65
Table 4. 8: Genetic diversity found within each STRUCTURE-based genetic clusters.	68
Table 4. 9: Within-cluster distance using STRUCTURE-based genetic clusters including strains with Q values > 0.80.....	72
Table 4. 10: Summary of differences in within-cluster Reynolds (1983) distance of STRUCTURE-defined clusters.....	73
Table 4. 11: Among-cluster genetic differentiation (F_{ST}) among each STRUCTURE-defined genetic cluster.	76

Table 4. 12: Genetic diversity found within *Trypanosoma brucei brucei*, *T. b. rhodesiense*, *T. evansi*, and *T. equiperdum* 85

LIST OF FIGURES

Figure 2. 1: Worldwide distribution of Surra).....	7
Figure 2. 2: Morphology of <i>T. evansi</i>	9
Figure 2. 3: Life cycle of <i>T. evansi</i> and reproduction.....	10
Figure 2. 4: Weight loss and emaciation in camels as a result of Surra.....	12
Figure 3. 1 Map of Africa showing in black the location of Kenya. The insert to the right shows the location of the <i>Trypanosoma evansi</i> (Tev) and <i>T. b. brucei</i> (Tbb) strains genotyped for this study (small black circles).....	27
Figure 3. 2: Map showing worldwide location of <i>Trypanosoma evansi</i> (Tev) (small black circles) and <i>Trypanosoma equiperdum</i> (Teq) (asterisk) strains genotyped for this study.....	27
Figure 3. 3: Diagnostic PCR for the GCT/Ala281 deletion in F1FO-ATP synthase subunit γ in <i>T. evansi</i> type A.....	36
Figure 4. 1:Parasitaemia profiles of individual mice infected with low and moderate virulence <i>T. evansi</i>	43
Figure 4. 2: Parasitaemia profiles of individual mice infected with high virulence.....	46
Figure 4. 3: Survival curves depicting the fraction of animals alive from the time (0) of parasite inoculation.....	48
Figure 4. 4: Percent (%) Packed Cell Volume change profiles of individual mice infected with low and moderate virulence <i>Trypanosoma evansi</i> isolates.....	50
Figure 4. 5: Bodyweight changes profiles of individual mice infected with low and moderate virulence <i>Trypanosoma evansi</i> isolates.....	53
Figure 4. 6 : STRUCTURE v2.3.4.....	56
Figure 4. 7: STRUCTURE v2.3.4 plot of individual assignments with K values of 2 through 7.....	57
Figure 4. 8: Plot of assignment scores of all isolates using STRUCTURE v2.3.4 with K=7..	58

Figure 4. 9: Evaluation of the genetic differentiation between isolates of <i>Trypanosoma brucei</i> <i>brucei</i> and <i>T. b. rhodesiense</i> (Tb) and <i>T. evansi</i> (Tev) genetic clusters using principal components analysis (PCA) of microsatellite data.....	63
Figure 4. 10: Distance tree based on 15 microsatellite markers and Reynolds distances using the UPGMA method implemented in the R package, “PopPR” v2.3.....	70
Figure 4. 11: Summary of pairwise Reynolds (1983) genetic distances computed in the R package “PopPR” v2.3.0.....	74
Figure 4. 12: STRUCTURE v2.3.4 plot of delta K (K=1 through 20).....	79
Figure 4. 13 : STRUCTURE results for K values 2-10.....	80
Figure 4. 14 : Plot of STRUCTURE v2.3.4 assignment scores with K=9.....	81
Figure 4. 15: Evaluation of the genetic differentiation between (A) all isolates, and (B) only <i>T. evansi</i> (Tev) and <i>T. equiperdum</i> (Teq) isolates, using principal components analysis (PCA) of microsatellite data.....	83
Figure 4. 16: Distance tree based on Reynolds distances using the UPGMA method implemented in the R package, “PopPR” v2.3.....	84

CHAPTER ONE

INTRODUCTION

1.1 Background information

African trypanosomes are the causative agents of Human African Trypanosomiasis (HAT, or Sleeping sickness) and African Animal Trypanosomiasis (AAT, Nagana). *Trypanosoma congolense*, *Trypanosoma vivax* and/or *Trypanosoma evansi* are the predominant causative agents of AAT (Mattioli *et al.*, 2004) while *Trypanosoma brucei rhodesiense* and/or *Trypanosoma brucei gambiense* are the HAT causative parasites. The AAT has been associated induce abortions, weight loss, meat and milk yield reductions, and eventually death in livestock (Desquesnes *et al.*, 2013). Morbidity and mortality of up to 30% and 3%, respectively, have been reported in camels (Ngaira *et al.*, 2003; Tekle and Abebe, 2001). *Trypanosoma evansi* originated in Africa and is an agent of surra throughout tropical and subtropical regions of the world, including Africa and Asia, with diverse mammalian hosts that include camels, horses, cattle, buffaloes, small ruminants and dogs with significant (Herrera *et al.*, 2004; Ngaira *et al.*, 2003; Tekle and Abebe, 2001), where, presently, it causes surra disease that affects a variety of animals including camels, horses, cattle, buffaloes, small ruminants and dogs (Ngaira *et al.*, 2003). The disease is therefore endemic in many regions of Africa and Asia where thousands of animals die during outbreaks (Enwezor and Sackey, 2005). *Trypanosoma evansi* share the same taxa with *Trypanosoma brucei brucei*, *T. b. gambiense*, *T. b. rhodesiense* and *T. equiperdum* (Brun *et al.*, 1998; Desquesnes *et al.*, 2013; Gibson, 2003; Herrera *et al.*, 2004; Ngaira *et al.*, 2003) among which all but *T. equiperdum* are restricted to sub-Saharan Africa and vectored by tsetse flies. *Trypanosoma evansi* and *T. equiperdum* are more widespread, including outside Africa where their transmission is mechanical and do not require tsetse fly vector. These parasites are responsible for surra in

wild and domestic animals (*T. evansi*) and dourine in equines (*T. equiperdum*). *Trypanosoma evansi* expresses Rode Trypanozoon antigen (RoTat) type 1.2 (type A), a predominant variable surface glycoprotein (VSG) in most strains of *T. evansi* (Verloo *et al.*, 2001), including those isolated from surra endemic regions (Abdel, 1991). A surra causative *T. evansi* strain devoid of VSG RoTat 1.2 (type B) has been identified in Kenya (Njiru *et al.*, 2006). While *T. evansi* type A strain can be identified by RoTat type 1.2 based serologically and by polymerase chain reaction (PCR) techniques (Ngaira *et al.*, 2003; Ngaira *et al.*, 2004; Ngaira *et al.*, 2005), there are no similar tools for detection of *T. evansi* type B, significantly impeding assessment of prevalence and virulence of this strain remains largely unknown in nature. This forms a major constraint to treatment and deployment of rational control strategies of surra (Enwezor and Sacky, 2005; Njiru *et al.*, 2010). It was thus essential to elucidate and identify the nature of virulence of the parasite.

Since the adaptation to mechanical transmission in *T. evansi*, the parasite does not require any biological cycle to be completed in the vector, *T. evansi* is also transmitted by non-tsetse blood-feeding flies (Antoine-Moussiaux *et al.*, 2009). *Trypanosoma evansi* locks the trypanosome in the bloodstream stages in vertebrates where the parasite multiplies by longitudinal binary fission (Luckins, 1988; Borst and Hoeijmakers, 1979). Tsetse-independent transmission has enabled these parasites to move out of the tsetse fly belt in sub-Saharan Africa. Another consequence of their inability to complete their development in tsetse flies is that both *T. evansi* and *T. equiperdum* strains do not undergo sexual reproduction. Although these peculiarities unite all *T. evansi* (and *T. equiperdum*) strains, there is significant variation in other traits. (Luckins, 1988). This study was therefore essential so as to quantify patterns of inter-strains genetic diversity in order to understand the evolutionary origin of different *T. evansi* strains. Subsequently, the findings have enabled an

understanding of the distribution, incidence and impact of surra in most countries which were previously poorly understood (Urakawa *et al.*, 2001).

In addition to their ability to bypass the tsetse fly vector, all *T. evansi* (and *T. equiperdum*) strains analyzed so far are also characterized by having no or dysfunctional kinetoplast DNA, a trait referred to as dyskinetoplastidy (Lai *et al.*, 2008). Where present, kDNA has suffered homogenization of the minicircle component, which consists of more than 200 distinct classes in a tsetse transmission competent strain of *T. brucei* (Lai *et al.*, 2008; Steinert and Van Assel, 1980). In all *T. evansi* strains analyzed to date, kDNA is dominated by either type A or type B minicircles. Minicircle heterogeneity is essential for mitochondrial gene expression in trypanosomes. As a consequence of its dyskinetoplastidy, (Carnes *et al.*, 2015), *T. evansi* can therefore no longer complete cyclical development in the tsetse fly, and this could be one of the driving forces for the switch to mechanical transmission. It was therefore important to screen for genetic polymorphism in additional *T. evansi* isolates from across the world to understand the origin and timing of the *T. evansi* spatial expansion, evaluate if only a few genetically similar strains were responsible for the spread, and identify the *T. brucei* genetic background most likely to give rise to *T. evansi* strains.

1.2 Statement of the problem

Camel trypanosomiasis (surra) is endemic in many regions of Africa and Asia where thousands of animals die during disease outbreaks each year. Unlike most pathogenic trypanosomes that have consistently maintained their endemic foci and host, *T. evansi* has been emerging in non-endemic areas and infecting new hosts. Therefore, most control and eradication programs against *T. evansi* are limited to treating animals, using trypanocidal drugs that have been available in the market for over 50 years, resulting in the development of resistant strains. It is also thought that *T. evansi* is under-diagnosed and the level of

infection is greater than frequently reported due to absence of diagnostic tools that can differentiate Types A and B of the parasite. The virulence of *T. evansi* therefore remains largely unknown. While it is agreeable that it is imperative to develop novel, effective control tools and strategies, it is also essential to elucidate the nature of virulence of the parasite to the host and its genetic aspects. To address this, the current study focused on understanding of virulence in *T. evansi* in camels, and to quantify levels and patterns of genetic diversity among these isolates, so as to understand the evolutionary origin of different *T. evansi* strains in Kenya and other parts of the world. These approaches provide information that are useful in the design of intervention strategies and in the monitoring of disease spread by providing data on the rate and modality of novel genotypic combinations that have been introduced in the circulating *T. evansi* strains.

1.3 Objectives of the Study

1.3.1 General Objective

To characterize virulence, evolutionary relationship and global expansion in *T. evansi* isolates from surra endemic regions.

1.3.2 Specific objectives

1. To determine levels of virulence of selected *T. evansi* isolates from various surra endemic regions in mice model.
2. To determine evolutionary origins of *T. evansi* in Kenya.
3. To determine the origin and dynamics of *T. evansi* from Kenya to other continents.

1.3.3 Research questions

1. What are the different levels of virulence in mice model in *T. evansi* isolates sampled from various surra endemic regions?

2. What are the evolutionary origins of *T. evansi* in Kenya?
3. What are the origins and dynamics of global expansion of *T. evansi*?

1.4 Significance of the study

This study characterized virulence of *T. evansi* parasites and established evolutionary origin and expansion of *T. evansi* in relation to other *T. brucei* sub-species. Two strains of *T. evansi* (types A and B) have been reported, which have not been adequately characterized (Njiru *et al.*, 2010). While *T. evansi* type A strain can be identified by RoTat type 1.2 based serologically and by polymerase chain reaction (PCR) techniques (Ngaira *et al.*, 2003; Ngaira *et al.*, 2004; Ngaira *et al.*, 2005), there are no similar tools for detection of *T. evansi* type B, significantly impeding assessment of prevalence of this strain in nature and forms a major constraint to treatment and deployment of rational control strategies of surra (Enwezor and Sacky, 2005; Njiru *et al.*, 2010). The absence of the tools that precisely distinguish these strains of the parasite necessitate in-depth assessment of the key virulence indicators as baseline information that will aid in development of *T. evansi* type specific diagnostic tools. Additionally, assessment of phylogenetic relationship in the various parasite strains enriched the current understanding of how *T. evansi* evolved and adapted to various regions where surra is endemic. Such information in turn lends insight and provides better understanding of the molecular and evolutionary basis of the differential epidemiology of surra in endemic regions despite their very similar genetic background.

CHAPTER TWO

LITERATURE REVIEW

2.1 Geographic distribution and economic impact of surra

Trypanosomiasis is a widespread constraint on livestock production, mixed farming and human health in tropical Africa. World Health Organization approximate 300,000 to 500,000 cases and over 60 million people are at risk of HAT infections in 37 countries (~ 40%)of Africa (WHO, 2017; Cecchi *et al.*, 2008). However, rate of new infections and mortality has reduced to 6743 in 2011 and 7197 in 2012 due to concerted control efforts of different stakeholders (WHO, 2014). Data on AAT impact is not readily available. However, direct agricultural losses as a result of trypanosomiasis are about US\$ 500 million annually while indirect losses arising from inability of farmers to keep livestock in trypanosomiasis endemic areas are about US\$ 5 billion per annum (Ogbaje *et al.*, 2010). Economic losses due to *T. evansi* infections have not been determined. However, most estimates, based on mortality and chemotherapeutic interventions, suggest US\$ 1.1 and US\$ 28 million losses in Philippines and Indonesia respectively (Manuel, 1998; Payne *et al.*, 1991). The indirect costs of *T. evansi* have not been adequately defined (Reid, 2002).

Surra is endemic in many tropical and subtropical countries, wherever biting-fly vectors are present, with vectors most major impact in arid and semi-arid areas (Dieleman, 1986). The disease occurs in most countries of Southeast Asia (Luckins, 1988), North and East Africa, Middle East, Indian sub-continent, central Asia, southern China and South America (Davila *et al.*, 1999; Njiru *et al.*, 2004; Reid and Copeman, 2000) (Figure 2.1). Camels and water buffalo, most affected by surra, are important for draught power, meat, milk and capital investment for low- income farmers in many areas where the disease is endemic (Luckins, 1988).

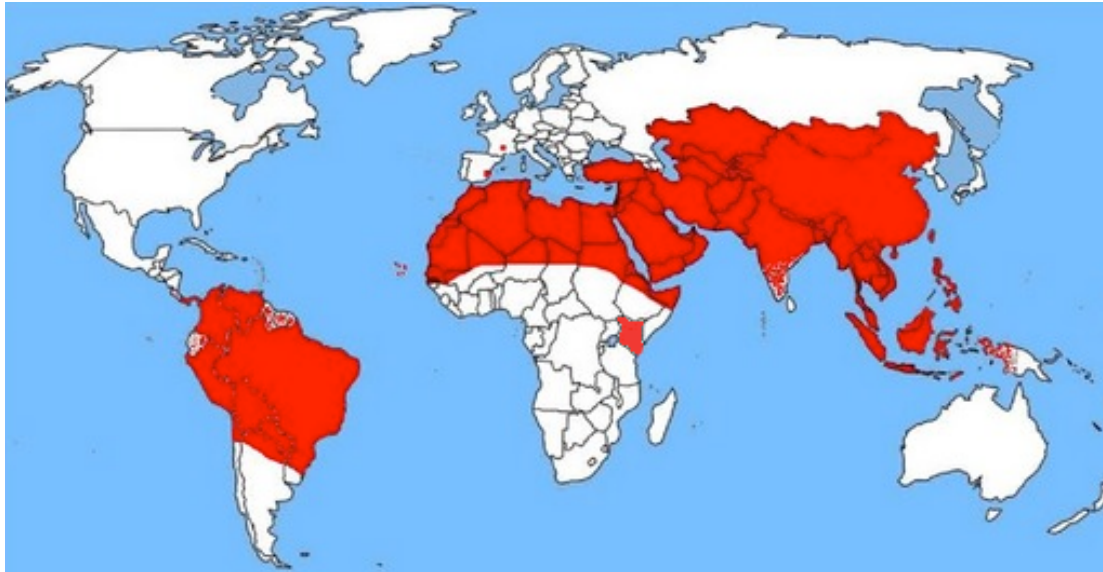


Figure 2. 1: Worldwide distribution of Surra (Desquesnes *et al.*, 2013).

2.2 Morphology

Trypanosomes are kinetoplastida unicellular parasites with a single flagellum, (Beverley, 1996). Kinetoplastid protozoa, including the genera *Leishmania* and *Trypanosoma*, are ancient eukaryotic organisms (Beverley, 1996) infecting wide range of hosts (Clayton *et al.*, 1995). The kinetoplast is a network of mitochondrial DNA with mini and maxi circles. Kinetoplast is attached to the basal body of the flagellum (Robinson and Gull, 1991). All *T. evansi* (and *T. equiperdum*) strains are characterized dyskinetoplastidy, presence of dysfunctional kinetoplast DNA. Where present, kDNA has suffered homogenization of the minicircle component, which consists of more than 200 distinct classes in a tsetse transmission competent strain of *T. brucei* (Steinert and Van Assel, 1980). The *T. evansi* kDNA is dominated by type A or type B minicircles (Birhanu *et al.*, 2016; Borst *et al.*, 1987; Carnes *et al.*, 2015; Njiru *et al.*, 2006). Minicircle heterogeneity is essential for mitochondrial gene expression in trypanosomes (Jensen *et al.*, 2008). As a consequence of its dyskinetoplastidy, *T. evansi* cannot complete cyclical development in tsetse fly, a possible driving forces for the switch to mechanical transmission (Borst *et al.*, 1987; Lai *et al.*, 2008; Lun *et al.*, 1992). Although these peculiarities unite all *T. evansi* (and *T. equiperdum*) strains,

there is significant variation in traits such as virulence among parasite strains and animal host species (De Menezes *et al.*, 2004). Replication of the trypanosomes occurs by binary fission with the flagellum and kinetoplast dividing together (Robinson and Gull, 1991). Diskinetoplastid forms among trypanosomes occur in nature, and can be induced by mutation or treatment with some trypanocides (Brun *et al.*, 1998).

Trypanosoma evansi is morphologically and genetically close to *T. brucei* where their blood stream forms are morphologically indistinguishable. The *T. evansi* is monomorphic and occur in a long slender form due to lack of cyclical transmission within insect vector (Figure 2.2). Blood slender form *T. evansi* is 15-33 μ m (mean length 24 μ m, width 1.5-2.2 μ m) and is amenable to pleomorphism (Hoare, 1972). The *T. evansi* is extracellular in host blood, lymph, lymph nodes, and extravascularly interstitial connective tissue (Reid *et al.*, 2001; Reid and Copeman, 2000; Tuntasuvan *et al.*, 2000). Trypanosomes in mammals may initially replicate in the dermal collagen and interstitial fluid of the skin at site of inoculation before moving into general circulation of the host.

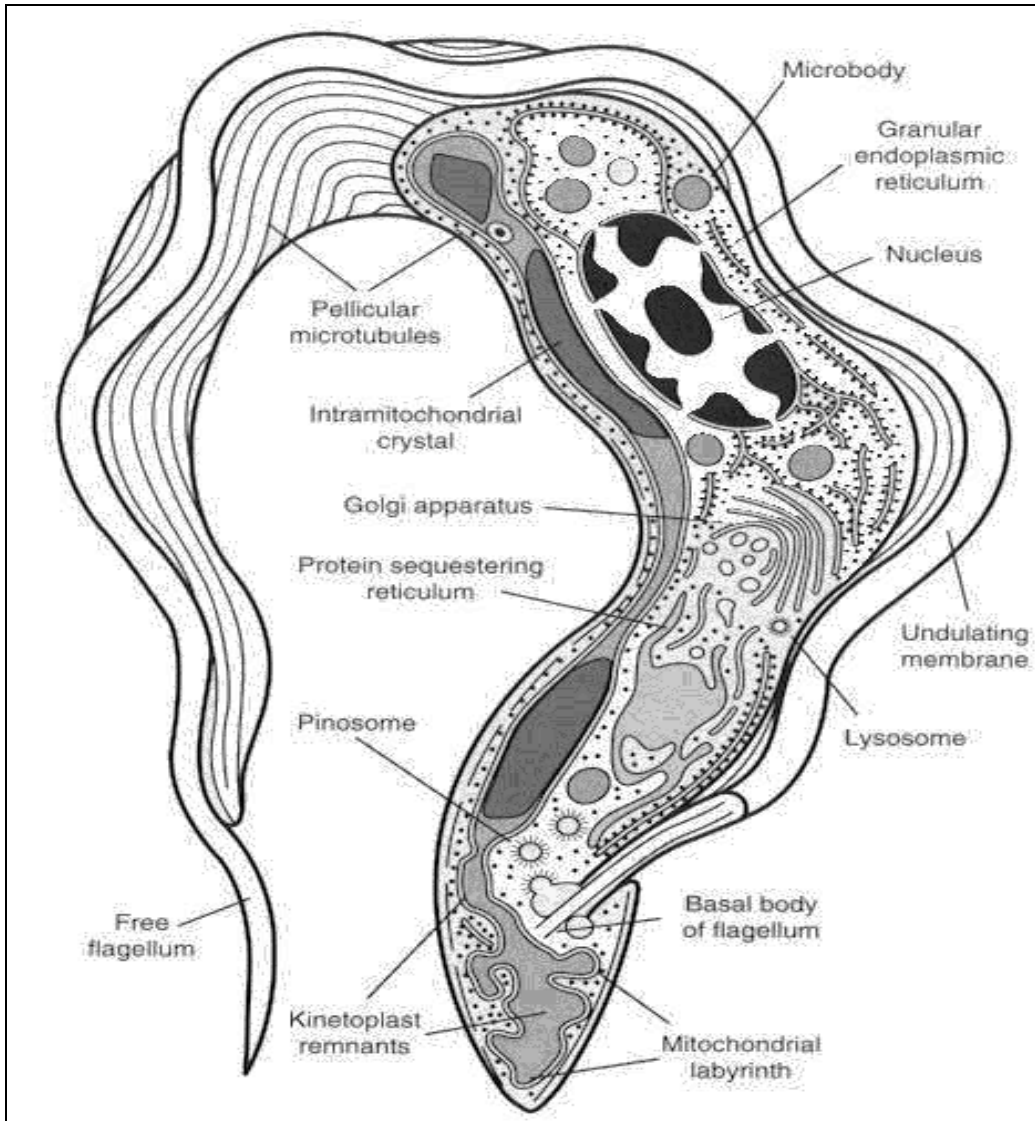


Figure 2. 2: Morphology of *T. evansi* (gsbs.utmb.edu/microbook/images/fig77_1.JPG)

2.3 Life cycle

The *T. evansi* does not undergo development or multiplication in insect vectors due to lacks maxicircle DNA vital for biological development in vector (Borst *et al.*, 1987). Consequently a procyclic or insect forms does not exist in *T. evansi* (Osir *et al.*, 1999). The non-cyclical transmission of *T. evansi* is aided by biting flies and therefore in the absence of tsetse flies, the transmission is maintained in the ecosystem (Eyob and Matios, 2013). The parasite does multiply by binary fission exclusively in the animal host (Brun *et al.*, 1998) (Figure 2.3).

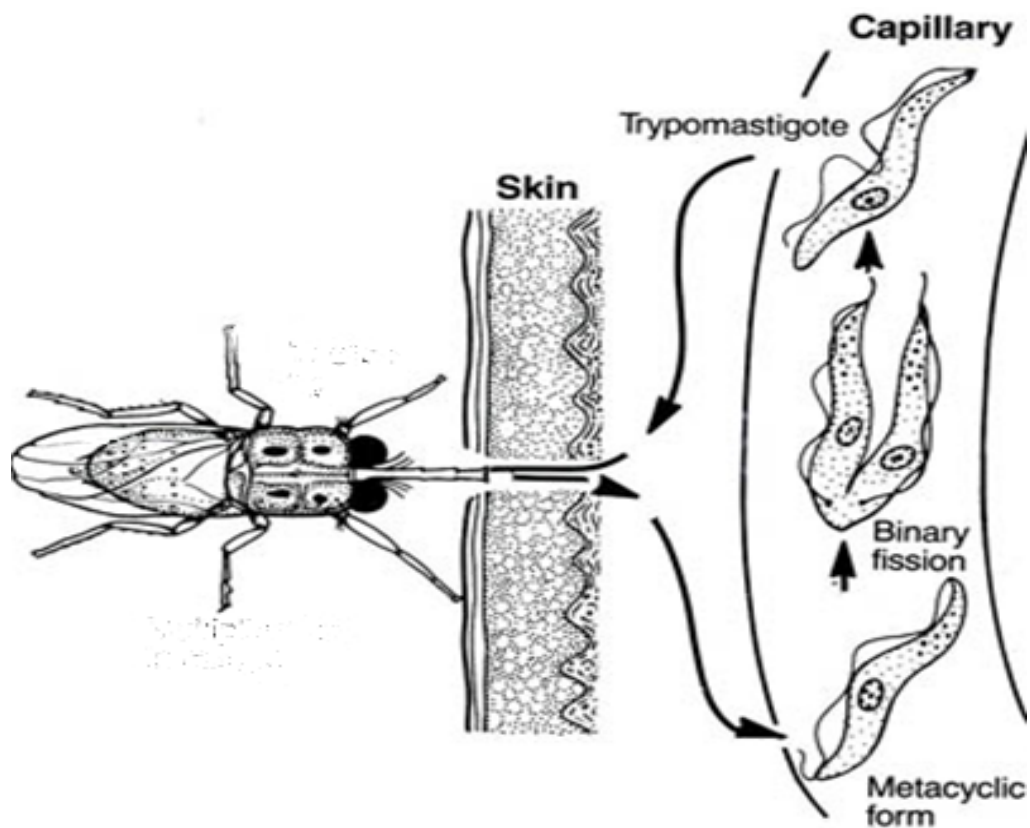


Figure 2. 3: Life cycle of *T. evansi* and reproduction

This figure shows the fly infecting the host and the parasites (metacyclic form) are released into the blood stream where they divide to give rise to trypomastigotes that are picked up by the fly to infect another host. (<http://www.vet.uga.edu/VPP/clerk/womack/index.php>).

2.4 Vectors

Trypanosomes are mainly transmitted via saliva of biting insects. Trypanosomes evolved from parasites of non-haematophagous insects, with transition to mammalian hosts occurring when insects acquired blood-sucking habits (Hoare, 1967). Many trypanosome species currently require an insect intermediate host (Jenni *et al.*, 1986; Lauricella *et al.*, 2005). African trypanosomes are in the salivarian group. The subgenus *Trypanozoon* comprises *Trypanosoma brucei* spp. (*T. brucei* group), *T. evansi* and closely related *T. equiperdum*. Tsetse flies (*Glossina spp*) are the invertebrate intermediate hosts of *T. brucei* group. *Trypanosoma evansi* is mechanically transmitted by haematophagous biting flies such as horseflies (*Tabanidae*) and stable flies (*Stomoxys*) (Luckins, 1988) where tsetse flies are its mechanical vectors in tsetse fly belt of Africa (Uilenberg, 1998). The adaptation to

mechanical transmission has allowed *T. evansi* to move beyond the confines of the tsetse fly belt in Africa and become the most geographically dispersed trypanosome species (Jensen *et al.*, 2008). In Central and South America *T. evansi* is transmitted by vampire bats (*Desmodus rotundus*) (Hoare, 1967), which are hosts and vectors of the parasite (Hoare, 1965). *Trypanosoma evansi* may also be spread by ingestion of fresh meat from infected animals (Herrera *et al.*, 2004).

2.5 Host ranges of Surra

Trypanosoma evansi has a wide host range. In most domestic and many wild animals *T. evansi* is pathogenic with clinical signs depending on strain pathogenicity, host species, general stresses on the host and local epidemiological conditions (Dieleman, 1986; Hoare, 1972). The *T. evansi* infect domestic animals including camels, horses and cattle, deer (Reid *et al.*, 1999; Desequences *et al.*, 2013) buffalo, mules, sheep, cats and pigs (Dieleman, 1986). Equines, camels, dogs, deer and Asian elephants are more frequently diagnosed with surra than buffaloes and cattle, possibly because they exhibit relatively more severe clinical signs (Herrera *et al.*, 2004). Horses may develop sub-clinical trypanosomiasis, though the disease generally causes multiple crises and relapses and is often fatal (Dieleman, 1986; Hoare, 1972). Camels usually develop acute disease (Figure 2.4), though they may survive to develop chronic infection or even undergo spontaneous recovery (Gutierrez *et al.*, 2006). The disease is usually fatal within six months in dogs (Aquino *et al.*, 2002; Morrison *et al.*, 1981). Bovines are more likely to develop cryptic disease, especially in endemic areas (Hoare, 1972). Pigs can be infected, but have mild or no clinical signs and goats develop chronic infection (Dargantes *et al.*, 2005).

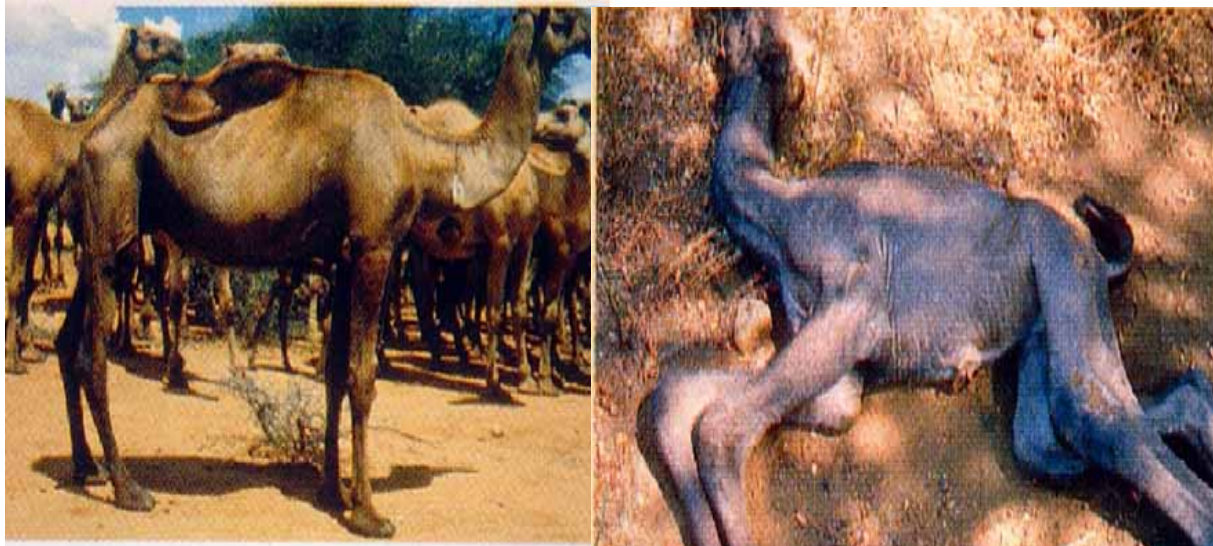


Figure 2. 4: Weight loss and emaciation in camels as a result of Surra (osp.mans.edu.eg)

Severity of outcome of *T. evansi* infection in livestock can be ranked from highest to lowest where camels, horses, dogs and Asian elephants are more susceptible than sheep and goats, which in turn are more susceptible than bovines and pigs. Wildlife susceptible to *T. evansi* include coatis (*Nasua nasua*) and capybaras (*Hydrochoeris hydrochoeris*) in South America (Herrera *et al.*, 2002; Herrera *et al.*, 2004). Experimental infection of marsupials including agile wallabies (*Macropus agilis*) and dusky pademelons (*Thylogale brunii*) resulted in acute disease with 100% mortality (Reid *et al.*, 2001). Unlike in tsetse-transmitted trypanosomiasis, wildlife are not important with *T. evansi* reservoirs of infection (Nantulya *et al.*, 1989), with coatis and capybaras as exceptions (Herrera *et al.*, 2004). Camels (in Africa) and horses are probably the main reservoir hosts in Africa and Asia (Hoare, 1972).

The *T. evansi* is not generally infective to humans due to presence of a resistance factor in human serum, but has minimal human infectivity (Joshi *et al.*, 2005). A *T. evansi* infection in India was attributed to rare mutation in ApoL-I gene of the patient ((Powar *et al.*, 2006; Vanhamme and Pays, 2004), a key effector molecule responsible for trypanosome lysis in human serum (Poelvoorde *et al.*, 2004). Lysis of trypanosomes by normal human serum can

be neutralised when serum resistance associated protein (SRA) interacts with human apoL-I in lysosome (Poelvoorde *et al.*, 2004; Vanhamme *et al.*, 2003; Xong *et al.*, 1998).

2.6 Diagnosis and Parasitological tests

Detection of parasites in blood is impeded by intermittent parasitaemia (Mahmoud and Gray, 1980), necessitating a need for more sensitive diagnostic techniques. Parasitological methods used in the diagnosis of *T. evansi* in camels are considered easy, rapid and economic. However, they are not sufficient to detect all trypanosome-infected animals, especially in case of low parasitaemia and chronic form of the disease. One of these methods is carried out by the direct microscopic examination of wet or stained blood films (Murray *et al.*, 1977), with a limited sensitivity. Other tests include haematocrit centrifugation, mini anion-exchange using DEAE–cellulose and inoculation in laboratory mice (Brun *et al.*, 1998). *Trypanosoma evansi* infections are consequently under-diagnosed.

2.6.1 Serological tests

In addition to the use of parasitological or molecular tools for detecting *T. evansi* infection, serological tests that prove the immune contact between the host and the parasite are quite useful. Antibody techniques including complement fixation test (CFT) immune trypanolysis (TL) assay (Van Meirvenne *et al.*, 1995), an enzyme–linked immunosorbent assay for *T. evansi* (ELISA/*T.evansi*) detects immunoglobulin G and thus for already established infections, a card agglutination test (CATT/*T. evansi*) detects immunoglobulin M thus picks early infections and a latex agglutination test (Desquesnes *et al.*, 2013). All these tests are based on Rotat 1. 2 VSG and not *T. evansi* type B found in Kenya (Thao *et al.*, 2009).

2.6.2 RoTat 1.2 gene

Rode Trypanozoon antigen type 1.2 (RoTat 1.2) is a predominant variable antigen type (VAT) in early in infection in most *T. evansi* strains responsible for antigenic variation. The

variable surface glycoprotein of *T. evansi* RoTat 1.2 is used as an antigen in different antibody detection assays for *T. evansi*. The VAT was cloned from *T. evansi* isolated from Indonesian water buffalo in 1982 (Urakawa *et al.*, 2001). Tests using RoTat 1.2 do not cross-react with antibodies to other pathogenic trypanosomes, although they cannot distinguish between infections with trypanosomes currently classified as *T. evansi* and *T. equiperdum* (Claes *et al.*, 2002; Claes *et al.*, 2004). The RoTat 1.2 gene is a fairly specific marker for *T. evansi* type A strains, but is not present in *T. evansi* type B strains isolated from Kenya, which may limit its diagnostic utility (Claes *et al.*, 2004; Ngaira *et al.*, 2005; Njiru *et al.*, 2006). Due to the limited diagnostic utility, *T. evansi* type B is not picked by the tests, thus the prevalence (approximately 2.4%) of this parasite could be higher in the field than earlier reported (Njiru *et al.*, 2010). Undiagnosed *T. evansi* cases continue to perpetuate transmission in the areas of disease foci and form the sources of infection in new areas. Despite this information, very little is known on the precise distribution, incidence, and impact of Surra in majority of the countries affected.

2.7 Control of surra

2.7.1 Vector control

Vector control of *T. evansi* infection is limited because of the large number and diversity of biting fly species, in addition the high mobility and prolificacy as seen with the tabanid species. There is no obvious way of developing exclusion zones for animals on grazing land and limited likelihood that vector control will be successful compared to tsetse-transmitted trypanosomes (Luckins, 1997) using insecticides and traps. The vector populations of surra can be attempted using traps and/or impregnated screens or using insecticides on livestock. The efficient traps for the mechanical vectors are the Nzi trap (Desquesnes *et al.*, 2013) which is capable of catching large tabanid and stomoxys species. However, so far, these traps

have been used to study insects and monitor control campaigns rather than for actual insect control (Desquesnes *et al.*, 2013).

2.7.2 Parasite Control

Trypanosoma evansi being a blood parasite, is killed by injecting various trypanocidal drugs in the infected host and providing concentration that is lethal to the parasite. Treatment of surra depends largely on four drugs: suramin, diminazene, cymelarsan and quinapyramine. These drugs have been on the market more than 50 years. One of the most important risks for the future use of these trypanocides is the development and the dissemination of resistance strains that have developed in different locations around the world depending on which drugs are frequently used (Geerts *et al.*, 2001; Gillingwater *et al.*, 2007). For example, resistance of *T. evansi* to suramin has been reported in isolates from Sudan to China (Delespaux and de Koning, 2007).

2.8 Virulence

Virulence, is a term that refers to the degree of pathology caused by an organism. The extent of the virulence is usually correlated with the ability of the pathogen to multiply within the host. An organism (species or strain) may exhibit different levels of virulence. In order to compete for transmission to new hosts, some pathogens, including *T. evansi*, extract resources from the host, thereby causing damage (Mackinnon *et al.*, 2008). This damage will depend on the level of virulence of the pathogen as the host immunity can aggravate selection for virulence. Under the trade-off hypothesis, it is assumed that there are both fitness benefits and costs associated with virulence. The cost is assumed to be host death because, for most pathogens, transmission stops when the host dies (Mackinnon *et al.*, 2008). The benefits associated with virulence are assumed to be production of more transmission forms per unit time, and/or increased persistence in a live host. Pathogens therefore run the risk of killing

their host and completely lose their ongoing source of transmission to new hosts. Virulence has been reported in many pathogens (Berngruber *et al.* 2013; Little *et al.*, 2008; Mackinnon *et al.* 2008), measured by the survival rate of the host following infection. Little *et al.* (2008) proved that relative growth rates of two parasite isolates studied depended on the host genotype.

However, it is generally acknowledged that naïve animals succumb to an infection faster than the animals that have been previously exposed to surra (Mackinnon *et al.*, 2008). The trade-off hypothesis and its assumptions has been well-covered in malaria (Mackinnon *et al.* 2008). Depending on pathogen types, evolutionary outcomes may occur. Other studies have reported that cysteine proteases (CPs), papain family, are expressed during infective stages of the life cycle of the parasite and are suspected to act as pathogenic factors in mammalian host, where they also trigger prominent immune responses (De Menezes *et al.*, 2004). The pathogenicity of *T. evansi* varies among different strains and in different animal species (Luckins, 1988). *Trypanosoma evansi* infection is usually regarded as a serious disease of horses and camel, causing high mortality, whereas the disease is typically mild in other domestic animals (Mekata *et al.*, 2013). However, there are growing concerns about the appearance of highly virulent *T. evansi*, and there are no reports about the virulence of the strains of *T. evansi* in general (Sistrom *et al.*, 2014). As such, the current study generated data that would assist in comparison as well as a deeper understanding of virulence as a phenotype of *T. evansi*. These findings provides an insight towards the development of novel approaches for management of the disease in camels.

2.9 Genetic studies

Over the last three decades, population genetic and genomic studies have provided important insights into the biology of *T. brucei* and epidemiology of Human African trypanosomiasis (HAT) or sleeping sickness and animal African trypanosomiasis (AAT) (Balmer *et al.*, 2011).

It is assumed that *T. evansi* originated in Africa from camels infected by *T. brucei* on the edge of the African tsetse fly belt and then spread via camel trade and transport across the Sahara into North Africa, Asia and the Middle East (Hoare, 1967). The exact nature of the genetic relationship between *T. brucei* and *T. evansi* has been the subject of ongoing debate, with some evidence suggesting that *T. evansi* should be considered a sub species or distinct species, separate from *T. brucei* (Wendy, 2003; Lai *et al.*, 2008). The fine scale ecological and evolutionary processes underlying disease dynamics and the distinction of the different parasite forms are still not very well understood.

There is evidence for *T. b. brucei* that origins of lethal *T. brucei* includes common origins of antigenic variation, a key trait in immune system evasion. Antigenic variation is conserved in all African trypanosomes and appears to be under purifying selection (Sistrom *et al.*, 2014). There is also some positive correlation between Linkage Disequilibrium (LD) and chromosome length on the *T. brucei* as supported by smaller chromosomes with higher recombination rates than larger ones (Balmer *et al.*, 2011; Sistrom *et al.*, 2014). The *T. evansi*, *T. equiperdum*, *T. b. gambiense* and *T. b. rhodesinse* are lethal strains that are genetically subspecies of *T. brucei* that originated from *T. b. brucei*.

Evidence that *T. evansi* and *T. equiperdum* originated from *T. b. brucei* come from kinetoplast DNA, Internal Transcribed Spacer (ITS) sequence data and microsatellite genotypes. These data show that *T. evansi* and *T. equiperdum* are polyphyletic and are nested phylogenetically within the more genetically diverse *T. b. brucei* (Carnes *et al.*, 2015). Genomic studies support that *T. evansi* evolved recently from *T. b. brucei*. Annotated *T. evansi* genome has extensive similarity to *T. b. brucei* reference strain, with 94.9% of predicted *T. b. brucei* coding sequences (CDS) (Ziková *et al.*, 2008). The *T. evansi* has retained genes also present in *T. brucei*, but are non-functional. For example, the *T. evansi* genome contains several genes that are essential for *T. brucei* survival in insect host vectors

(i.e. kinetoplast genes involved exclusively in oxidative phosphorylation), but appear to be completely unnecessary for *T. evansi* survival or transmission (Carnes *et al.*, 2015). The loss of function in these genes in *T. evansi* is relatively recent since there is not a single case of gene loss in the kinetoplast, a region of the genome involved in survival of *T. b. brucei* in insect hosts (Sistrom *et al.*, 2014). Thus, structural and functional genomic evidence for a recent *T. evansi* origin from *T. b. brucei* is strong.

However, available data is insufficient to provide an understanding of where, when and how many times this evolutionary event took place. Also, the apparent links between efficient mechanical transmissions, kDNA loss that have led to the enormous evolutionary success of this parasites remain unclear. Insights into these questions will be critical to clearly define the pool of parasites responsible for animal disease, to understand the emergence of new disease foci, and to eventually understand how animal infectivity interacts with other important traits such as animal host range (Balmer *et al.*, 2011), virulence and drug-resistance. It was also important to study the evolution and the genetic diversity among different *T. evansi* strains and understand its evolutionary origins in the endemic regions with emphasis on Kenya.

Despite the genetic and genomic evidence that *T. evansi* originated from *T. b. brucei* somewhere in Africa, details of *T. evansi* origins are poorly understood. Some studies (Claes *et al.*, 2002; Salim *et al.*, 2011; Villareal *et al.*, 2013) found that the four *T. evansi* strains sampled were included in the single population genetics study completed to date, three strains were genetically distinct from all other *T. brucei* subspecies, and there was a single non-distinct *T. evansi* strain from Kenya (Sistrom *et al.*, 2014). It was suggested that this pattern of genetic similarity can be an artifact resulting from the limited number and type of isolates included in these studies. This is especially true for the *T. evansi* isolates that only included the common kDNA type A lineage (i.e. kDNA minicircle type A configuration and RoTat 1.2

positive). Indeed, other studies that have included both type A and type B *T. evansi* isolates have found similar results to what was found in this study, using a larger geographic and taxonomic diversity of isolates (Carnes *et al.*, 2015). Interestingly, previous comparative genomic analysis (Carnes *et al.*, 2015) and with classical parasitological characterization, indicates high similarity between *T. evansi* and *T. b. brucei* except for variable patterns of loss of part or all of their kDNA (Borst *et al.*, 1987; Carnes *et al.*, 2015; Lai *et al.*, 2008; Schnauffer, Domingo, & Stuart, 2002). Together, Siström's (2014) preliminary work supports multiple origins of *T. evansi* from *T. b. brucei* and indicated a need for further analysis including a broader sample of *T. evansi* from Africa and spatial expansion on a global scope. It is on this background of uncertainties that the current study was designed to determine the origin and dynamics of global expansion in *T. evansi*.

CHAPTER THREE

MATERIALS AND METHODS

3.1 Study design

This was a laboratory-based study that involved use of cryopreserved trypanosomes, to investigate virulence, evolutionary trends and spatial expansion of *T. evansi*. The study involved screening of *T. evansi* isolates by PCR to confirm species and type (A and B). Selected isolates were used to infect experimental laboratory mice (swiss white mice). These mice were preferable because they are small, easy to handle, readily available. They also reproduce quickly and have a short lifespan of two to three years, so several generations of mice can be observed in a relatively short period of time. They are also relatively inexpensive. Most of these mice are inbred, thus are almost identical genetically. This helps make the results more uniform. Parameters related to virulence which were parasitaemia, survival time, Packed Cell Volume (PCV) and bodyweights recorded and analyzed. Blood samples was also collected from infected mice and DNA extracted from the parasites for evolutionary and spatial expansion studies. For studies on evolutionary trends and spatial expansion, fifteen microsatellite loci were used. The detailed methodologies are provided in the following sections.

3.2 Determination of differential virulence of *T. evansi* isolates in mice

Under this objective the experimental procedure is as described below:

3.2.1 Source of *T. evansi* isolates

Isolates of *T. evansi* were provided by Kenya Trypanosomiasis Research Institute (KETRI) Cryobank, Muguga, Kenya, where collections of trypanosomes from different regions are maintained (Muchiri *et al.*, 2015). All isolates were screened for presence of *T. evansi* types

A and B using type-specific polymerase chain reaction (PCR). The procedure for PCR-screening of the isolates is described under section 3.2.2. From the PCR-screening the types A and B isolates were selected for further analyses as shown in Table 3.1.

Table 3. 1: Selected *Trypanosoma evansi* isolates for virulence studies.

<i>T. evansi</i> strains	Region	Country	Host	Year Isolated
KETRI 4034	Brazil	Brazil	Dog	1986
KETRI 4035	Colombia	Colombia	Horse	1973
KETRI 4036	Kazakstan	Kazakhstan	Bactrian camel	1995
KETRI 4037	Phillipines	Philippines	Water buffalo	1996
KETRI 4038	Indonesia	Indonesia	Water buffalo	1982
KETRI 4039	China	China	Water buffalo	1983
KETRI 4040	Vietnam	Vietnam	Water buffalo	1998
KETRI 2479	Nguranit	Kenya	Camel	1979
KETRI 2446	Marsabit	Kenya	Camel	1979
KETRI 2737	Galana	Kenya	Camel	1985
KETRI 3266	Samburu	Kenya	Camel	1990
KETRI 3552	Isiolo	Kenya	Camel	1994
KETRI 3567	Athi river	Kenya	Camel	1994
KETRI 3573	Nguranit	Kenya	Camel	1994
KETRI 3575	Nguranit	Kenya	Camel	1994
KETRI 3576	Nguranit	Kenya	Camel	1994
KETRI 3580	Loglogo	Kenya	Camel	1994

3.2.2 PCR-Screening of *T. evansi* isolates

DNA was extracted from cryo-preserved isolates (thawed at room temperature) and diluted in 100 µl of Tris-EDTA buffer (pH 8.0) using DNeasy Blood and Tissue kit (Qiagen, Hilden, Germany) according to manufacturer's instructions. In brief, samples were first lysed using proteinase K. Buffering conditions were adjusted to provide optimal DNA binding conditions and the lysate was loaded onto the DNeasy Mini spin column. During centrifugation, DNA was selectively bound to the DNeasy membrane as contaminants pass through. Remaining contaminants and enzyme inhibitors were removed in two efficient wash steps and DNA was then eluted in buffer, ready for use. The extracted DNA was used as template for PCR-screening of Rotat 1.2 and minicircle genes for *T. evansi* types A and B, respectively. The

PCR for *T. evansi* type A was performed using a set of ILO7957 and ILO8091 primers that amplified sequences encoding RoTat1.2 VSG gene, targeting 488 bp fragment of the RoTat 1.2 variant (Urakawa *et al.*, 2001). Briefly, amplification, parameters used were; initial denaturation 94°C for 30 s, followed by 30 cycles 52°C for 30s, and annealing 72°C for 60 s, followed by a 10-min extension at 72°C for 5 min. The PCR primers for type B were EVAB1 and EVAB2 targeting a 433 bp fragment (Njiru *et al.*, 2006) with amplification conditions employed as; the initial denaturation step at 94°C for 5 min, followed by 30 cycles of denaturation at 94°C for 30s, annealing at 60°C for 30s and extension at 72°C for 60s. The PCR products were analyzed on ethidium bromide-stained 1.5% agarose gels according to standard protocols (Sambrook *et al.*, 1989). The products were further purified on the agarose gels, and identity of the genes confirmed by sequencing.

3.2.3 Experimental animals

This study used 6-8-week-old male Swiss White mice, each weighing 25-30g live body weight. The animals were obtained from Animal Breeding Unit at KALRO-BioRI, Muguga, Kenya. The mice were housed in standard mouse cages and maintained on a diet consisting of commercial pellets (Unga® Kenya Ltd (Muchiri *et al.*, 2015). All animal experiments were approved by the Institutional Animal Care and Use Committee (IACUC) at KALRO-BioRI (Appendix 1). Briefly, the animals were housed in standard cages where water was provided *ad libitum* as previously described (Kagira *et al.*, 2007). All mice were acclimatized for two-weeks, during which time they were screened and treated for the ecto- and endo-parasites using ivermectin (Ivermectin®, Anupco, Suffolk, England (Ndung'u *et al.*, 2008). During the two-week quarantine period, pre-infection data was collected on body weights and packed cell volume twice a week prior to inoculation with trypanosomes.

3.2.4 *T. evansi* isolates and preparation of inoculum

A total of 17 isolates from different geographic regions and mammalian host species were used in the study (Table 3.1). Seven of the isolates were obtained from Swiss Tropical Institute, Basel (STIB) while the rest were obtained from the KALRO-BioRI, Trypanosome cryobank (Murilla *et al.*, 2014). The parasite stabilates obtained from BioRI trypanosome bank were thawed, and their viability validated through microscopy. The parasites were diluted in Phosphate buffered Saline Glucose (PSG; pH 8.0), for validation of viability (Gichuki and Brun, 1999). The parasites were considered viable if motile parasites were observed through wet film under a microscope. Two immunosuppressed donor mice were each inoculated intraperitoneally (I.P) with 200ul of 1×10^5 of viable trypanosomes/ml as previously described (Gichuki and Brun, 1999). Immunosuppression was achieved by administration of cyclophosphamide at 300mg/kg per animal at 100mg/kg bodyweight per day for 3 consecutive days (Murilla *et al.*, 2016). The animals were monitored for trypanosomes daily until parasites were detected in the peripheral blood. Thereafter, the parasitaemia was monitored three times a week up to the first peak (1×10^9 trypanosomes) parasitaemia (Herbert and Lumsden, 1976). At peak parasitaemia, the mice were euthanized by placing them in a chamber containing carbon dioxide (CO₂) and bled from the heart into a tube containing EDTA (Gichuki and Brun, 1999).

The blood was pooled and parasitaemia density determined. The pooled blood was diluted in PSG buffer (pH 8.0). The number of trypanosomes was quantified using an improved Neabauer chamber and viewed under microscope (Seamer *et al.*, 1993). The first count (C1) and the second count (C2) were made through all the 16 squares of the haemocytometer and the average count C_{av} calculated as Number of trypanosomes = Average count x dilution factor x 10⁴ trypanosomes/ml. After establishing number and viability of parasites obtained

from donor mice, parasites were serially diluted in PSG to a final concentration of 5×10^5 trypanosomes/ml (Seamer *et al.*, 1993).

3.2.5 Trypanosome inoculation into experimental mice

Six mice were used per isolate while six additional animals were used as non-infected controls. The experimental mice were inoculated I.P with 1×10^5 trypanosomes in 200 μ l of PSG (pH=8.0). The mice in the control group were similarly injected with 200 μ l of PSG per mouse. All the infected animals were maintained as described above for 60 days' post infection (dpi).

3.2.6 Evaluation of parasitaemia in infected mice

A drop of blood from snipping of the mouse-tail was placed on a clean slide and covered using a cover slip as a wet blood smear and examined under a microscope (Seamer *et al.*, 1993). The parasitaemia score was estimated which correlated to a score sheet, as outlined by Herbert and Lumsden (1976). Parasitaemia was determined daily and recorded for the first 14 days. This period taken from parasite inoculation to the first appearance of trypanosomes in blood was recorded for all groups. Thereafter, parasitaemia was determined and recorded twice weekly up to 60 dpi. Any observed mortalities were recorded on daily basis.

3.2.7 Survival

Each mouse was monitored daily for a period of 60 dpi (endpoint). The end point of the infected mice was determined by a PCV drop of 35% and below, consistent high parasitaemia levels of 1×10^9 /ml for at least three consecutive days, lethargy and hackle hair clinical signs. At this point, affected animal(s) were sacrificed immediately by CO₂ asphyxiation in accordance with guidelines of the IUCAC as described by (O'brien, 1998) and recorded as dead animal(s). Mice surviving beyond this period (60 dpi), were sacrificed using CO₂ and the survival time recorded as 60 days and categorized as censored data. Log rank *p* and the

Wilcoxon *p*-values were determined and used to test that the survival curves are identical in all the *T. evansi* populations (O'brien, 1998).

3.2.8 Assessment of Packed Blood Cell Volume (PCV) in infected and uninfected mice

Blood from infected mice and uninfected controls was collected from the tail vein using heparinized capillary tubes and sealed with plasticine at one end (Naessens *et al.*, 2005). The sealed capillaries were centrifuged in a haematocrit centrifuge at 10,000 revolutions per minute, for five minutes. The PCV was read using the haematocrit reader and expressed as a percentage (%) of the total blood volume (Naessens *et al.*, 2005). The PCV data was collected twice weekly for the experimental period of 60 days post-infection.

3.2.9 Assessment of body weights in infected and uninfected mice

Body weights of mice were determined using an analytical balance (Mettler Toledo PB 302 ®, Switzerland) (Ezz El-Arab *et al.*, 2006) and expressed in grams prior and after inoculation. Data on live body weights was recorded twice a week for a period of two weeks before inoculation and over the experimental period of 60 days' post-infection. The differences in the weights were recorded.

3.2.10 Data analysis

Analysis was done to test the significant differences between the isolates in PCV, parasitaemia and body weights. The data obtained from the study was summarized as means \pm standard error, while the differences between and within the means was analysed using one-way ANOVA. All analysis was conducted using GenStat (Nelder and Baker, 1972). $P \leq 0.05$ were considered statistically significant.

3.3 Determination of multiple evolutionary origin and dynamics of global expansion of *T. evansi*

In order to determine the multiple evolutionary origin and dynamics of spatial expansion from Africa to multiple continents of *T. evansi* isolates, studies were undertaken on the parasite population genetics. This comparative study was undertaken on Kenyan isolates and DNA from isolates collected from *T. evansi* endemic regions of the world.

3.3.1 Trypanosome isolates

For the purpose of this work, and in line with microbiological convention, the term isolate and strains were defined as follows. An isolate constituted samples obtained from particular animal at a particular time while a strain was an isolate or group of isolates that distinguishable from other isolates by phenotypic and or genotypic characterization (Dijkshoorn *et al.*, 2000). A total of 41 *T. evansi* isolates were analyzed. The majority of these isolates were from Kenya (Figure 3.1) and currently stored at the KETRI cryobank (Murilla *et al.*, 2014) based at KALRO-BRI (Kikuyu, Kenya). For spatial expansion an additional 17 isolates of *T. evansi* and *T. equiperdum* were analyzed and majority of the isolates were from Asia as shown in Figure 3.2.

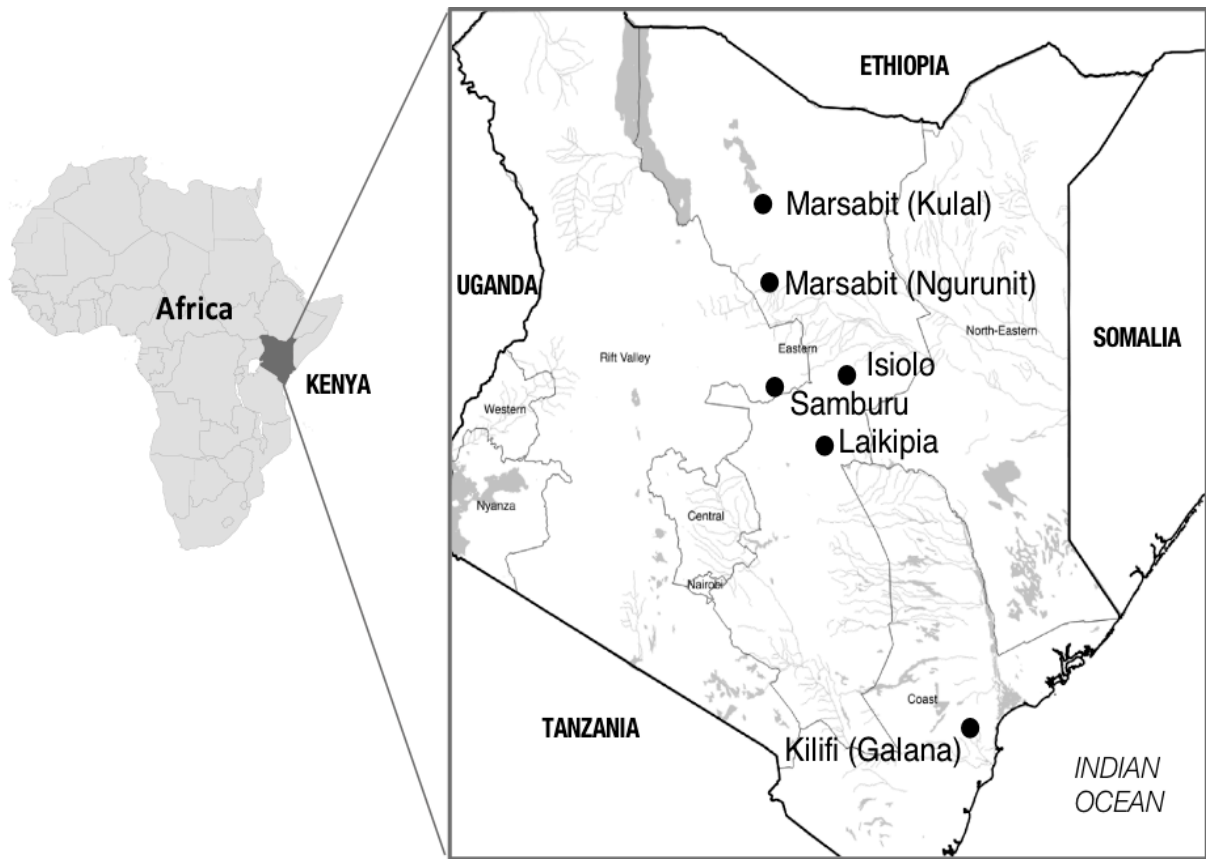


Figure 3. 1 Map of Africa showing in black the location of Kenya. The insert to the right shows the location of the *Trypanosoma evansi* (Tev) and *T. b. brucei* (Tbb) strains genotyped for this study (small black circles).

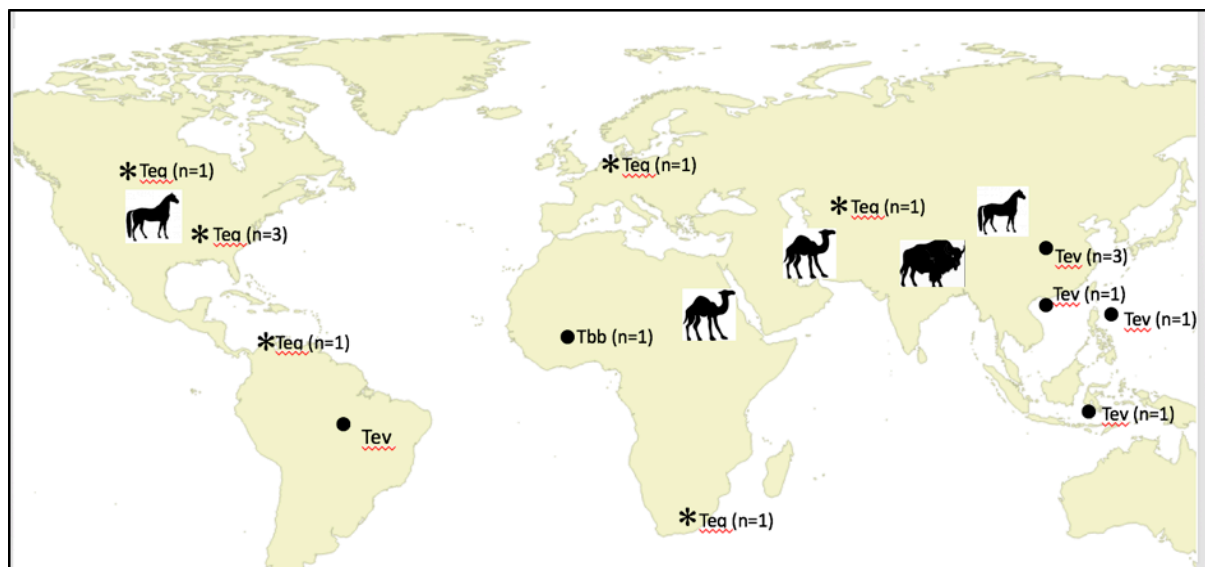


Figure 3. 2: Map showing worldwide location of *Trypanosoma evansi* (Tev) (small black circles) and *Trypanosoma equiperdum* (Teq) (asterisk) strains genotyped for this study.

These samples had been collected at several time points and some had previously been classified as *T. evansi* based on host species (camel vs. non-camel), region of isolation, and kDNA minicircle type (Table 3.2).

Table 3. 2: Sample details and PCR assay results of *T. evansi* genotyped for this study.

Sample ID	Isolate ^{source} [reference]	kDNA type	PCR assay				Host	County (town) / Country	Year of isolation
			ITS 1	S R A	Ro Tat 1.2	A 281d el			
K2469	KETRI2469 ^a	A†	+	-	-	+	Camel	Marsabit (Kulal)	1979
K2444	KETRI2444 ^a	A†	+	-	-	+	Camel	Marsabit (Kulal)	1979
K2467	KETRI2467 ^a	A†	+	-	-	+	Camel	Samburu	1979
K3789	KETRI3789 ^a	A†	+	-	-	+	Camel	Samburu	2003
K3793 [#]	KETRI3793 ^a	Unkn.	+	-	-	n/a	Camel	Laikipia	1995
K3930	KETRI3930 ^a	A†	+	-	-	+	Camel	Samburu	2003
K3931	KETRI3931 ^a	A†	+	-	-	+	Camel	Marsabit (Kulal)	2003
K2443	KETRI2443 ^a [1]	A	+	-	-	+	Camel	Marsabit (Kulal)	1979
K2450 [#]	KETRI2450 ^a [1]	Unkn.	+	-	-	n/a	Camel	Kilifi (Galana)	1979
K2455	KETRI2455 ^a [1]	A†	+	-	-	+	Camel	Kilifi (Galana)	1979
K2458	KETRI2458 ^a [1]	A†	+	-	-	+	Camel	Kilifi (Galana)	1979
K2465	KETRI2465 ^a [1]	A†	+	-	-	+	Camel	Marsabit (Kulal)	1979
K2466	KETRI2466 ^a [1]	A†	+	-	-	+	Camel	Marsabit (Kulal)	1979
K2470	KETRI2470 ^a [1]	A†	+	-	-	+	Camel	Marsabit (Kulal)	1979
K2439	KETRI2439 ^a [1]	A	+	-	+	+	Camel	Marsabit (Kulal)	1979
K2441	KETRI2441 ^a [1]	A†	+	-	+	+	Camel	Marsabit (Kulal)	1979
K2442	KETRI2442 ^a [1]	A†	+	-	+	+	Camel	Marsabit (Kulal)	1979
K2446	KETRI2446 ^a	A†	+	-	+	+	Camel	Marsabit (Kulal)	1979
K2449	KETRI2449 ^a	A†	+	-	+	+	Camel	Kilifi (Galana)	1979
K2451	KETRI2451 ^a [1]	A†	+	-	+	+	Camel	Kilifi (Galana)	1979
K2453	KETRI2453 ^a [1]	A†	+	-	+	+	Camel	Marsabit (Kulal)	1979
K2454	KETRI2454 ^a [1]	A	+	-	+	+	Camel	Marsabit (Kulal)	1979
K2456	KETRI2456 ^a [2]	A	+	-	+	+	Camel	Kilifi (Galana)	1979
K2457	KETRI2457 ^a [1]	A†	+	-	+	+	Camel	Marsabit (Kulal)	1979
K2479**	KETRI2479 ^a	B	+	-	-	-	Camel	Marsabit	1979
K2481	KETRI2481 ^a [1]	A†	+	-	+	+	Camel	Marsabit (Kulal)	1979
K3548	KETRI3548 ^a [1]	A†	+	-	+	+	Camel	Isiolo	1994
K3550	KETRI3550 ^a [1]	A†	+	-	+	+	Camel	Isiolo	1994
K3551	KETRI3551 ^a [1]	A†	+	-	+	+	Camel	Isiolo	1994
K3552	KETRI3552 ^a [1]	Non-A/B	+	-	+	-	Camel	Isiolo	1994
K3553	KETRI3553 ^a	A†	+	-	+	+	Camel	Isiolo	1994
K3556	KETRI3556 ^a [1]	A†	+	-	+	+	Camel	Isiolo	1994
K3557	KETRI3557 ^a [1]	Non-A/B	+	-	+	-	Camel	Isiolo	1994
K3558	KETRI3558 ^a [1]	A†	+	-	+	+	Camel	Isiolo	1994
K3576*	KETRI3576 ^a [1]	Unkn.	+	-	+	n/a	Camel	Marsabit	1994
STIB810	STIB810 ^b [6]	A	+	-	+	n/a	Buffalo	China	1985
C13	C13 [4]	A	+	-	+	n/a	Camel	Kenya	1981

[#] *T. evansi* assignment based on camel host alone

1 (Njiru and Constantine, 2007)

† kDNA type based on A281del PCR assay alone	2 (Masiga <i>et al.</i> , 2006)
^a Kenya Trypanosomiasis Research Institute	3 (Borst <i>et al.</i> , 1987)
^b Swiss Tropical Institute Basel	4 (Gibson <i>et al.</i> , 1983)
** high virulence	5 (Claes and Büscher, 2007)
* low virulence	

Provided are details showing sample ID, strain isolated with source and reference, kinetoplast DNA (kDNA) type, PCR assay results (ITS1 + indicates pathogenic African trypanosome, SRA – indicates not *T. b. rhodesiense*, RoTat 1.2 + indicates serological diagnostic antigen variant, A281del + indicates deletion of a GTC (Ala) triplet in F₀F₁-ATPase subunit γ unique to *T. evansi* isolates of kDNA type A, n/a indicates failure of the positive PCR control), host of isolation, the locality of origin and year of isolation. See also Table 3.2 for strains genotyped in previous studies.

Virulence of two of these isolates, K2479 (Gibson *et al.*, 1983; Masiga *et al.*, 2006) and K3576, were experimentally characterized in mice, based on relative levels of parasitaemia and host survivorship in infected mice. The remaining *T. evansi* isolates came from multiple sources (Tables 3.3) and have been well-characterized in past studies and, in some cases, were part of recent genetic studies (Balmer *et al.*, 2011; Borst *et al.*, 1987; Carnes *et al.*, 2015; Gibson *et al.*, 1983; Lun *et al.*, 1992).

Table 3. 3: Sample details of strains from previous studies showing sample ID, publication, taxon, kDNA, host of isolation, and locality of origin.

Sample ID	Publication	Taxon	kDNA type	Host	Locality of origin
RoTat1.2 (OB106)	(Urakawa <i>et al.</i> , 2001; Birhanu <i>et al.</i> , 2016; Balmer <i>et al.</i> , 2011; Carnes <i>et al.</i> , 2015)	Tev	A	Water buffalo	Indonesia
STIB708 (KETRI2489, OB35)	(Balmer <i>et al.</i> , 2011; Carnes <i>et al.</i> , 2015)	Tev	A	Camel	Kenya
STIB806K (OB2)	(Lun <i>et al.</i> , 1992; Carnes <i>et al.</i> , 2015)	Tev	A	Buffalo	China
STIB811 (OB42)	(Lun <i>et al.</i> , 1992; Carnes <i>et al.</i> , 2015)	Tev	A	Buffalo	China
RE091	(Echodu <i>et al.</i> , 2015)	Tbb		Porcine	Uganda
RE133	(Echodu <i>et al.</i> , 2015)	Tbb		Porcine	Uganda
RE086	(Echodu <i>et al.</i> , 2015)	Tbb		Porcine	Uganda
UTRO2509	(Echodu <i>et al.</i> , 2015)	Tbb		Human	Uganda
UTRO2516	(Echodu <i>et al.</i> , 2015)	Tbb		Human	Uganda
RE042	(Echodu <i>et al.</i> , 2015)	Tbr		Human	Uganda
OB21	(Balmer <i>et al.</i> , 2011)	Tbr		<i>Glossina pallidipes</i>	Uganda
F783	(Balmer <i>et al.</i> , 2011)	Tbb		n/a	Uganda
K2355	(Gibson <i>et al.</i> , 2015)	Tbr		Human	Uganda
OB091	(Balmer <i>et al.</i> , 2011)	Tbb		n/a	Uganda
OB59	(Balmer <i>et al.</i> , 2011)	Tbb		Lion	Tanzania
OB71	(Balmer <i>et al.</i> , 2011)	Tbb		Lion	Tanzania
OB67	(Balmer <i>et al.</i> , 2011)	Tbb		Lion	Tanzania
OB63	(Balmer <i>et al.</i> , 2011)	Tbb		Lion	Tanzania
OB68	(Balmer <i>et al.</i> , 2011)	Tbb		Lion	Tanzania
OB61	(Balmer <i>et al.</i> , 2011)	Tbb		Lion	Tanzania
OB52	(Balmer <i>et al.</i> , 2011)	Tbb		n/a	Kenya
OB74	(Balmer <i>et al.</i> , 2011)	Tbb		Lion	Tanzania
OB69	(Balmer <i>et al.</i> , 2011)	Tbb		Lion	Tanzania
cp12	(Balmer <i>et al.</i> , 2011)	Tbb		Cow	Kenya
cp16	(Balmer <i>et al.</i> , 2011)	Tbb		<i>Glossina pallidipes</i>	Kenya
OB70	(Balmer <i>et al.</i> , 2011)	Tbb		Lion	Tanzania
OB76	(Balmer <i>et al.</i> , 2011)	Tbb		Lion	Tanzania
OB62	(Balmer <i>et al.</i> , 2011)	Tbb		Lion	Tanzania
OB72	(Balmer <i>et al.</i> , 2011)	Tbb		Lion	Tanzania
cp13	(Balmer <i>et al.</i> , 2011)	Tbb		Cow	Kenya
cp6	(Balmer <i>et al.</i> , 2011)	Tbb		Lion	Zambia
cp17	(Balmer <i>et al.</i> , 2011)	Tbb		Cow	Kenya

cp24	(Balmer <i>et al.</i> , 2011)	Tbb	Giraffe	Zambia
cp29	(Balmer <i>et al.</i> , 2011)	Tbb	<i>Glossina morsitans</i>	Zambia
cp15	(Balmer <i>et al.</i> , 2011)	Tbb	<i>Glossina pallidipes</i>	Kenya
cp5	(Balmer <i>et al.</i> , 2011)	Tbb	<i>Glossina pallidipes</i>	Kenya
cp14	(Balmer <i>et al.</i> , 2011)	Tbb	<i>Glossina pallidipes</i>	Kenya
OB58	(Balmer <i>et al.</i> , 2011)	Tbb	Kongoni	Uganda
OB56	(Balmer <i>et al.</i> , 2011)	Tbb	Hyena	Tanzania
OB54	(Balmer <i>et al.</i> , 2011)	Tbr	Lion	Tanzania
OB53	(Balmer <i>et al.</i> , 2011)	Tbr	n/a	Tanzania
OB57	(Balmer <i>et al.</i> , 2011)	Tbr	Hyena	Tanzania
OB31	(Balmer <i>et al.</i> , 2011)	Tbb	Bovine	Somalia
OB10	(Balmer <i>et al.</i> , 2011)	Tbb	Kongoni	Tanzania
cp19	(Balmer <i>et al.</i> , 2011)	Tbb	Sheep	Kenya
OB027	(Balmer <i>et al.</i> , 2011)	Tbr	Human	Uganda
cp26	(Balmer <i>et al.</i> , 2011)	Tbb	<i>Glossina pallidipes</i>	Zambia
cp7	(Balmer <i>et al.</i> , 2011)	Tbb	Hyena	Zambia
cp27	(Balmer <i>et al.</i> , 2011)	Tbb	<i>Glossina morsitans</i>	Zambia
OB30	(Balmer <i>et al.</i> , 2011)	Tbb	<i>Glossina fuscipes</i>	Uganda
OB088	(Balmer <i>et al.</i> , 2011)	Tbb	<i>Glossina pallidipes</i>	Kenya
OB22	(Balmer <i>et al.</i> , 2011)	Tbr	Human	Tanzania
OB051	(Balmer <i>et al.</i> , 2011)	Tbb	Hippo	Uganda
OB64	(Balmer <i>et al.</i> , 2011)	Tbb	Kongoni	Tanzania
OB55	(Balmer <i>et al.</i> , 2011)	Tbb	Hyena	Tanzania
OB078	(Balmer <i>et al.</i> , 2011)	Tbr	Human	Kenya
OB066	(Balmer <i>et al.</i> , 2011)	Tbr	Kongoni	Tanzania
STIB366	(Balmer <i>et al.</i> , 2011)	Tbb	n/a	Uganda
OB75	(Balmer <i>et al.</i> , 2011)	Tbb	Hyena	Tanzania
OB65	(Balmer <i>et al.</i> , 2011)	Tbr	Kongoni	Tanzania
OB60	(Balmer <i>et al.</i> , 2011)	Tbb	Lion	Tanzania
OB153	(Balmer <i>et al.</i> , 2011)	Tbb	Porcine	Cameroon
OB155	(Balmer <i>et al.</i> , 2011)	Tbb	Porcine	Cameroon
OB095	(Balmer <i>et al.</i> , 2011)	Tbr	n/a	Ethiopia
OB006	(Balmer <i>et al.</i> , 2011)	Tbr	Human	Uganda
OB113	(Balmer <i>et al.</i> , 2011)	Tbb	Ox	Burkina Faso
cp8	(Balmer <i>et al.</i> , 2011)	Tbb	Cow	Uganda
OB026	(Balmer <i>et al.</i> , 2011)	Tbr	Human	Ethiopia
OB12	(Balmer <i>et al.</i> , 2011)	Tbb	Kongoni	Tanzania
OB024	(Balmer <i>et al.</i> , 2011)	Tbr	Human	Kenya

Provided are details showing sample ID, strain isolated with source and reference, kinetoplast DNA (kDNA) type, n/a indicates host of isolation is unknown, host of isolation and the locality of origin

To provide a spatial breadth to the study and to be able to connect it with previous microsatellite analyses, 66 *T. b. brucei* and *T. b. rhodesiense* isolates were also included (Table 3.3) from across sub-Saharan Africa that have also been extensively characterized (Balmer *et al.*, 2011; Carnes *et al.*, 2015; Echodu *et al.*, 2015). These isolates included at least one representative from each of the genetic clusters previously identified in sub-Saharan Africa (Balmer *et al.*, 2011). Thus, the final sample set consisted of 107 *T. brucei* and *T. evansi* isolates, including four from buffalo in Asia and 103 from a variety of mammalian hosts in Africa, with a special focus on isolates from camels (Table 3.2) and wildlife (Table 3.3) in Kenya.

3.3.2 DNA extractions and PCR based diagnostic tests

DNA was extracted from all isolates using Qiagen DNeasy Blood and Tissue Kit (Qiagen, Germany), following manufacturer's protocols. To further classify presumptive *T. evansi* samples not previously well classified (Njiru *et al.*, 2005), a set of four diagnostic PCR tests for 37 isolates was carried out, including the 34 strains for which certain classification was not available (Table 3.2). For spatial expansion PCR tests were conducted for 17 isolates

Table 3. 4: Sample details and PCR assay results of *T. evansi* (Tev) and *T. equiperdum* (Teq) genotyped for this study

Sample ID	Taxon ^{source, refs}	kDNA type	PCR assay results				Host	Locality of origin	Year of isolation
			ITS 1	SR A	RoT at1.2	A281del			
OVI	Teq [1]	Unkn.	+	-	-	-	Horse	South Africa	1975
BoTat1.1	Teq [1]	Unkn.	+	-	-	-	Horse	Morocco	1924
Canadian	Teq [1]	Unkn.	+	-	+	-	Horse	Canada	Unkn.
ATCC30019	Teq [1]	A†	+	-	+	+	Horse	France	1903
STIB 818	Teq [1]	A†	+	-	+	+	Horse	Beijing, China	1979
RoTat1.2	Tev [1]	A†	+	-	+	+	Water	Indonesia	1982
STIB 806K	Tev ^b [1]	A†	+	-	+	+	Unkn.	China	1983
STIB 811	Tev ^b [1]	A†	+	-	+	+	Buffalo	Hunan Province,	1982
KETRI3793	Tev ^a	Unkn.	+	-	-	-	Camel	Laikipia, Kenya	1995
KETRI2444	Tev ^a	A†	+	-	-	+	Camel	Kulal, Kenya	1979
KETRI3558	Tev ^a [2]	A†	+	-	+	+	Camel	Isiolo, Kenya	1994
C13	Tev [5]	A†	+	-	+	+	Camel	Kenya	1981
KETRI3576	Tev ^a [2]	Unkn.	+	-	+	-	Camel	Ngurunit, Kenya	1994
KETRI3557	Tev ^a [2]	Unkn.	+	-	+	-	Camel	Isiolo, Kenya	1994
KETRI3552	Tev ^a [2]	Unkn.	+	-	+	-	Camel	Isiolo, Kenya	1994
STIB 708	Tev ^a [3]	Unkn.	+	-	+	-	Camel	Malindi, Kenya	1982
KETRI2479**	Tev ^a	B†	+	-	-	-	Camel	Ngurunit, Kenya	1979

† kDNA type based on A281del PCR assay alone

^a Kenya Trypanosomiasis Research Institute

^b Swiss Tropical Institute Basel

** high virulence

Tev *T. evansi*

Teq *T. equiperdum*

1 (Claes *et al.*, 2002)

2 (Njiru and Constantine, 2007)

3 (Balmer *et al.*, 2011)

4 (Borst *et al.*, 1987)

5 (Gibson *et al.*, 1983)

6 (Goudet, 1995)

Table showing sample ID, strain isolated with source and reference, kinetoplast DNA (kDNA) type, PCR assay results (ITS1 + indicates pathogenic African trypanosome, SRA – indicates not *T. b. rhodesiense*, RoTat 1.2 + indicates serological diagnostic antigen variant, A281del + indicates deletion of a GTC (Ala) triplet in F₀F₁-ATPase subunit γ unique to *T. evansi* isolates of kDNA type A, n/a indicates failure of the positive PCR control), host of isolation, the locality of origin and year of isolation.

First, PCR amplification of a 480 bp fragment of the Internal Transcribed Spacer (ITS1) of the ribosomal DNA was used (Njiru *et al.*, 2005), to confirm all strains were pathogenic African trypanosomes. PCR amplification of a 284 bp fragment of the serum resistance-associated (SRA) gene (Radwanska *et al.*, 2002) was then used, to confirm strains that were not *T. b. rhodesiense*.

Then, a PCR assay was performed to identify strains with VSG antigen type RoTat 1.2, used in serological and PCR-based diagnosis, that targets a 488 bp fragment of the RoTat 1.2 variant, as per previous protocol (Urakawa *et al.*, 2001). Although this gene occurs in most *T. evansi* type A (Ngaira *et al.*, 2005; Urakawa *et al.*, 2001), *T. evansi* type B and some *T. evansi* type A strains may not have it (Ngaira *et al.*, 2004; Ngaira *et al.*, 2005). In addition, *T. evansi* strains can lose the kinetoplast entirely (Carnes *et al.*, 2015) which would lead to a false negative result in a diagnostic PCR assay for type A minicircles. Thus, as an alternative to identify type A *T. evansi*, a novel PCR assay was designed. This assay targets a 3-bp deletion (GTC codon, corresponding to alanine 281) in the nuclear encoded subunit γ (systematic TriTrypDB ID Tb927.10.180) of the mitochondrial F₀F₁-ATPase. This deletion is unique to all *T. evansi* type A screened so far and to some closely related strains that had been classified as *T. equiperdum* (Carnes *et al.*, 2015). This mutation is critical to compensate for loss of functional kinetoplast DNA in this group of *T. evansi*/*T. equiperdum* (Dean *et al.*, 2013). The assay consisted of two PCR reactions, a diagnostic and a control PCR reaction (Figure 3.3).

1a = *T. evansi* type A (e.g. STIB805), allele a
1b = *T. evansi* type A (e.g. STIB805), allele b (A281del)
2a = other trypanozoon (e.g. *T. b. brucei* Lister 427), allele a
2a = other trypanozoon (e.g. *T. b. brucei* Lister 427), allele b

```

1a ATGTCGGGCAAGCTTCGTCCTTACAAAGAAAACTTGAGGGGTACAACCGGTTTACTCTATCGTTAAAACATTAAGAT 80
1b ATGTCGGGCAAGCTTCGTCCTTACAAAGAAAACTTGAGGGGTACAACCGGTTTACTCTATCGTTAAAACATTAAGAT 80
2a ATGTCGGGCAAGCTTCGTCCTTACAAAGAAAACTTGAGGGGTACAACCGGTTTACTCTATCGTTAAAACATTAAGAT 80
2b ATGTCGGGCAAGCTTCGTCCTTACAAAGAAAACTTGAGGGGTACAACCGGTTTACTCTATCGTTAAAACATTAAGAT 80
5'-ATGTCGGGCAAGCTT (primer F1)

1a GGTGACTTTGGCAAAGTATCGTGC GGCGCAGGGACGGATAAGGACACGCGATTTACGCTCTGCTATACGGAGTTGGCGT 160
1b GGTGACTTTGGCAAAGTATCGTGC GGCGCAGGGACGGATAAGGACACGCGATTTACGCTCTGCTATACGGAGTTGGCGT 160
2a GGTGACTTTGGCAAAGTATCGTGC GGCGCAGGGACGGATAAGGACACGCGATTTACGCTCTGCTATACGGAGTTGGCGT 160
2b GGTGACTTTGGCAAAGTATCGTGC GGCGCAGGGACGGATAAGGACACGCGATTTACGCTCTGCTATACGGAGTTGGCGT 160

1a TCAGCAAACCACAAGCATCGAGAGATGCCGTGGTTCGACGCAAGAAATGCCCTTGTTTACATACCGATAAATACGAATCGT 240
1b TCAGCAAACCACAAGCATCGAGAGATGCCGTGGTTCGACGCAAGAAATGCCCTTGTTTACATACCGATAAATACGAATCGT 240
2a TCAGCAAACCACAAGCATCGAGAGATGCCGTGGTTCGACGCAAGAAATGCCCTTGTTTACATACCGATAAATACGAATCGT 240
2b TCAGCAAACCACAAGCATCGAGAGATGCCGTGGTTCGACGCAAGAAATGCCCTTGTTTACATACCGATAAATACGAATCGT 240

1a GGGTCATGCGGTGCCCTGAACAGCAATATTGTGCGTGTGATCGATTCCGTGGTGTGCGAGTAAGATGGTATTGATGCCGGT 320
1b GGGTCATGCGGTGCCCTGAACAGCAATATTGTGCGTGTGATCGATTCCGTGGTGTGCGAGTAAGATGGTATTGATGCCGGT 320
2a GGGTCATGCGGTGCCCTGAACAGCAATATTGTGCGTGTGATCGATTCCGTGGTGTGCGAGTAAGATGGTATTGATGCCGGT 320
2b GGGTCATGCGGTGCCCTGAACAGCAATATTGTGCGTGTGATCGATTCCGTGGTGTGCGAGTAAGATGGTATTGATGCCGGT 320

1a TGGCAAACGTTGGTATAGACTCGTTTTCTAAACTGTATCCCGATGAATTCAGATACGGTATCATTAACGATATGAAGGAAT 400
1b TGGCAAACGTTGGTATAGACTCGTTTTCTAAACTGTATCCCGATGAATTCAGATACGGTATCATTAACGATATGAAGGAAT 400
2a CGGCAAACGTTGGTATAGACTCGTTTTCTAAACTGTATCCCGATGAATTCAGATACGGTATCATTAACGATATGAAGGAAT 400
2b TGGCAAACGTTGGTATAGACTCGTTTTCTAAACTGTATCCCGATGAATTCAGATACGGTATCATTAACGATATGAAGGAAT 400

1a CAATGCATTTTGGTTATGCAACCTTTGTAATTGAAAATGCATATGAAGTGTCCAAGGATGCGGATCGGTATCAGGTGATT 480
1b CAATGCATTTTGGTTATGCAACCTTTGTAATTGAAAATGCATATGAAGTGTCCAAGGATGCGGATCGGTATCAGGTGATT 480
2a CAATGCATTTTGGTTATGCAACCTTTGTAATTGAAAATGCATATGAAGTGTCCAAGGATGCGGATCGGTATCAGGTGATT 480
2b CAATGCATTTTGGTTATGCAACCTTTGTAATTGAAAATGCATATGAAGTGTCCAAGGATGCGGATCGGTATCAGGTGATT 480

1a TTCAATCGTTTCGTTTCTGCGGGTGTCCAAGGAATGCCGTTTACAACATTCATCATATGAGAAGTGGAAGAGGACCT 560
1b TTCAATCGTTTCGTTTCTGCGGGTGTCCAAGGAATGCCGTTTACAACATTCATCATATGAGAAGTGGAAGAGGACCT 560
2a TTCAATCGTTTCGTTTCTGCGGGTGTCCAAGGAATGCCGTTTACAACATTCATCATATGAGAAGTGGAAGAGGACCT 560
2b TTCAATCGTTTCGTTTCTGCGGGTGTCCAAGGAATGCCGTTTACAACATTCATCATATGAGAAGTGGAAGAGGACCT 560

1a TGCCGATGCCGCTAGCTCGGACAACCAGAAGAATCGTTACCTTTTTGCGAATGCGCTGCAGAATGAGGAGGAACAGCTTA 640
1b TGCCGATGCCGCTAGCTCGGACAACCAGAAGAATCGTTACCTTTTTGCGAATGCGCTGCAGAATGAGGAGGAACAGCTTA 640
2a TGCCGATGCCGCTAGCTCGGACAACCAGAAGAATCGTTACCTTTTTGCGAATGCGCTGCAGAATGAGGAGGAACAGCTTA 640
2b TGCCGATGCCGCTAGCTCGGACAACCAGAAGAATCGTTACCTTTTTGCGAATGCGCTGCAGAATGAGGAGGAACAGCTTA 640

1a TTCGGGACTTCTTTGATTTTCATGCTGCGCTCGCGTCTCAATGCCGTTGGAGAAAACGAGCTTCCGAGCAAGCTGCC 720
1b TTCGGGACTTCTTTGATTTTCATGCTGCGCTCGCGTCTCAATGCCGTTGGAGAAAACGAGCTTCCGAGCAAGCTGCC 720
2a TTCGGGACTTCTTTGATTTTCACGCTGCGCTCGCGTCTCAATGCCGTTGGAGAAAACGAGCTTCCGAGCAAGCTGCC 720
2b TTCGGGACTTCTTTGATTTTCACGCTGCGCTCGCGTCTCAATGCCGTTGGAGAAAACGAGCTTCCGAGCAAGCTGCC 720

1a CGTCTGGTTGCTGTTGAGGGTCAGTTGACTAATATCAGCAGCCTGCAACAGAGAACTAGCTCGCTTTACAACAAGACACG 800
1b CGTCTGGTTGCTGTTGAGGGTCAGTTGACTAATATCAGCAGCCTGCAACAGAGAACTAGCTCGCTTTACAACAAGACACG 800
2a CGTCTGGTTGCTGTTGAGGGTCAGTTGACTAATATCAGCAGCCTGCAACAGAGAACTAGCTCGCTTTACAACAAGACACG 800
2b CGTCTGGTTGCTGTTGAGGGTCAGTTGACTAATATCAGCAGCCTGCAACAGAGAACTAGCTCGCTTTACAACAAGACACG 800

1a GCAGTTTGGTATTACGGCGGCGCTAATTGAAATCTTTCT--ATGAGTTCGTTGGAAGGCA 859
1b GCAGTTTGGTATTACGGCGGCGCTAATTGAAATCTTTCTTCTGCTATGAGTTCGTTGGAAGGCA 863
2a GCAGTTTGGTATTACGGCGGCGCTAATTGAAATCTTTCTGCTATGAGTTCGTTGGAAGGCA 863
2b GCAGTTTGGTATTACGGCGGCGCTAATTGAAATCTTTCTGCTATGAGTTCGTTGGAAGGCA 863

```

||||| |||||

AAAGA---TACTCAAGCAACCTT-5' (R1 = A281del specific)

||||| |||||

TACTCAAGCAACCTTCCGT-5' (R2 = +ve control)

Figure 3. 3: Diagnostic PCR for the GCT/Ala281 deletion in F1FO-ATP synthase subunit γ in *T. evansi* type A. Shown are nucleotides 1–859 (GCT deletion) and 1–863 (‘wild type’), respectively, of gene *TevSTIB805.10.220* / *Tb427.10.180* (systematic TriTrypDB.org IDs). Primer combination F1/R1 will give an 855-bp amplicon if the deletion is present. Primer combination F1/R2 will give an 863-bp amplicon for most if not all isolates from the group of 5 closely related named taxa includes *T. evansi* (also known as subgenus *Trypanozoon*).

The diagnostic reaction (using primer combination F1/R1) is designed to amplify an 855 bp fragment of F₀F₁-ATPase subunit γ , if at least one allele in the strain has this 3-bp deletion (named A281del). The control PCR reaction (using primer combination F1/R2) amplifies an 863 bp long fragment of the same region, regardless of kDNA type. Both PCR reactions were carried out in 10 μ l volumes consisting of 5 μ l 2X Type-It (Qiagen), 0.25 μ M of each primer, 10 ng of genomic DNA and dH₂O. A touchdown thermal cycling protocol included a 5min initial denaturation at 95 °C, 10 cycles touchdown (95 °C for 30 sec, 50 °C minus 1 °C per cycle for 30 sec, and 72 °C for 1 min), and 30 cycles amplification (95 °C for 30 sec, 40 °C for 30 sec, and 72 °C for 1 min), followed by a 7 min final extension period. All PCR runs included the isolates RoTat1.2 (OB106), a *T. evansi* type A, and cp24, a *T. b. brucei* from (Balmer *et al.*, 2011), as positive and negative controls, respectively (Table 3.2).

3.3.3 Microsatellite genotyping

Fifteen microsatellite loci validated in previous studies and using the same previously published protocols were used extensively (Balmer *et al.*, 2006; Siström *et al.*, 2013). Primer sequences were present for amplification and chromosomal locations (Table 3.5).

Table 3. 5: PCR primers used in microsatellite marker amplification

Locus	Forward Primer	Reverse Primer	Motif	Size	Location	Source
TB8/11	[FAM]- TGTAGCAGTGG TACGCAC	CACCCAACGC ATGTAAGC	AT	97–127	8	(Sistrom <i>et al.</i> , 2013)
TB2/19	[HEX]- CTGGTGCGTGT AACTGTG	GAAGTGAGG ACATGCACG	AT	84–104	2	(Balmer <i>et al.</i> ,2006)
TB11/13	[FAM]- CAAGAACTCTG CATTGAGC	ATCTGTTGGC GATGGTGA	AT	125-161	11	(Balmer <i>et al.</i> ,2006)
TB6/7	[HEX]- AAGCTGACAGG TGGTTGA	GAACATGCGT GCGTGTG	AT	104-136	6	(Balmer <i>et al.</i> ,2006)
TB1/8	[FAM]- AGGTTTAGTGC ATGTCGGA	CCTGTTGTAC GGAGGTCA	CA	97-117	1	(Balmer <i>et al.</i> ,2006)
TB5/2	[HEX]- CAACCGAAAGT AAGGGGAAC	TCTCGCCTTC TTTGCCC	AT	83-107	5	(Balmer <i>et al.</i> ,2006)
TB10/5	[FAM]- AAAGGCGATAT GTTATTATTGA	ATTGGGTATA CTGTCCCTCA	TA	79-115	10	(Balmer <i>et al.</i> ,2006)
TB9/6	[HEX]- TGATTCATTGG TTAAGACAGG	AATGATAACT GCGGATTACA C	AC	124-158	9	(Balmer <i>et al.</i> ,2006)
Tryp52	[ALEXA 532]- GCATCATTGAC GTCGACCC	TAACAACCAC TGGGACCGC	GT	201-231	11	(Sistrom <i>et al.</i> , 2013)
Tryp54	[ROX]- AGTCGGCGTGA TGGTACTC	TTCAGCCCAC AAACAACCG	AAAT	144-176	10	(Sistrom <i>et al.</i> , 2013)
Tryp55	[FAM]- AATTCAACCCC AACAGCCC	CTCGTTCAAT GACTTGCCCC	GT	208-246	5	(Sistrom <i>et al.</i> , 2013)
Tryp59	[ALEXA 532]- GAGGCAATCGC AGTGTGTG	CGCACGTTTC ACCATCCTC	GT	209-225	9	(Sistrom <i>et al.</i> , 2013)
Tryp62	[ROX]- AAGGCGACCAA CTTCAACC	GTTGTCATCG GCTTGCTCC	AC	153-177	11	(Sistrom <i>et al.</i> , 2013)
Tryp65	[ALEXA 546]- GGAGGTAAACT TGATTCGGGTG	ACGACAACA GCGACAAAG C	ATT	207-234	9	(Sistrom <i>et al.</i> , 2013)
Tryp67	[FAM]- GTTGCTGAGGT GCAACTGG	GTCGTCAGGC ACCAAACG	GTT	151-178	7	(Sistrom <i>et al.</i> , 2013)

Table with general information about the motif, size range in bp (size), chromosome location (location), and source of the protocol used.

Amplifications were performed with fluorescently-labelled forward primers (6-FAM and HEX) using a standard PCR in 13 μ l reaction volumes containing 1 μ l of genomic DNA at approximately 100 ng/ μ l of genomic DNA, 5 μ l of Type-it Master Mix (Qiagen, Germany) and 1 μ l each of forward and reverse primers (10 μ M starting concentration). PCR products were then multiplexed, combined with size standard (Applied Biosystems ROX500) and highly deionized formamide, and genotyped on an ABI 3730xl DNA Analyzer (Applied Biosystems Inc, USA) at the DNA Analysis Facility on Science Hill at Yale University (<http://dna-analysis.yale.edu/>). Alleles were scored using the program GeneMarker v 2.4.0 (Soft Genetics, State College, PA, USA) with manual editing of the automatically scored peaks.

3.3.4 Identification of distinct genetic clusters

To evaluate evolutionarily distinct genetic clusters within the dataset, all 107 *T. b. brucei*, *T. b. rhodesiense*, and *T. evansi* strains were included in Bayesian cluster analyses using STRUCTURE v2.3.4 (Pritchard *et al.*, 2000). STRUCTURE runs indicated a K value (number of clusters) of less than ten. Thus, 20 runs were performed with a burn-in of 5,000 and a total of 250,000 iterations to assess the optimal K value with the Evanno method (Evanno *et al.*, 2005), using the Clustering Markov Packager Across K (CLUMPAK) (Goudet, 1995). For final assignments of strains to clusters, 10 runs were performed for K values one through ten with a burn in of 50,000 and 250,000 iterations. Each strain was assessed for probability of assignment (Q) to each of the K clusters identified in the STRUCTURE analysis. The current analyses considered $Q > 0.80$ as a “certain assignment”, and $Q < 0.80$ as an “uncertain assignment”. Evolutionary relationships were further evaluated and the level of genetic differentiation among and within *T. evansi* and *T. brucei* genetic

clusters and strains of uncertain assignment using principal components analysis (PCA) of microsatellite data in the “adeget” package in R v3.0.2 (R Development Core Team). The centroid and region encompassing 95% of the variance observed within *T. brucei* subgroups was identified in the STRUCTURE analysis.

3.3.5 Estimating levels of genetic diversity and differentiation

In order to compare levels of genetic diversity and differentiation among *T. evansi* strains with that found among *T. brucei* (*T. b. brucei* + *T. b. rhodesiense*) isolates levels of diversity, were estimated within the STRUCTURE defined clusters as well as levels of differentiation between and within clusters. For these analyses, only strains with high probability of assignment ($Q > 0.80$) to STRUCTURE-based clusters at three levels were included: (i) all strains regardless of taxonomy, (ii) *T. brucei* strains only, and (iii) *T. evansi* isolates only.

To understand diversity within clusters at these three levels, allelic richness was estimated (A_R) in FSTAT v1.2 (Goudet, 1995) (Goudet, 2005) observed and expected heterozygosity (H_O and H_E) and the related Fisher’s inbreeding coefficient (F_{IS}) in the R package HIERFSTAT v0.4-10 (Goudet, 2005). To understand patterns of within-cluster genetic distance at these three levels, pairwise genetic distance between strains was calculated using the Reynolds distances (Reynolds *et al.*, 1983). A distance tree was estimated using the UPGMA method implemented in the “PopPR” v2.3.0 package (Kamvar *et al.*, 2014; 2015) in R with 1000 bootstrap replicates. Significant differences was then tested in within-cluster genetic distances with an analysis of variance (ANOVA) followed by a Tukey-Kramer HSD test performed in JMP v11.2 (SAS Institute Inc., Cary, NC, USA, 1989– 2012). Finally, to understand patterns of among-cluster differentiation at the same three levels, pairwise F_{ST} was estimated in ARLEQUIN v.3.5 (Wright, 1951) with Wright’s statistics (Wright, 1951), following the variance method (Claes *et al.*, 2002), using 10,000 permutations, 1,000,000 Markov chain steps, and 10,000 dememorization steps to obtain exact p-values.

3.4 Estimating levels of genetic diversity for spatial expansion of *T. evansi*

In order to compare levels of genetic diversity within each named subspecies (*T. b. brucei*, *T. b. rhodesiense*, *T. evansi*, and *T. equiperdum*), the allelic richness (A_R) in FSTAT v1.2 (Goudet, 2005), observed and expected heterozygosity (H_O and H_E) and the related Fisher's inbreeding coefficient (F_{IS}) in the R package HIERFSTAT v0.4-10 (Goudet, 2005) was estimated.

CHAPTER FOUR

RESULTS

4.1 Comparison of virulence in mice model of selected *T. evansi* isolates

4.1.1 Parasitaemia profiles and survival of infected mice

Following inoculation of groups of mice with 17 different *T. evansi* isolates, the parasites were detected in tail blood within 1-3 days with rapid rise in parasitaemia, attaining peak within 3 days [Figures 4.1(A-I) and 4.2(A-H)]. Based on parasitaemia profiles and survival of the animals following infection, three distinct virulent groups were identified that consisted of 1) low, exhibiting high intermittent parasitaemia, survival 31-60 days post infection (dpi), 2) moderate, exhibiting high persistent parasitaemia, survival 11-30 dpi; and 3) high, exhibiting high persistent parasitaemia, survival period 0-10 dpi. Animals in the high virulent group died before any clinical signs were manifested (Table 4.1).

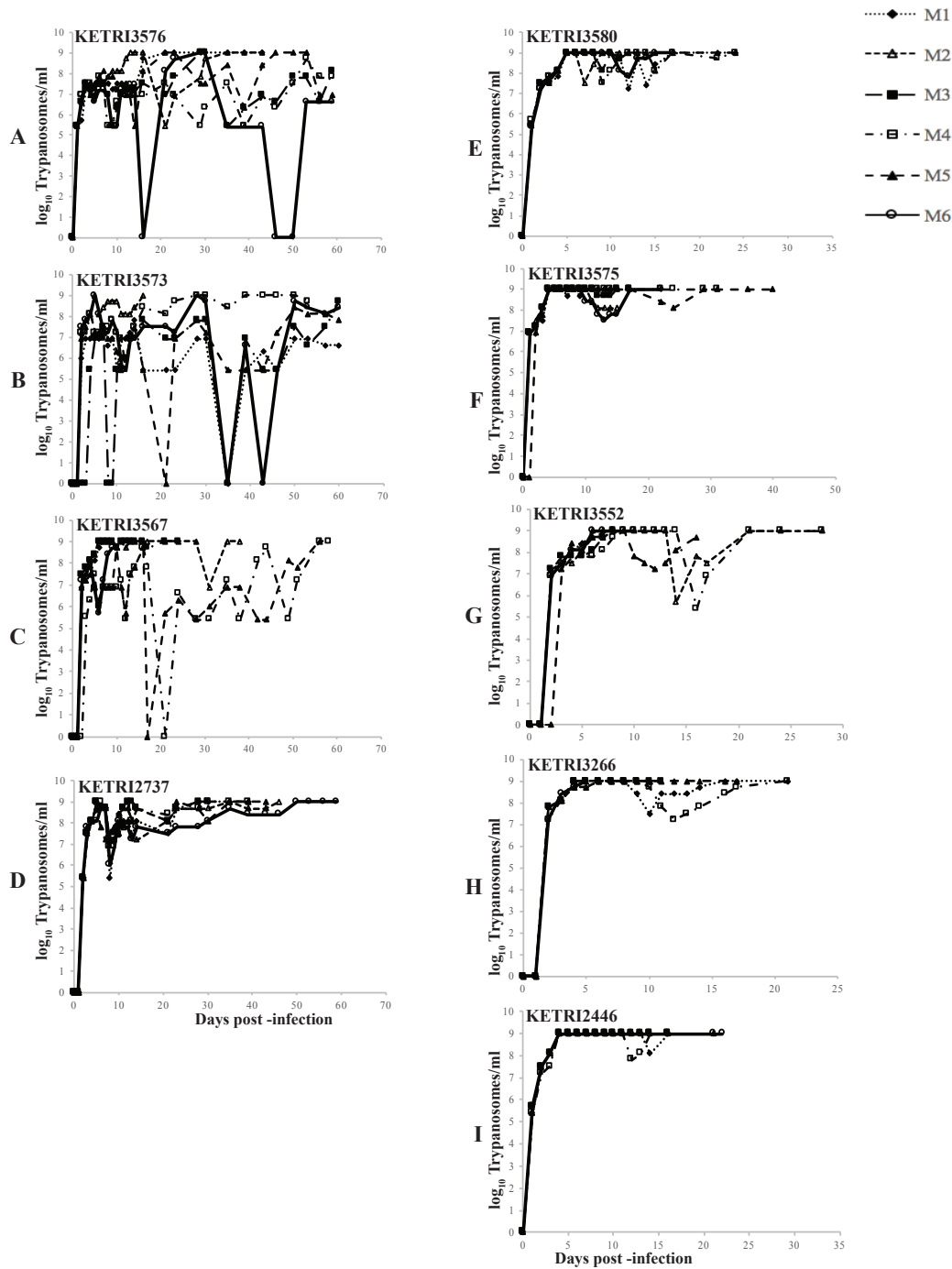


Figure 4. 1: Parasitaemia profiles of individual mice infected with low and moderate virulence *T. evansi*. (A-D) Parasitaemia profiles of individual mice infected with low virulence *Trypanosoma evansi* isolates; KETRI 3576, 3573, 3567 and 2737. (M=mouse). (E-I) Parasitaemia profiles of mice infected with moderate virulence *Trypanosoma evansi* isolates; KETRI 3580, 3575, 3552, 3266 and 2446. (M = mouse).

Table 4. 1: Sample details of *T. evansi* phenotyped for this study

Isolate ID ^{source}	Locality of origin	Host	Year of isolation	kDNA Type	Average survival time (range dpi;n=6)	Virulence levels
KETRI 3576 ^a	Ngurunit, Kenya	Camel	1994	A	55.33(44-60)	Low
KETRI 3573 ^a	Ngurunit, Kenya	Camel	1994	A	52.17(18-60)	Low
KETRI 2737 ^a	Galana, Kenya	Camel	1985	A	43.83(32-60)	Low
KETRI 3567 ^a	Athiriver, Kenya	Camel	1994	A	33.83(10-60)	Low
KETRI 3575 ^a	Ngurunit, Kenya	Camel	1994	A	26.83(16-40)	moderate
KETRI 3580 ^a	Loglogo, Kenya	Camel	1994	A	20.67(12-27)	moderate
KETRI 2446 ^a	Marsabit, Kenya	Camel	1979	A	17.5 (11-24)	moderate
KETRI 3552 ^a	Isiolo, Kenya	Camel	1994	A	17.17(9-29)	moderate
KETRI 3266 ^a	Samburu, Kenya	Camel	1990	A	15.67(6-22)	moderate
KETRI 4035 ^b	Colombia	Horse	1973	A	10.83(9-18)	High
KETRI 2479 ^a	Ngurunit, Kenya	Camel	1979	B	10.17(8-15)	High
KETRI 4036 ^b	Kazakhstan	Bactrian camel	1995	A	6.33(5-7)	High
KETRI 4039 ^b	China	Water buffalo	1983	A	5.83(5-7)	High
KETRI 4034 ^b	Brazil	Dog	1986	A	5.83(5-6)	High
KETRI 4038 ^b	Indonesia	Water buffalo	1982	A	5.00(5)	High
KETRI 4040 ^b	Vietnam	Water buffalo	1998	A	5.00 (5)	High
KETRI 4037 ^b	Philippines	Water buffalo	1996	A	4.5 (4-5)	High

^a Kenya Trypanosomiasis Research Institute

n= number of infected mice

Dpi= days post infection

Table showing sample ID, strain isolated with source and reference, kinetoplast DNA (kDNA) type, virulence levels based on survival of infected Swiss White mice following infection, locality of origin, host of isolation, and the year of isolation.

Three of four isolates (KETRI 3576, 3573, 3567) classified as of low virulence exhibited high intermittent parasitaemia, with more than one parasitaemia wave in some animals (Figures 4.1A-D). Highest parasitaemia score attained was 1×10^9 trypanosomes/ml where each mouse attained this score at least once in the first ten dpi. The mean survival period of mice in this group ranged between 31 to 60 dpi. Significant differences ($p < 0.001$) in parasitaemia profiles were observed between individual animals infected with same isolate and between isolates (Table 4.2).

Table 4. 2: Comparison of mean parasitaemia values between various *Trypanosoma evansi* isolates following infection of mice at different virulence levels.

Country of origin	Isolate ID	Virulence	Mean
Kenya	KETRI 3575	Moderate	8.0±0.08 a
Kenya	KETRI 3580	Moderate	7.8±0.17 ab
Kenya	KETRI 2446	Moderate	7.8±0.15 ab
Kenya	KETRI 3266	High	7.5±0.1 bc
Kenya	KETRI 2737	Low	7.4±0.03 bc
Kenya	KETRI 2479	High	7.1±0.16 cd
Philippines	KETRI 4035	High	7.1±0.17 cd
Kenya	KETRI 3552	Moderate	6.8±0.24 de
Kenya	KETRI 3576	Low	6.8±0.15 de
Kenya	KETRI 3567	Low	6.7±0.37 def
Vietnam	KETRI 4039	High	6.6±0.09 efg
Kazakhstan	KETRI 4038	High	6.2±0.06 fgh
Kenya	KETRI 3573	Low	6.1±0.39 gh
Indonesia	KETRI 4040	High	6.1±0.1 gh
Swiss	KETRI 4037	High	6.0±0.13 h
Brazil	KETRI 4036	High	5.2±0.21 i
Colombia	KETRI 4034	High	5.0±0.04 i
LSD	0.53		
CV (%)	6.8		

NB: Means followed by the same letter do not significantly differ ($p < 0.001$).

Whereas three of the four isolates exhibited high intermittent parasitaemia in infected mice, one isolate (KETRI 2737) exhibited high and persistent parasitaemia (Figure 4.1D). Differences at individual animal level were not observed with this particular isolate.

In contrast, high persistent parasitaemia with peak score of 9.0 was recorded in mice infected with KETRI 2446, 3266, 3552, 3575 and 3580 isolates (Figure 4.1E to I). The pre-patent period ranged between 1-3 days with the animals surviving for periods ranging between 10-30 days. There were no significant differences in parasitaemia profiles ($p=0.05$) between individual animals infected with any of the isolates in this group except KETRI 3552, whose profile was significantly different from the rest of the isolates (Table 4.2). These isolates were classified as moderate virulence (Figure 4.1E to I).

Animals infected with one isolate from Kenya (Type B; KETRI 2479) and six from Asia and South America (KETRI 4034, 4035, 4036, 4037, 4038, 4039, 4040) exhibited very high

persistent parasitaemia, however, this was of a shorter duration when compared to the moderate virulence group. Pre-patent periods were similar to those observed in the low and moderate virulence groups, with maximum survival period of ten dpi. Significant differences ($p < 0.05$) were observed between isolates of this group (Figure 4.2A to H) and were classified as high virulence.

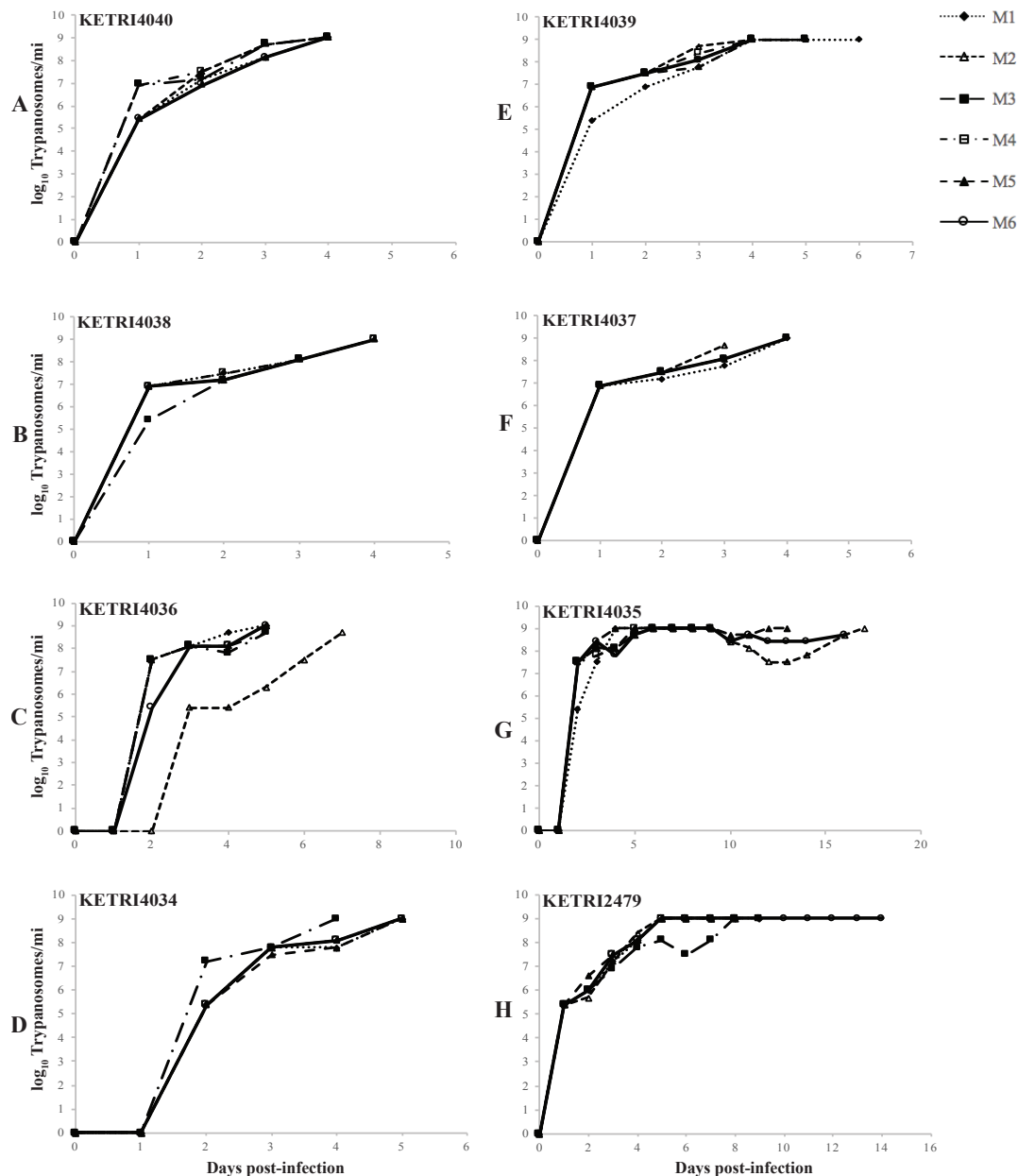


Figure 4. 2: Parasitaemia profiles of individual mice infected with high virulence (A-H). Parasitaemia profiles of individual mice infected with high virulence *Trypanosoma evansi* isolates; KETRI 4040, 4038, 4036, 4034, 4039, 4037, 4035 and 2479. (M = mouse).

Comparison of pre-patent periods showed that all animals were detected positive (with parasites in the peripheral blood) by microscopy between 1-3 days of infection with high parasitaemia score of 1×10^9 trypanosomes/ml attained at least once within 10 days. There were significant differences ($p < 0.05$) in parasitaemia scores between the three groups. Four of five isolates classified as moderately virulent had a mean log parasitaemia score above 7.5 (range 7.8 ± 0.15 - 8.0 ± 0.08), three of four low virulent isolates with a mean log score above 6.5 (range 6.7 ± 0.37 - 7.4 ± 0.03) while six of nine high virulent isolates had a mean log score of approximately 6.5 and below (range 5.0 ± 0.04 - 6.6 ± 0.09). These results show that the mean parasitaemia scores of the high virulent isolates were low with high death rates recorded within a short period when compared to the moderate and low virulent parasites. This observation demonstrated that the *T. evansi* isolates investigated for virulence had different outcomes related to parasitaemia score and survival of infected mice. Of importance to note was that very high parasitaemia scores (above 7.0) were not always associated with short survival of the infected animals (Figures 4.1E to I and 4.2A to H).

4.1.2 Survival

Survival curves are shown in Figures 4.3A, 4.3B and 4.3C, depicting the fraction of animals alive from the time of parasite inoculation (time 0; Figure 4.3A). Among the low virulence group isolate, KETRI 2737 depicted four successful event times (survival) when compared to two event times for animals infected with KETRI 3573 (high and intermittent parasitaemia).

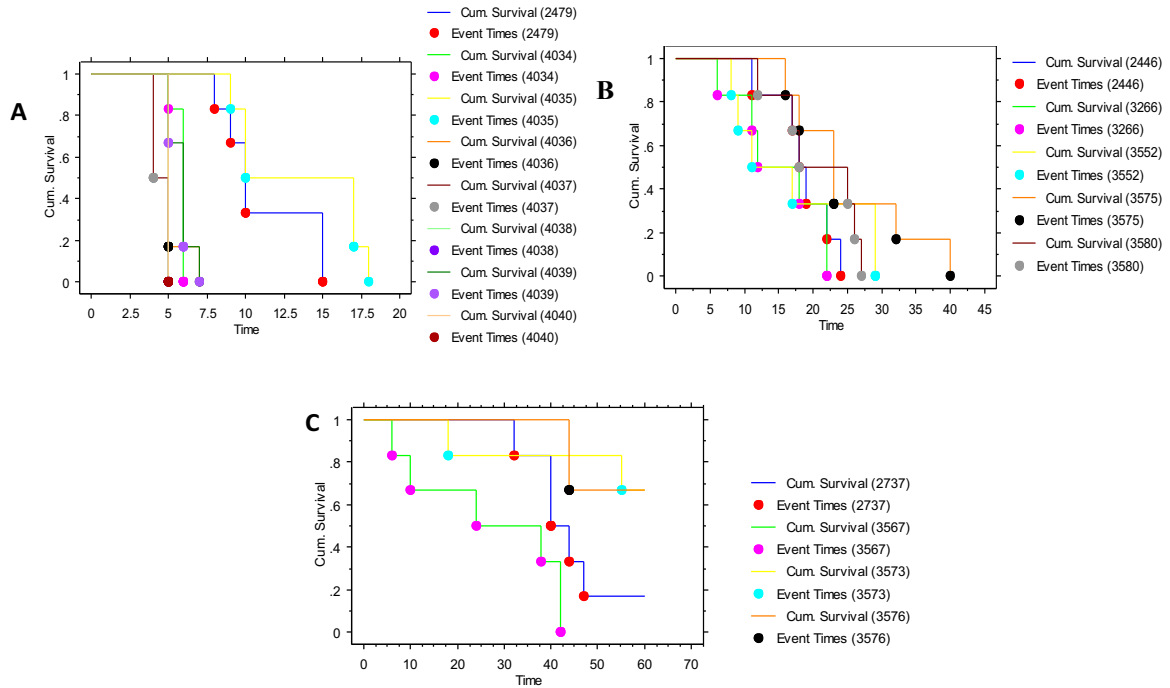


Figure 4. 3: Survival curves depicting the fraction of animals alive from the time (0) of parasite inoculation: (A) Survival curves of *Trypanosoma evansi* isolates of high virulence. (B) Survival curves of *Trypanosoma evansi* isolates of medium virulence. (C) Survival curves of *Trypanosoma evansi* isolates of low virulence.

Log rank p and the Wilcoxon p-values are provided in Table 4.3. Both the log rank and the Wilcoxon p values obtained for the low virulence and high virulence showed significant differences ($p < 0.01$) in survival at both early and later days of infection (Figures 4.1A to D and 4.2A to H).

Table 4. 3: Rank tests for survival time of Swiss White mice infected with *Trypanosoma evansi* isolates of varied virulence obtained from different endemic regions of the world.

Virulence Categories	Rank Test	Chi-square	DF	P-value
Low	Logrank (mantel-Cox)	18.129	3	0.0004
	Breslow-Gehan-Wilcoxon	16.091	3	0.0011
Moderate	Logrank (mantel-Cox)	3.810	3	0.2827
	Breslow-Gehan-Wilcoxon	3.650	3	0.3018
High	Logrank (mantel-Cox)	70.470	8	<0.0001
	Breslow-Gehan-Wilcoxon	56.933	8	<0.0001

Animals infected with parasites of moderate virulence showed significant similarities between individual animals within and between isolates (Figures 4.1E to I).

4.1.3 Packed blood cell volume

The control (non-infected) animals generally maintained their pre-infection PCV values (29.9 ± 0.99) throughout the observation period of 60 days. However, gradual decline in PCV was recorded in mice infected with different isolates classified as low virulence (Figures 4.4 A to D).

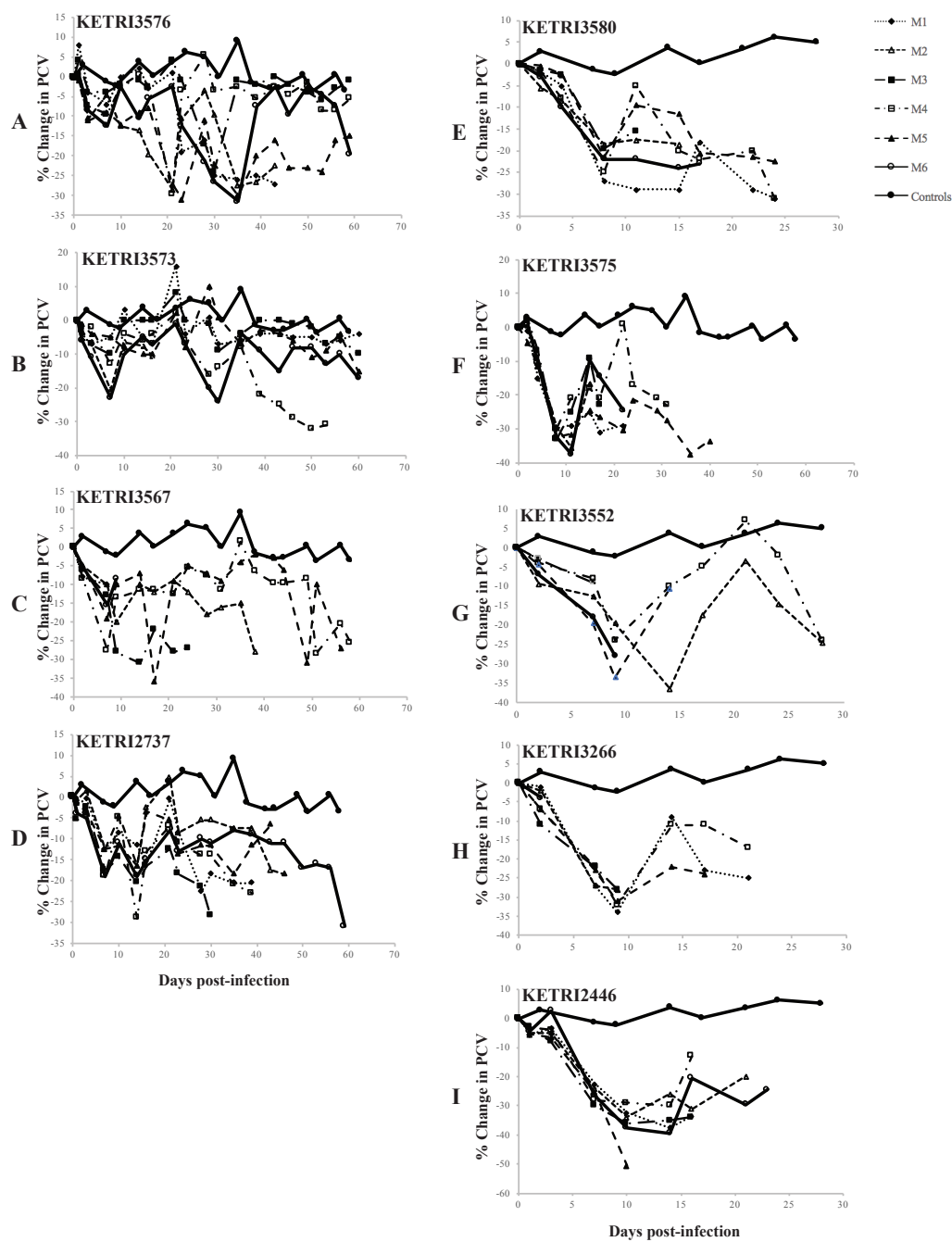


Figure 4. 4: (A-D) percent (%) Packed Cell Volume change profiles of individual mice infected with low virulence *Trypanosoma evansi* isolates; KETRI 3576, 3573, 3567 and 2737. (E-I) Percent (%) Changes in Packed Cell Volume of individual mice infected with moderate virulence *Trypanosoma evansi* isolates; KETRI 3580, 3575, 3552, 3266 and 2446. (M = mouse).

Table 4. 4: Comparison of Packed Cell Volume change (%) between various *Trypanosoma evansi* isolates collected from different countries.

Country of Origin	Isolate ID	Virulence	Mean
-	Controls	-	29.9±0.99 a
Brazil	KETRI 4036	High	2.0±0.88 b
Indonesia	KETRI 4040	High	-3.3±1.36 bc
Kazakhstan	KETRI 4038	High	-4.0±0.53 bc
Vietnam	KETRI 4039	High	-4.6±1.42 bc
Swiss	KETRI 4037	High	-5.5±1.11 bcd
Colombia	KETRI 4034	High	-10.4±6.64 cde
Kenya	KETRI 3573	Low	-13.5±3.92 def
Kenya	KETRI 2479	High	-15.1±2.12 ef
Kenya	KETRI 3576	Low	-16.4±3.93 efg
Kenya	KETRI 3552	Moderate	-17±3.95 efg
Philippines	KETRI 4035	High	-19.6±3.38 fgh
Kenya	KETRI 3567	Low	-24.7±4.29 gh
Kenya	KETRI 2737	Low	-26.5±1.31 hi
Kenya	KETRI 3580	Moderate	-28.3±3.72 hi
Kenya	KETRI 3266	High	-34±2.13 ij
Kenya	KETRI 2446	Moderate	-34.7±3.54 ij
Kenya	KETRI3575	Moderate	-40.4±2.57 j
LSD	8.8		
CV (%)	51.8		

NB: Means followed by the same letter do not significantly differ ($p < 0.0001$)

Rapid decline in PCV was observed in mice infected with isolates of moderate virulence (Figures 4.4 E to I) when compared with the control group. This group of isolates exhibited high and persistent parasitaemia with animal survival periods ranging from 11-30 dpi. No marked differences were observed between individual animals and different isolates in this group. No PCV profiles are available for the high virulence group due to the high and short duration of parasitaemia and short survival period that ranged from 4-10 days. The drop in PCV approximately 3% suggesting that the animals died before they became anemic. There were significant differences in % PCV values between the controls and infected animals (Table 4.4). The drop in % PCV values was significantly higher ($p < 0.05$; range -17±3.95 to -40.4±2.57) in mice infected with medium virulent parasites when compared with low (range -13.5±3.92 to -26.5±1.31) and high virulence (range -4.0±0.53 to -10.4±6.64 in 4 of 7

isolates). Generally, the results showed that very high and persistent parasitaemia levels were associated with rapid drop in PCV values.

4.1.4 Body weight profiles

Gradual increase in live body weights of 9.0 ± 2.13 g was observed in all animals in the control group within the 60 days observation period. A similar trend was observed in profiles of animals infected with isolates classified as low virulence (7.8 ± 3.17 to 17 ± 2.2 ; survival period 31-60 days; Figures 4.5A to D), three of which were significantly higher ($p < 0.001$) than those of controls, suggesting significant increase in bodyweight with exception of KETRI 2737 (Figure 4.5D). When compared to the control animals, rapid decline in bodyweights was observed in mice infected with four of the moderate virulent isolates (KETRI 2446, 3266, 3552 and 3575) as shown in Figure 4B. However, no weight loss was observed in animals infected with the isolate KETRI 3580 within the same category of classification (Figure 4.5E). No body weight profiles are available for the high virulence group due to the short survival period that ranged from 4-10 days.

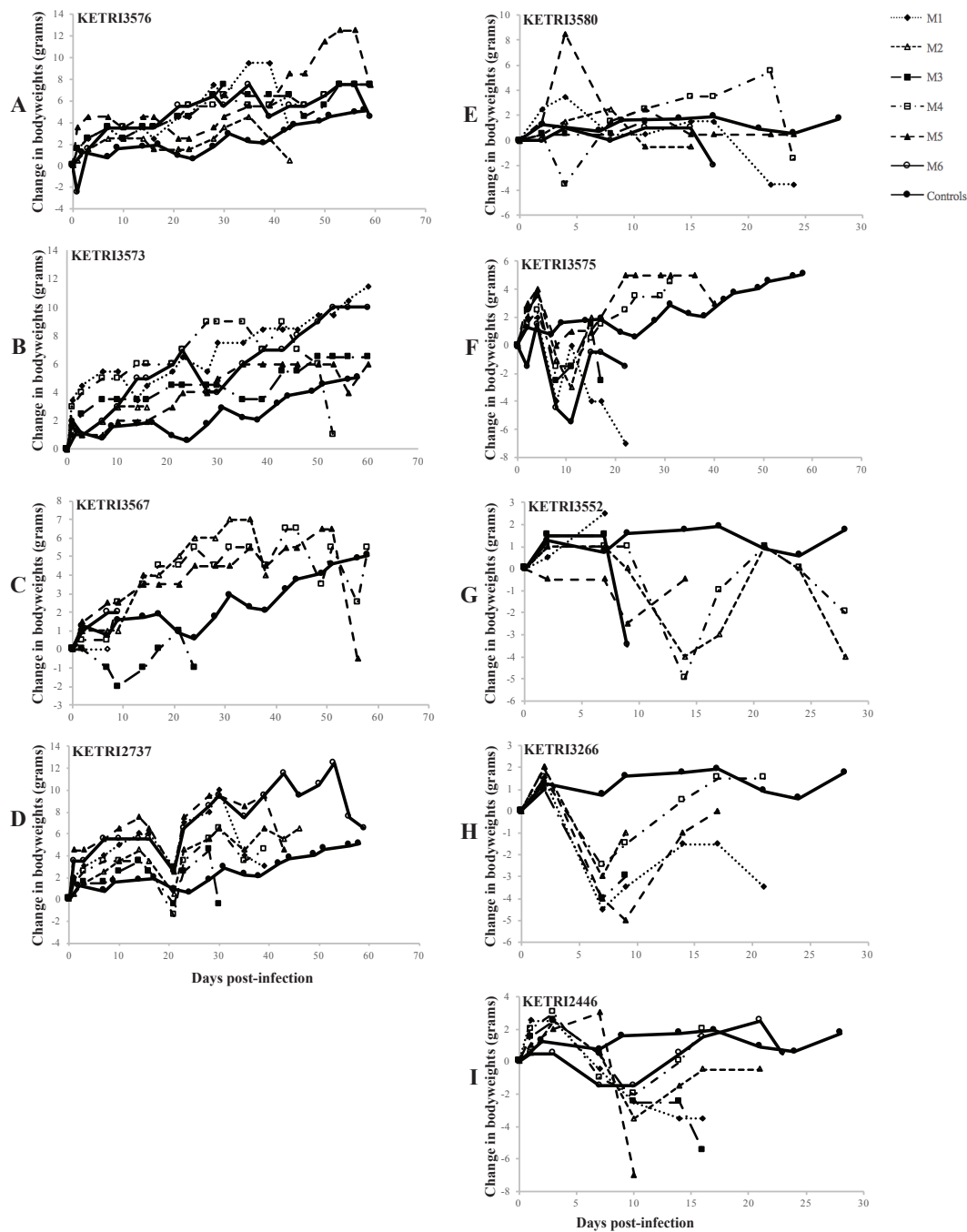


Figure 4. 5:(A-D) bodyweight changes profiles of individual mice infected with low virulence *Trypanosoma evansi* isolates; KETRI 3576, 3573, 3567 and 2737. (E-I) bodyweight change profiles of individual mice infected with moderate virulence of *Trypanosoma evansi* isolates; KETRI 3580, 3575, 3552, 3266 and 2446 (M = mouse). Comparison of bodyweight changes showed significantly higher body weight increase in animals that were infected with low virulent parasites than in control animals (Table 4.5).

Table 4. 5: Comparison of bodyweights change (%) between various *Trypanosoma evansi* isolates collected from different countries.

Country of origin	Isolate ID	Virulence	Mean
Kenya	KETRI 3573	Low	17±2.2 a
Kenya	KETRI 2737	Low	16.3±3.22 a
Kenya	KETRI 3576	Low	16.2±2.04 a
-	Controls	-	9.0±2.13 b
Kenya	KETRI 3567	Low	7.8±3.17 bc
Kenya	KETRI 2479	High	6.9±0.93 bc
Indonesia	KETRI 4040	High	6.3±0.89 bcd
Vietnam	KETRI 4039	High	4.5±1.11 bcde
Kazakhstan	KETRI 4038	High	4.3±0.71 bcdef
Kenya	KETRI 3580	High	3.0±0.99 cdef
Kenya	KETRI 3575	Moderate	1.4±2.82 defg
Swiss	KETRI 4037	High	0.7±1.34 efg
Colombia	KETRI 4034	High	0.4±0.58 efg
Kenya	KETRI 3552	Moderate	-0.3±1.28 efg
Brazil	KETRI 4036	High	-0.6±0.46 fg
Kenya	KETRI 2446	Moderate	-0.7±0.8 fg
Kenya	KETRI 3266	High	-2.7±1.4 g
Philippines	KETRI 4035	High	-9.9±2.11 h
LSD	5.0		
CV (%)	98.9		

NB: Means followed by the same letter do not significantly differ (p-value < 0.001)

However, significant loss ($p < 0.001$) in body weights was observed in animals infected with moderate virulent *T. evansi* parasites when compared with controls and low virulent groups.

The above results demonstrated a strong association between parasitaemia levels, PCV, body weights and survival of infected animals leading to the classification of low, moderate and high virulence.

4.2 Evolutionary origin of *T. evansi* in Kenya

4.2.1 PCR-based diagnostic tests

Results from the PCR assays are presented in Table 3.2. All KETRI isolates amplified in PCR test diagnostic for ITS1 region of African trypanosomes considered pathogenic. Members of the subgenera *Nannomonas* (*T. congolense*), *Duttonella* (*T. vivax*) and *Trypanozoon* (*T. brucei*, *T. evansi*, *T. equiperdum*). In contrast, *T. lewisi* and *T. theileri*, which are considered non-pathogenic but can be found in many areas of the world, including

Kenya, have been reported to not give a positive signal, presumably because their ITS region is more divergent. All isolates were also SRA negative, confirming absence of *T. b. rhodesiense* isolates. For the A281del PCR assay, five isolates could not be determined because they failed to amplify in the positive control reaction (n/a in Table 3.2). Of those that amplified, 29 isolates were found to be A281del positive, indicating that they are *T. evansi* type A, and 3 isolates that were A281del negative, indicating that they could be either type B or something else, but not type A. Only 20 of the isolates tested were positive for the RoTat 1.2 gene (including, as expected, STIB810 and C13), indicating a diversity of VSG antigen types in our dataset. Although it has been reported that type A *T. evansi* isolates are typically RoTat1.2 positive.

4.2.2 Identification of distinct genetic clusters

The current results suggested a K-value of 2, and thus the presence of two distinct genetic clusters, as the most likely hierarchical level of population structure that best fits the method's assumptions (Figure 4.6).

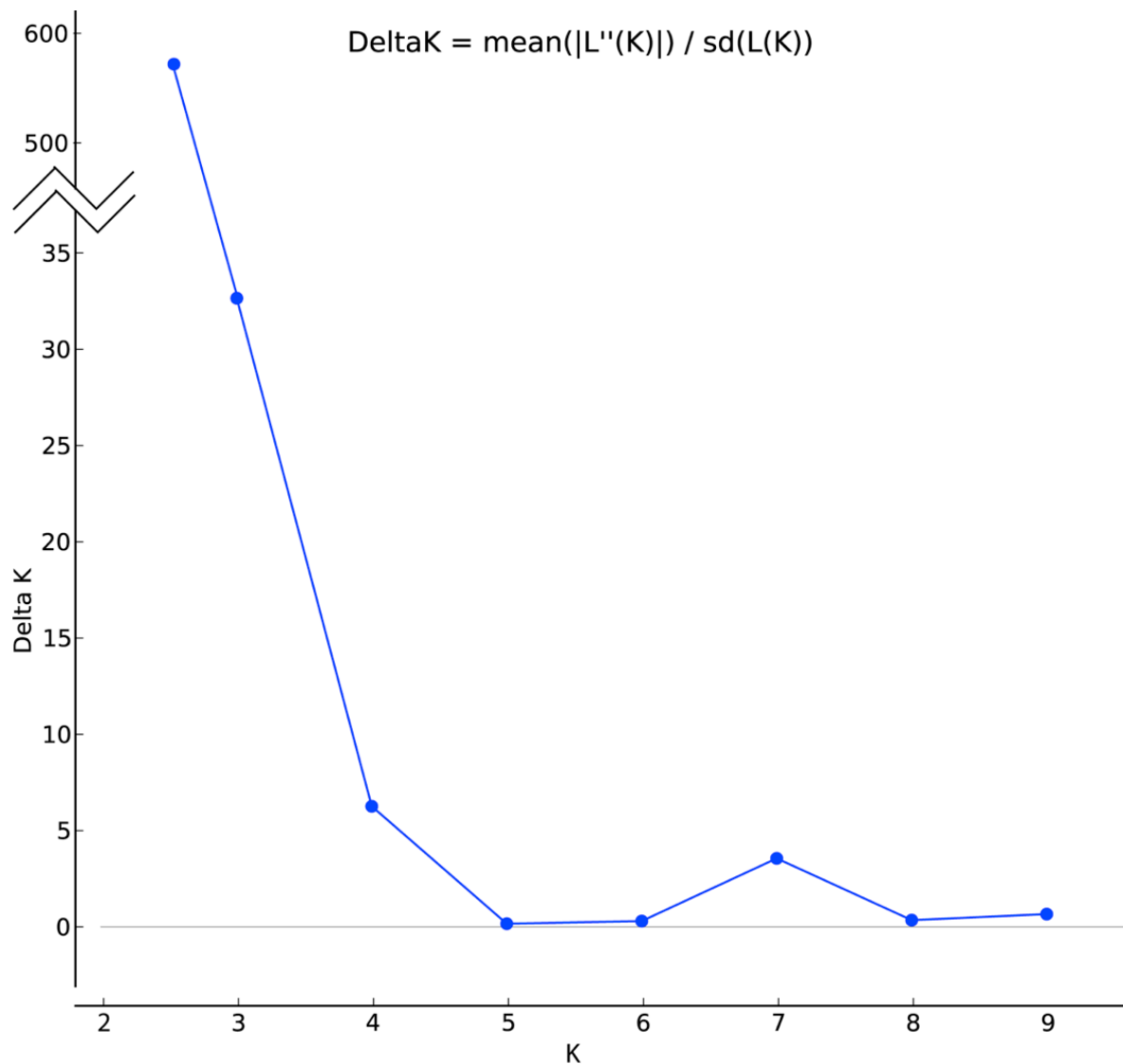


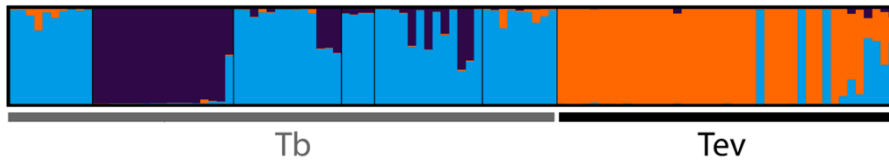
Figure 4. 6 : STRUCTURE v2.3.4 plot of delta K for K values of 2 to 9 based on 20 runs each performed with a burn-in of 5,000 and a total of 250,000 iterations. Although K=2 had the highest delta K and thus explained the highest hierarchical level in the data, a K value of 7 was the next hierarchical level with a peak in delta K and was able to distinguish structure within *Trypanosoma brucei brucei* and *T. b. rhodesiense*.

One of these two clusters (Figure 4.7; top panel, orange colour) includes most but not all *T. evansi* isolates, while the other includes all of the *T. b. brucei* and *T. b. rhodesiense* isolates (Figure 4.7; top panel, blue colour). The next best fit of K=7 was able to distinguish structures within *T. brucei*, suggesting the presence of seven distinct genetic units. Assignment to these clusters for the 107 isolates analyzed is shown in Figure 4.8A.

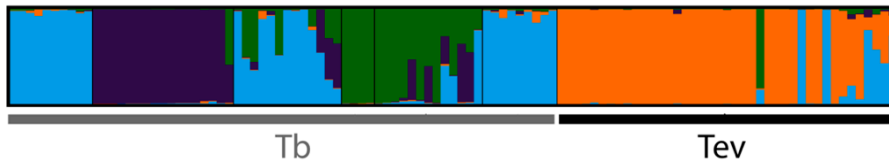
K=2



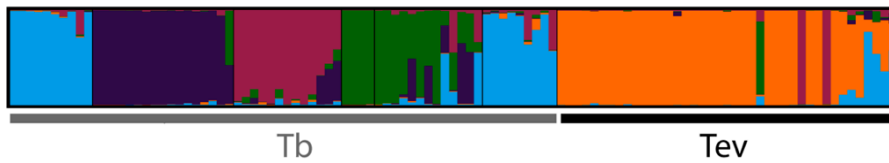
K=3



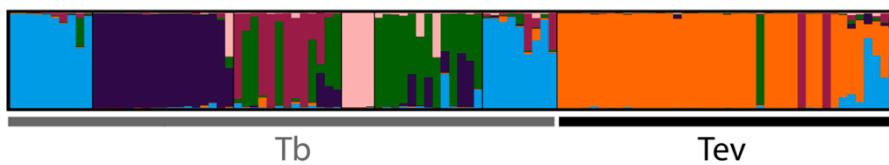
K=4



K=5



K=6



K=7

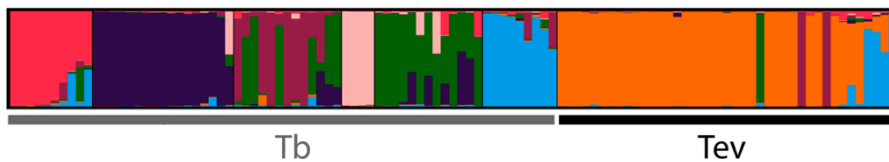


Figure 4. 7: STRUCTURE v2.3.4 (Pritchard *et al.*, 2000)plot of individual assignments with K values of 2 through 7. Each vertical bar represents a strain's probability of assignment to one of K genetic clusters, with *T. brucei* (Tb) strains on the left (light grey horizontal bar) and *T. evansi* (Tev) strains on the right (dark grey horizontal bar). Individuals with 100% probability of assignment to one cluster are represented by bars of only one colour,

individuals with multiple assignment to different genetic cluster are represented by bars with multiple colours.

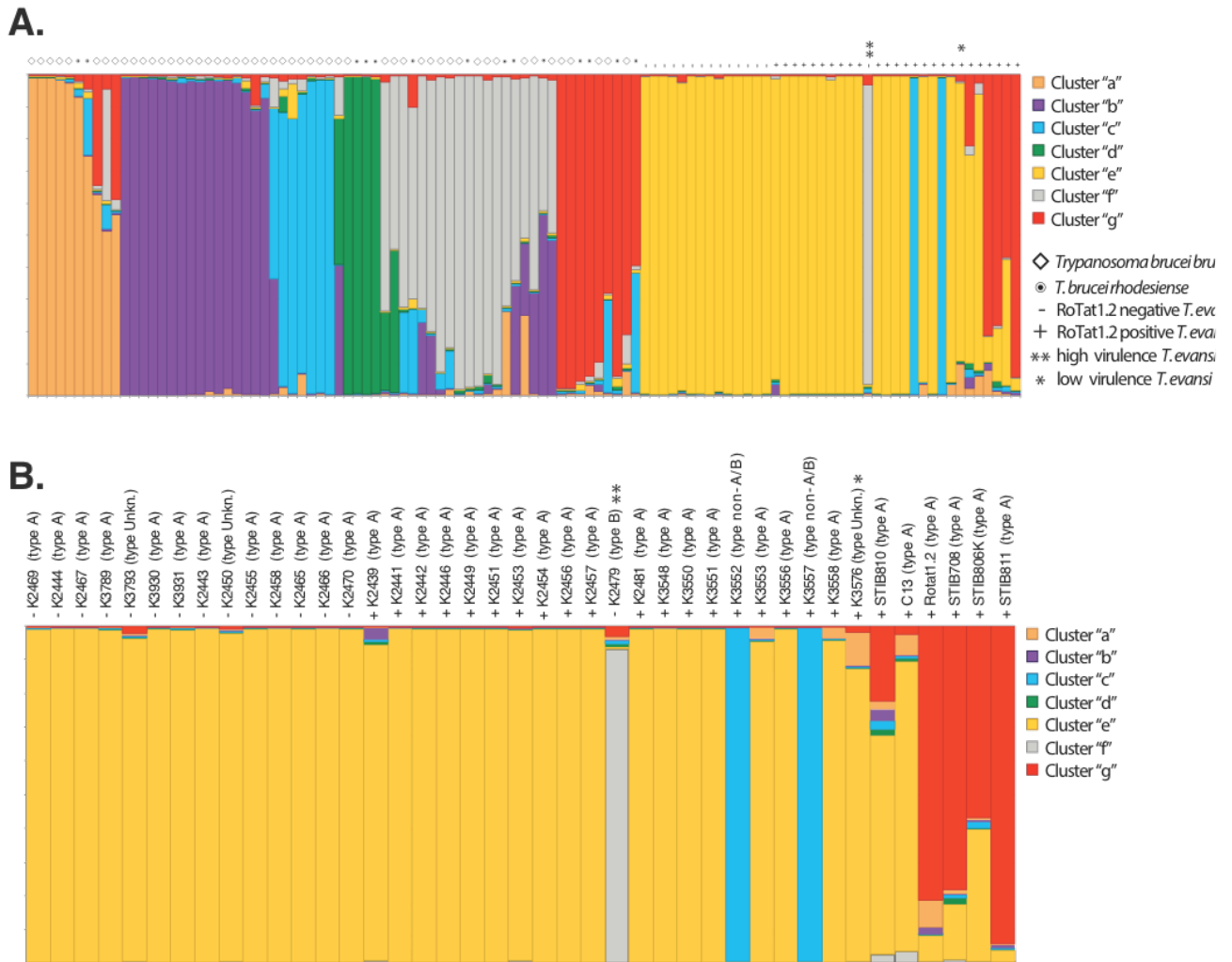


Figure 4. 8: Plot of assignment scores of all isolates using STRUCTURE v2.3.4 (Pritchard *et al.*, 2000) with K=7 of (A) all isolates, and (B) the close up of *Trypanosoma evansi* isolates (Tev) with labels added showing isolate ID and kDNA type in parentheses (based on literature, where available, or predicted from the A281del PCR assay). Each vertical bar represents an isolate's probability of assignment to one of seven genetic clusters "a" through "g" shown in orange, purple, blue, green, yellow, grey and red, as presented in the legend to the right. *T. b. brucei* is indicated with a diamond, *T. b. rhodesiense* is indicated with a bullet point, and *T. evansi* is indicated by a plus "+" if RoTat 1.2 positive and minus "-" if RoTat 1.2 negative. The high virulence isolate is marked with a double asterix "**", and the low virulence isolate is marked by a single asterix "*". Note that Tev isolates in panel B are ordered according to Table 1 and not strictly according to cluster assignment.

While the majority of the isolates (78%) had high level of assignment to only one cluster (Q > 0.80; colours in bars in Figure 4.8 represent scores listed in Table 4.6),

Table 4. 6: Assignment scores from STRUCTURE v2.3.4 clustering analysis with K=7

A.									
Sample ID	Taxon	Genetic cluster	"a"	"b"	"c"	"d"	"e"	"f"	"g"
RE091	Tbb	"a" (orange)	0.99	0.00	0.00	0.00	0.00	0.00	0.00
RE133	Tbb	"a" (orange)	0.99	0.00	0.00	0.00	0.00	0.00	0.00
RE086	Tbb	"a" (orange)	0.99	0.00	0.00	0.00	0.00	0.00	0.00
UTRO2509	Tbb	"a" (orange)	0.98	0.00	0.00	0.00	0.01	0.00	0.00
UTRO2516	Tbb	"a" (orange)	0.98	0.00	0.01	0.00	0.00	0.00	0.01
RE042	Tbr	"a" (orange)	0.93	0.00	0.02	0.00	0.02	0.01	0.02
OB021	Tbr	Uncertain	0.75	0.00	0.18	0.00	0.02	0.01	0.05
F783	Tbb	Uncertain	0.63	0.01	0.01	0.00	0.00	0.01	0.34
K2355	Tbb	Uncertain	0.51	0.00	0.08	0.00	0.01	0.35	0.04
OB091	Tbb	Uncertain	0.56	0.01	0.00	0.00	0.00	0.03	0.39
OB59	Tbb	"b" (purple)	0.00	0.99	0.00	0.00	0.00	0.00	0.00
OB71	Tbb	"b" (purple)	0.00	0.99	0.00	0.00	0.00	0.00	0.00
OB67	Tbb	"b" (purple)	0.00	0.99	0.00	0.00	0.00	0.00	0.00
OB63	Tbb	"b" (purple)	0.00	0.99	0.00	0.00	0.00	0.00	0.00
OB68	Tbb	"b" (purple)	0.00	0.98	0.00	0.00	0.00	0.00	0.00
OB61	Tbb	"b" (purple)	0.00	0.98	0.00	0.00	0.00	0.01	0.00
OB52	Tbb	"b" (purple)	0.00	0.97	0.01	0.00	0.00	0.00	0.00
OB74	Tbb	"b" (purple)	0.01	0.98	0.00	0.01	0.00	0.00	0.00
OB69	Tbb	"b" (purple)	0.00	0.98	0.00	0.00	0.00	0.01	0.00
cp12	Tbb	"b" (purple)	0.01	0.97	0.00	0.00	0.00	0.00	0.00
cp16	Tbb	"b" (purple)	0.01	0.97	0.01	0.00	0.00	0.01	0.00
OB70	Tbb	"b" (purple)	0.02	0.96	0.00	0.00	0.00	0.00	0.01
OB76	Tbb	"b" (purple)	0.01	0.97	0.02	0.00	0.00	0.00	0.00
OB62	Tbb	"b" (purple)	0.00	0.94	0.00	0.01	0.02	0.01	0.01
OB72	Tbb	"b" (purple)	0.00	0.89	0.00	0.00	0.01	0.00	0.10
cp13	Tbb	"b" (purple)	0.00	0.92	0.05	0.00	0.00	0.02	0.01
cp6	Tbb	Uncertain	0.01	0.36	0.53	0.00	0.00	0.09	0.01
cp17	Tbb	"c" (blue)	0.03	0.00	0.85	0.05	0.02	0.03	0.02
cp24	Tbb	"c" (blue)	0.00	0.00	0.86	0.00	0.11	0.02	0.01
cp29	Tbb	"c" (blue)	0.07	0.00	0.87	0.01	0.00	0.04	0.01
cp15	Tbb	"c" (blue)	0.00	0.01	0.97	0.01	0.00	0.00	0.00
cp5	Tbb	"c" (blue)	0.01	0.00	0.98	0.00	0.00	0.00	0.01
cp14	Tbb	"c" (blue)	0.00	0.00	0.98	0.00	0.00	0.01	0.00
OB58	Tbb	Uncertain	0.00	0.40	0.00	0.45	0.01	0.12	0.01
OB56	Tbb	"d" (green)	0.00	0.00	0.00	0.99	0.00	0.00	0.00
OB54	Tbr	"d" (green)	0.00	0.00	0.00	0.99	0.00	0.00	0.00
OB53	Tbr	"d" (green)	0.00	0.00	0.00	0.99	0.00	0.00	0.00
OB57	Tbr	"d" (green)	0.00	0.00	0.00	0.98	0.01	0.00	0.00
OB31	Tbb	Uncertain	0.01	0.01	0.01	0.24	0.00	0.71	0.02
OB10	Tbb	Uncertain	0.00	0.00	0.00	0.44	0.00	0.54	0.00
cp19	Tbb	Uncertain	0.01	0.00	0.25	0.01	0.01	0.72	0.00

OB027	Tbr	Uncertain	0.00	0.00	0.26	0.01	0.03	0.60	0.10
cp26	Tbb	Uncertain	0.00	0.23	0.04	0.00	0.00	0.72	0.00
cp7	Tbb	Uncertain	0.00	0.18	0.01	0.00	0.00	0.79	0.01
cp27	Tbb	"f" (grey)	0.00	0.02	0.05	0.00	0.00	0.92	0.01
OB30	Tbb	"f" (grey)	0.02	0.00	0.12	0.01	0.00	0.84	0.01
OB088	Tbb	"f" (grey)	0.00	0.00	0.00	0.01	0.00	0.98	0.00
OB22	Tbr	"f" (grey)	0.01	0.00	0.00	0.01	0.00	0.97	0.00
OB051	Tbb	"f" (grey)	0.00	0.01	0.01	0.01	0.00	0.97	0.00
OB64	Tbb	"f" (grey)	0.01	0.03	0.00	0.02	0.01	0.92	0.02
OB55	Tbb	"f" (grey)	0.02	0.01	0.00	0.01	0.00	0.96	0.01
OB078	Tbr	Uncertain	0.26	0.00	0.01	0.00	0.00	0.72	0.01
OB066	Tbr	Uncertain	0.00	0.34	0.00	0.00	0.01	0.63	0.01
STIB366	Tbb	Uncertain	0.25	0.22	0.00	0.01	0.01	0.50	0.01
OB75	Tbb	Uncertain	0.01	0.31	0.00	0.00	0.00	0.67	0.00
OB65	Tbr	Uncertain	0.00	0.56	0.00	0.00	0.01	0.41	0.01
OB60	Tbb	Uncertain	0.00	0.48	0.01	0.01	0.00	0.48	0.01
OB153	Tbb	"g" (red)	0.00	0.00	0.01	0.00	0.00	0.00	0.98
OB155	Tbb	"g" (red)	0.01	0.00	0.00	0.00	0.00	0.00	0.98
OB095	Tbr	"g" (red)	0.01	0.00	0.01	0.00	0.02	0.01	0.96
OB006	Tbr	"g" (red)	0.03	0.00	0.00	0.00	0.00	0.02	0.94
OB113	Tbb	"g" (red)	0.01	0.02	0.01	0.00	0.01	0.05	0.89
cp8	Tbb	Uncertain	0.01	0.00	0.29	0.00	0.01	0.01	0.68
OB026	Tbr	"g" (red)	0.00	0.00	0.01	0.01	0.02	0.01	0.94
OB12	Tbb	"g" (red)	0.08	0.00	0.00	0.01	0.01	0.09	0.81
OB024	Tbr	Uncertain	0.01	0.00	0.37	0.00	0.01	0.01	0.59

B.										
Sample ID	RoTat 1.2	kDNA type	Genetic Cluster	"a"	"b"	"c"	"d"	"e"	"f"	"g"
K2469	-	A*	"e" (yellow)	0.00	0.00	0.00	0.00	0.99	0.00	0.00
K2444	-	A*	"e" (yellow)	0.00	0.00	0.00	0.00	0.99	0.00	0.00
K2467	-	A*	"e" (yellow)	0.00	0.00	0.00	0.00	0.99	0.00	0.00
K3789	-	A*	"e" (yellow)	0.00	0.00	0.00	0.00	0.99	0.00	0.00
K3793	-	Unkn.	"e" (yellow)	0.01	0.00	0.00	0.00	0.96	0.00	0.02
K3930	-	A*	"e" (yellow)	0.00	0.00	0.00	0.00	0.99	0.00	0.00
K3931	-	A*	"e" (yellow)	0.00	0.00	0.00	0.00	0.99	0.00	0.00
K2443	-	A	"e" (yellow)	0.00	0.00	0.00	0.00	0.99	0.00	0.00
K2450	-	Unkn.	"e" (yellow)	0.01	0.00	0.00	0.01	0.97	0.00	0.01
K2455	-	A*	"e" (yellow)	0.00	0.00	0.00	0.00	0.99	0.00	0.00
K2458	-	A*	"e" (yellow)	0.00	0.00	0.00	0.00	0.99	0.00	0.00
K2465	-	A*	"e" (yellow)	0.00	0.00	0.00	0.00	0.99	0.00	0.00
K2466	-	A*	"e" (yellow)	0.00	0.00	0.00	0.00	0.99	0.00	0.00
K2470	-	A*	"e" (yellow)	0.00	0.00	0.00	0.00	0.99	0.00	0.00
K2439	+	A	"e" (yellow)	0.00	0.03	0.01	0.01	0.94	0.01	0.00
K2441	+	A*	"e" (yellow)	0.00	0.00	0.00	0.00	0.99	0.00	0.00
K2442	+	A*	"e" (yellow)	0.00	0.00	0.00	0.00	0.99	0.00	0.00
K2446	+	A*	"e" (yellow)	0.00	0.00	0.00	0.00	0.99	0.00	0.00

K2449	+	A*	"e" (yellow)	0.00	0.00	0.00	0.00	0.99	0.00	0.00
K2451	+	A*	"e" (yellow)	0.00	0.00	0.00	0.00	0.99	0.00	0.00
K2453	+	A*	"e" (yellow)	0.00	0.00	0.00	0.00	0.98	0.01	0.01
K2454	+	A	"e" (yellow)	0.00	0.00	0.00	0.00	0.99	0.00	0.00
K2456	+	A	"e" (yellow)	0.00	0.00	0.00	0.00	0.99	0.00	0.00
K2457	+	A*	"e" (yellow)	0.00	0.00	0.00	0.00	0.99	0.00	0.00
K2479	-	B	"f" (grey)	0.01	0.00	0.01	0.01	0.01	0.93	0.03
K2481	+	A*	"e" (yellow)	0.00	0.00	0.00	0.00	0.99	0.00	0.00
K3548	+	A*	"e" (yellow)	0.00	0.00	0.00	0.00	0.99	0.00	0.00
K3550	+	A*	"e" (yellow)	0.00	0.00	0.00	0.00	0.99	0.00	0.00
K3551	+	A*	"e" (yellow)	0.00	0.00	0.00	0.00	0.99	0.00	0.00
K3552	+	non-A/B	"c" (blue)	0.00	0.00	0.99	0.00	0.00	0.00	0.00
K3553	+	A*	"e" (yellow)	0.04	0.00	0.00	0.00	0.95	0.00	0.00
K3556	+	A*	"e" (yellow)	0.00	0.00	0.00	0.00	0.99	0.00	0.00
K3557	+	non-A/B	"c" (blue)	0.00	0.00	0.99	0.00	0.00	0.00	0.00
K3558	+	A*	"e" (yellow)	0.04	0.00	0.00	0.00	0.95	0.00	0.00
K3576	+	Unkn.	"e" (yellow)	0.10	0.00	0.00	0.00	0.87	0.01	0.02
STIB810	+	A	Uncertain	0.02	0.03	0.03	0.02	0.65	0.03	0.22
C13	+	A	"e" (yellow)	0.06	0.01	0.00	0.01	0.86	0.04	0.02
RoTat1.2 (OB106)	+	A	"g" (red)	0.08	0.02	0.00	0.00	0.08	0.00	0.81
STIB708 (OB35)	+	A	Uncertain	0.01	0.00	0.01	0.02	0.16	0.01	0.78
STIB806 K (OB2)	+	A	Uncertain	0.01	0.01	0.02	0.00	0.39	0.01	0.57
STIB811 (OB42)	+	A	"g" (red)	0.00	0.01	0.00	0.00	0.04	0.00	0.94

Table showing sample ID, taxon, genetic cluster “a-g” (Figure 4.8) if probability of assignment (Q) above or equal to 0.8, or "uncertain" if $Q < 0.8$ for each strain of (A) *Trypanosoma brucei brucei* (Tbb) or *T. b. rhodesiense* (Tbr), and (B) *T. evansi* (Tev).

7 *T. b. rhodesiense*, 13 *T. b. brucei*, and 3 *T. evansi* isolates showed uncertain assignment to any one of seven clusters ($Q < 0.80$, bars with no single colour representing more than 80% in Figure 4.8) to any one of seven clusters (Figure 4.8A). This uncertain assignment could be due to a variety of factors, ranging from shared common ancestry or recent admixture to limitations of the genetic markers to separate such recently diverged taxa. Cluster “b” (purple) includes only *T. b. brucei* isolates and corresponds to the “Kiboko B” group (Balmer *et al.*, 2011). Cluster “a” (orange), “c” (blue), “d” (green), and “f” (grey) include both *T. b. brucei* and *T. b. rhodesiense* isolates. Cluster “g” (red) includes isolates from all the three

taxa, *T. b. brucei*, *T. b. rhodesiense*, and *T. evansi*. Cluster “e” (yellow) includes only *T. evansi* isolates.

The STRUCTURE results for *T. evansi* isolates are displayed in detail in Figure 4.8B. Also included are the results of the RoTat 1.2 PCR assay and information on the kDNA minicircle type (based on the literature, where available, or as predicted from our A281del PCR assays; see Tables 3.2 and 3.3). Although the majority of *T. evansi* isolates assigned to cluster “e” (yellow), there are 6 isolates that assigned with high Q values ($Q > 0.80$) to different STRUCTURE-defined genetic clusters, and 3 isolates (STIB810, STIB708 and STIB806K) with uncertain assignment ($Q < 0.80$). Of the isolates with high Q values to non “e” clusters, one isolate (K2479) assigned to cluster “f” (grey), two isolates (K3552 and K3557) to cluster “c” (blue), and two isolates (RoTat1.2 and STIB811) to cluster “g” (red), implying that some *T. evansi* isolates are genetically closer to *T. brucei* isolates than to each other and supporting the hypothesis of multiple independent origins of *T. evansi* isolates from *T. brucei*. All 33 isolates with kDNA minicircle type A were assigned to either cluster “e” or “g”, the single confirmed type B (K2479) assigned to cluster “f”, and the two isolates that could not be classified as type A or type B by our assays (K3552 and K3557) assigned to cluster “c” (Figure 4.8B). This result suggests an association of kDNA minicircle type A with the “e” and “g” clusters, and that the other isolates in our dataset associated with other dominant minicircle types (Table 3.3) are from genetically distinct lineages. In contrast, there was no assignment pattern for the isolates that typed as RoTat 1.2 positive or negative based on the PCR assay (Table 3.2), as the positive isolates assigned to three different clusters (“c”, “g”, and “e”; Figure 4.8B). The high virulence isolate, K2479 (a kDNA minicircle type B and RoTat 1.2 negative isolate), grouped with the “f” cluster, while the low virulence isolate, K3576 (a RoTat 1.2 positive isolate) assigns to the “e” cluster (Figure 4.8B). This separation into different clusters suggests independent evolution, but more samples from different

genetic backgrounds and virulence degrees are necessary to validate the generality of this observation.

The results of the multivariate analyses (PCA, Figure 4.9) largely confirmed the pattern of genetic structuring suggested by the Bayesian analyses (Figures 4.8A, B) and also provided additional insights on how the different STRUCTURE-based clusters are genetically similar.

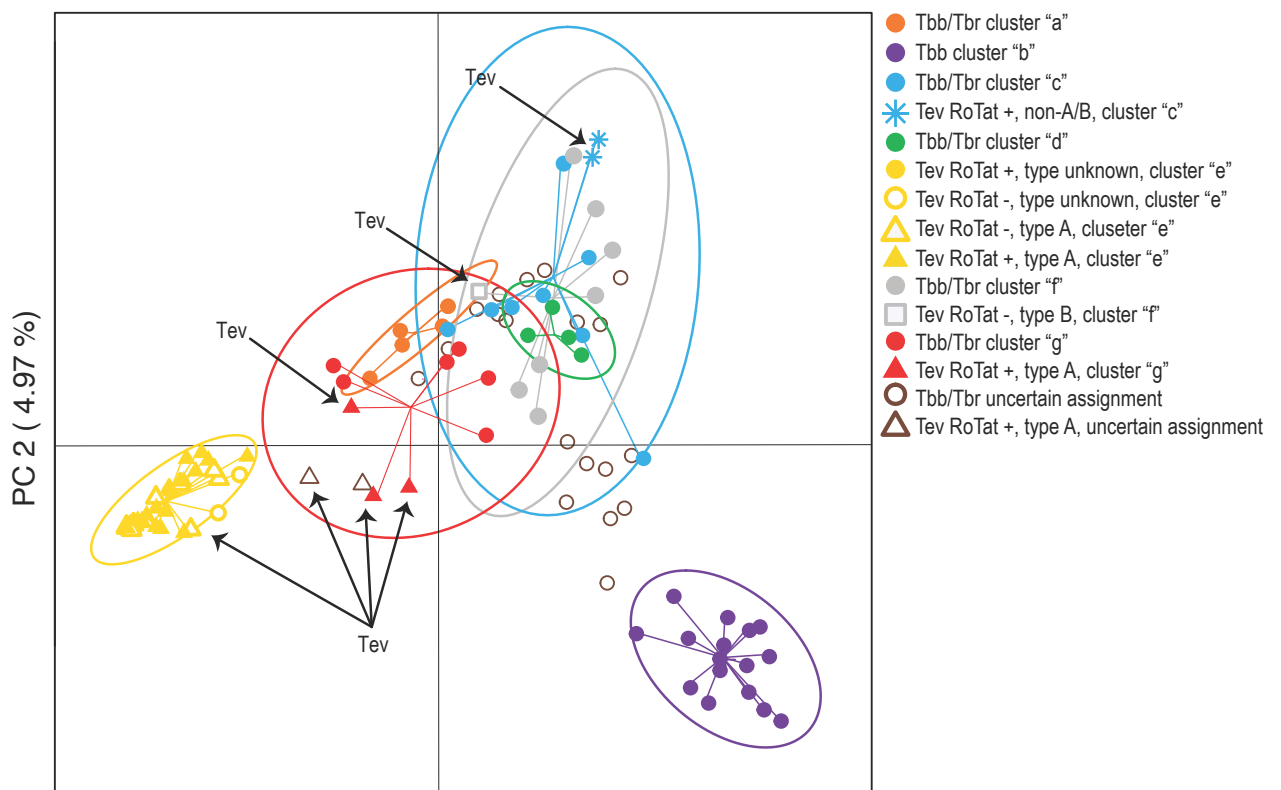


Figure 4. 9: Evaluation of the genetic differentiation between isolates of *Trypanosoma brucei brucei* and *T. b. rhodesiense* (Tb) and *T. evansi* (Tev) genetic clusters using principal components analysis (PCA) of microsatellite data. PCA was performed in R using the package “adegenet” (Jombart, 2008). Points representing individual genotypes are marked by colour of their STRUCTURE assignment following the key and connected by a line to the

centroid of an ellipse, which circumscribes a region encompassing 95% of the variance observed within each subgroup identified. Black arrows point out the *Tev* isolates.

Individuals from four of five STRUCTURE-defined clusters that include both *T. b. brucei* and *T. b. rhodesiense* isolates (clusters “a”, “c”, “d”, “f”, and “g”) grouped close together in the multivariate space defined by the first two PC axes, with isolates from the “a” and “g”, and isolates from the “c”, “d”, and “f” clusters being indistinguishable from one another along the first two components (PC 1 and 2). These close genetic relationships were also implied by the uncertain STRUCTURE cluster assignment of some *T. brucei*, which suggests some shared ancestry with all these clusters (Figure 4.8A, bars with no single dominant colour representing more than 80% of the size). On the other hand, the *T. b. brucei* “Kiboko B” isolates (cluster “b”, Figure 4.8A) were clearly genetically distinct from the other isolates (purple ellipsoid in Figure 4.9), as also suggested by the high Q values assignment of these isolates to a single STRUCTURE-based cluster (Figure 4.8A). The isolates included in STRUCTURE-based cluster “e” (yellow in Figure 4.8A, exclusively *T. evansi* isolates), were also separate from the others. However, they were proximal to cluster “g” isolates and to two *T. evansi* isolates with uncertain assignment (Figure 4.8B), indicating a close evolutionary relationship between the *T. evansi* and *T. brucei* isolates in these two clusters (Figure 4.9). As for the STRUCTURE analyses, some *T. evansi* isolates were closer to *T. brucei* isolates included in different clusters (“f”, “c”, and “g”; Figure 4.8B). Thus, both Bayesian and multivariate analyses suggest that some *T. evansi* isolates share closer evolutionary relationships with different *T. brucei* isolates than with each other.

4.2.3 Genetic diversity and levels of differentiation

To compare diversity and differentiation within and among *T. evansi* and *T. brucei*, basic diversity statistics, genetic distance, and F_{ST} among STRUCTURE-based clusters was

estimated at three levels defined as follows: (i) all of the 84 isolates with $Q > 0.80$ regardless of taxonomy (Table 4.7).

Table 4. 7: Assignment scores from STRUCTURE v2.3.4

A.									
Sample ID	Taxon	Genetic cluster	“a”	“b”	“c”	“d”	“e”	“f”	“g”
RE091	Tbb	"a" (orange)	0.99	0.00	0.00	0.00	0.00	0.00	0.00
RE133	Tbb	"a" (orange)	0.99	0.00	0.00	0.00	0.00	0.00	0.00
RE086	Tbb	"a" (orange)	0.99	0.00	0.00	0.00	0.00	0.00	0.00
UTRO2509	Tbb	"a" (orange)	0.98	0.00	0.00	0.00	0.01	0.00	0.00
UTRO2516	Tbb	"a" (orange)	0.98	0.00	0.01	0.00	0.00	0.00	0.01
RE042	Tbr	"a" (orange)	0.93	0.00	0.02	0.00	0.02	0.01	0.02
OB021	Tbr	uncertain	0.75	0.00	0.18	0.00	0.02	0.01	0.05
F783	Tbb	uncertain	0.63	0.01	0.01	0.00	0.00	0.01	0.34
K2355	Tbb	uncertain	0.51	0.00	0.08	0.00	0.01	0.35	0.04
OB091	Tbb	uncertain	0.56	0.01	0.00	0.00	0.00	0.03	0.39
OB59	Tbb	"b" (purple)	0.00	0.99	0.00	0.00	0.00	0.00	0.00
OB71	Tbb	"b" (purple)	0.00	0.99	0.00	0.00	0.00	0.00	0.00
OB67	Tbb	"b" (purple)	0.00	0.99	0.00	0.00	0.00	0.00	0.00
OB63	Tbb	"b" (purple)	0.00	0.99	0.00	0.00	0.00	0.00	0.00
OB68	Tbb	"b" (purple)	0.00	0.98	0.00	0.00	0.00	0.00	0.00
OB61	Tbb	"b" (purple)	0.00	0.98	0.00	0.00	0.00	0.01	0.00
OB52	Tbb	"b" (purple)	0.00	0.97	0.01	0.00	0.00	0.00	0.00
OB74	Tbb	"b" (purple)	0.01	0.98	0.00	0.01	0.00	0.00	0.00
OB69	Tbb	"b" (purple)	0.00	0.98	0.00	0.00	0.00	0.01	0.00
cp12	Tbb	"b" (purple)	0.01	0.97	0.00	0.00	0.00	0.00	0.00
cp16	Tbb	"b" (purple)	0.01	0.97	0.01	0.00	0.00	0.01	0.00
OB70	Tbb	"b" (purple)	0.02	0.96	0.00	0.00	0.00	0.00	0.01
OB76	Tbb	"b" (purple)	0.01	0.97	0.02	0.00	0.00	0.00	0.00
OB62	Tbb	"b" (purple)	0.00	0.94	0.00	0.01	0.02	0.01	0.01
OB72	Tbb	"b" (purple)	0.00	0.89	0.00	0.00	0.01	0.00	0.10
cp13	Tbb	"b" (purple)	0.00	0.92	0.05	0.00	0.00	0.02	0.01
cp6	Tbb	uncertain	0.01	0.36	0.53	0.00	0.00	0.09	0.01
cp17	Tbb	"c" (blue)	0.03	0.00	0.85	0.05	0.02	0.03	0.02
cp24	Tbb	"c" (blue)	0.00	0.00	0.86	0.00	0.11	0.02	0.01
cp29	Tbb	"c" (blue)	0.07	0.00	0.87	0.01	0.00	0.04	0.01
cp15	Tbb	"c" (blue)	0.00	0.01	0.97	0.01	0.00	0.00	0.00
cp5	Tbb	"c" (blue)	0.01	0.00	0.98	0.00	0.00	0.00	0.01
cp14	Tbb	"c" (blue)	0.00	0.00	0.98	0.00	0.00	0.01	0.00
OB58	Tbb	uncertain	0.00	0.40	0.00	0.45	0.01	0.12	0.01
OB56	Tbb	"d" (green)	0.00	0.00	0.00	0.99	0.00	0.00	0.00
OB54	Tbr	"d" (green)	0.00	0.00	0.00	0.99	0.00	0.00	0.00
OB53	Tbr	"d" (green)	0.00	0.00	0.00	0.99	0.00	0.00	0.00
OB57	Tbr	"d" (green)	0.00	0.00	0.00	0.98	0.01	0.00	0.00

OB31	Tbb	uncertain	0.01	0.01	0.01	0.24	0.00	0.71	0.02
OB10	Tbb	uncertain	0.00	0.00	0.00	0.44	0.00	0.54	0.00
cp19	Tbb	uncertain	0.01	0.00	0.25	0.01	0.01	0.72	0.00
OB027	Tbr	uncertain	0.00	0.00	0.26	0.01	0.03	0.60	0.10
cp26	Tbb	uncertain	0.00	0.23	0.04	0.00	0.00	0.72	0.00
cp7	Tbb	uncertain	0.00	0.18	0.01	0.00	0.00	0.79	0.01
cp27	Tbb	"f" (grey)	0.00	0.02	0.05	0.00	0.00	0.92	0.01
OB30	Tbb	"f" (grey)	0.02	0.00	0.12	0.01	0.00	0.84	0.01
OB088	Tbb	"f" (grey)	0.00	0.00	0.00	0.01	0.00	0.98	0.00
OB22	Tbr	"f" (grey)	0.01	0.00	0.00	0.01	0.00	0.97	0.00
OB051	Tbb	"f" (grey)	0.00	0.01	0.01	0.01	0.00	0.97	0.00
OB64	Tbb	"f" (grey)	0.01	0.03	0.00	0.02	0.01	0.92	0.02
OB55	Tbb	"f" (grey)	0.02	0.01	0.00	0.01	0.00	0.96	0.01
OB078	Tbr	uncertain	0.26	0.00	0.01	0.00	0.00	0.72	0.01
OB066	Tbr	uncertain	0.00	0.34	0.00	0.00	0.01	0.63	0.01
STIB366	Tbb	uncertain	0.25	0.22	0.00	0.01	0.01	0.50	0.01
OB75	Tbb	uncertain	0.01	0.31	0.00	0.00	0.00	0.67	0.00
OB65	Tbr	uncertain	0.00	0.56	0.00	0.00	0.01	0.41	0.01
OB60	Tbb	uncertain	0.00	0.48	0.01	0.01	0.00	0.48	0.01
OB153	Tbb	"g" (red)	0.00	0.00	0.01	0.00	0.00	0.00	0.98
OB155	Tbb	"g" (red)	0.01	0.00	0.00	0.00	0.00	0.00	0.98
OB095	Tbr	"g" (red)	0.01	0.00	0.01	0.00	0.02	0.01	0.96
OB006	Tbr	"g" (red)	0.03	0.00	0.00	0.00	0.00	0.02	0.94
OB113	Tbb	"g" (red)	0.01	0.02	0.01	0.00	0.01	0.05	0.89
cp8	Tbb	uncertain	0.01	0.00	0.29	0.00	0.01	0.01	0.68
OB026	Tbr	"g" (red)	0.00	0.00	0.01	0.01	0.02	0.01	0.94
OB12	Tbb	"g" (red)	0.08	0.00	0.00	0.01	0.01	0.09	0.81
OB024	Tbr	uncertain	0.01	0.00	0.37	0.00	0.01	0.01	0.59

B.										
Sample ID	RoTat 1.2	kDNA type	Genetic Cluster	"a"	"b"	"c"	"d"	"e"	"f"	"g"
K2469	-	A*	"e" (yellow)	0.00	0.00	0.00	0.00	0.99	0.00	0.00
K2444	-	A*	"e" (yellow)	0.00	0.00	0.00	0.00	0.99	0.00	0.00
K2467	-	A*	"e" (yellow)	0.00	0.00	0.00	0.00	0.99	0.00	0.00
K3789	-	A*	"e" (yellow)	0.00	0.00	0.00	0.00	0.99	0.00	0.00
K3793	-	Unkn.	"e" (yellow)	0.01	0.00	0.00	0.00	0.96	0.00	0.02
K3930	-	A*	"e" (yellow)	0.00	0.00	0.00	0.00	0.99	0.00	0.00
K3931	-	A*	"e" (yellow)	0.00	0.00	0.00	0.00	0.99	0.00	0.00
K2443	-	A	"e" (yellow)	0.00	0.00	0.00	0.00	0.99	0.00	0.00
K2450	-	Unkn.	"e" (yellow)	0.01	0.00	0.00	0.01	0.97	0.00	0.01
K2455	-	A*	"e" (yellow)	0.00	0.00	0.00	0.00	0.99	0.00	0.00
K2458	-	A*	"e" (yellow)	0.00	0.00	0.00	0.00	0.99	0.00	0.00
K2465	-	A*	"e" (yellow)	0.00	0.00	0.00	0.00	0.99	0.00	0.00
K2466	-	A*	"e" (yellow)	0.00	0.00	0.00	0.00	0.99	0.00	0.00
K2470	-	A*	"e" (yellow)	0.00	0.00	0.00	0.00	0.99	0.00	0.00
K2439	+	A	"e" (yellow)	0.00	0.03	0.01	0.01	0.94	0.01	0.00

K2441	+	A*	"e" (yellow)	0.00	0.00	0.00	0.00	0.99	0.00	0.00
K2442	+	A*	"e" (yellow)	0.00	0.00	0.00	0.00	0.99	0.00	0.00
K2446	+	A*	"e" (yellow)	0.00	0.00	0.00	0.00	0.99	0.00	0.00
K2449	+	A*	"e" (yellow)	0.00	0.00	0.00	0.00	0.99	0.00	0.00
K2451	+	A*	"e" (yellow)	0.00	0.00	0.00	0.00	0.99	0.00	0.00
K2453	+	A*	"e" (yellow)	0.00	0.00	0.00	0.00	0.98	0.01	0.01
K2454	+	A	"e" (yellow)	0.00	0.00	0.00	0.00	0.99	0.00	0.00
K2456	+	A	"e" (yellow)	0.00	0.00	0.00	0.00	0.99	0.00	0.00
K2457	+	A*	"e" (yellow)	0.00	0.00	0.00	0.00	0.99	0.00	0.00
K2479	-	B	"f" (grey)	0.01	0.00	0.01	0.01	0.01	0.93	0.03
K2481	+	A*	"e" (yellow)	0.00	0.00	0.00	0.00	0.99	0.00	0.00
K3548	+	A*	"e" (yellow)	0.00	0.00	0.00	0.00	0.99	0.00	0.00
K3550	+	A*	"e" (yellow)	0.00	0.00	0.00	0.00	0.99	0.00	0.00
K3551	+	A*	"e" (yellow)	0.00	0.00	0.00	0.00	0.99	0.00	0.00
K3552	+	non-A/B	"c" (blue)	0.00	0.00	0.99	0.00	0.00	0.00	0.00
K3553	+	A*	"e" (yellow)	0.04	0.00	0.00	0.00	0.95	0.00	0.00
K3556	+	A*	"e" (yellow)	0.00	0.00	0.00	0.00	0.99	0.00	0.00
K3557	+	non-A/B	"c" (blue)	0.00	0.00	0.99	0.00	0.00	0.00	0.00
K3558	+	A*	"e" (yellow)	0.04	0.00	0.00	0.00	0.95	0.00	0.00
K3576	+	Unkn.	"e" (yellow)	0.10	0.00	0.00	0.00	0.87	0.01	0.02
STIB810	+	A	uncertain	0.02	0.03	0.03	0.02	0.65	0.03	0.22
C13	+	A	"e" (yellow)	0.06	0.01	0.00	0.01	0.86	0.04	0.02
RoTat1.2 (OB106)	+	A	"g" (red)	0.08	0.02	0.00	0.00	0.08	0.00	0.81
STIB708 (OB35)	+	A	uncertain	0.01	0.00	0.01	0.02	0.16	0.01	0.78
STIB806K (OB2)	+	A	uncertain	0.01	0.01	0.02	0.00	0.39	0.01	0.57
STIB811 (OB42)	+	A	"g" (red)	0.00	0.01	0.00	0.00	0.04	0.00	0.94

* kDNA type is tentative because it is based on the A281del PCR assay only.

Clustering analysis with K=7 showing sample ID, taxon, genetic cluster "a-g" (Figure 4.8) if probability of assignment (Q) above or equal to 0.8, or "uncertain" if $Q < 0.8$ for each strain of (A) *Trypanosoma brucei brucei* (Tbb) or *T. b. rhodesiense* (Tbr), and (B) *T. evansi* (Tev).

(ii) the 46 *T. brucei* isolates with $Q > 0.80$ (Table 4.7A), and (iii) the 38 *T. evansi* isolates with $Q > 0.80$ (Table 4.7B). Basic diversity statistics are shown in Table 4.7. Allelic richness within clusters of all isolates (Table 4.8A) ranged from 2.10 in cluster "d" to 3.86 in cluster "f", indicating the lowest genetic diversity in cluster "d" that contains both *T. b. brucei* and *T. b. rhodesiense*, but not *T. evansi* (Figure 4.8), and the highest genetic diversity in cluster "f" that contains *T. b. brucei*, *T. b. rhodesiense*, and *T. evansi* (Figure 4.8). Observed and expected heterozygosity levels and the related inbreeding coefficient (F_{IS}) are also reported in

Table 4.7A. Within clusters including all isolates, H_O ranged from 0.50 in cluster “g” to 0.66 in cluster “e”, H_E ranged from 0.47 in cluster “d” to 0.78 in cluster “g”, and F_{IS} ranged from -0.30 in cluster "e" to 0.34 in cluster "f", spanning a wide range of heterozygosity and conformity to the expectations of Hardy-Weinberg (H-W) equilibrium. This is not surprising given the importance of random mating and sexual reproduction in the maintenance of H-W equilibrium, and the known variation of these life history traits among trypanosome taxa (Gibson, 2007; Weir *et al.*, 2015). For *T. brucei* only isolates (Table 4.8B), within cluster allelic richness estimates were very similar but slightly lower than the estimates based on all isolates (Table 4.8A).

Table 4. 8: Genetic diversity found within each STRUCTURE-based genetic clusters.

A.	N	A_R	H_O	H_E	F_{IS}
“a” (orange)	6	2.55	0.58	0.57	-0.02
“b” (purple)	16	3.07	0.55	0.61	0.10
“c” (blue)	10	3.67	0.63	0.76	0.16
“d” (green)	4	2.10	0.55	0.47	-0.20
“e” (yellow)	33	2.35	0.66	0.51	-0.30
“f” (grey)	8	3.86	0.53	0.78	0.34
“g” (red)	9	3.48	0.50	0.71	0.31
Overall	86	3.01	0.57	0.63	0.10

B.	N	A_R	H_O	H_E	F_{IS}
Tb “a” (orange)	6	2.55	0.58	0.56	-0.02
Tb “b” (purple)	16	3.07	0.55	0.61	0.10
Tb “c” (blue)	8	3.70	0.63	0.76	0.19
Tb “d” (green)	4	2.10	0.55	0.47	-0.18
Tb “f” (grey)	7	3.77	0.50	0.76	0.36
Tb “g” (red)	6	3.22	0.55	0.66	0.22
Tb overall	47	3.07	0.56	0.64	0.11

C	N	A_R	H_O	H_E	F_{IS}
Tev “c/f” (blue/grey)	3	n/a	0.69	0.72	0.06
Tev “e” (yellow)	33	2.35	0.66	0.51	-0.30
Tev “g” (red)	3	n/a	0.40	0.36	0.19
Tev overall	39	2.35	0.58	0.59	-0.09

(A) all isolates, (B) *T. brucei* (Tb) isolates only, and (C) *T. evansi* (Tev) isolates only. Sample size within the cluster (N), allelic richness (A_R) calculated in *FSTAT v1.2* (Goudet, 2005), and observed heterozygosity (H_O), expected heterozygosity under Hardy-Weinberg expectations (H_E), and the inbreeding coefficient (F_{IS}) calculated in the R package *HIERFSTAT v0.4-10* (Goudet, 1995, 2005). Allelic richness could not be calculated in clusters made up of less than 4 individuals (marked n/a).

H_O ranged from 0.50 to 0.63, H_E ranged from 0.47 to 0.76, and F_{IS} values were mostly positive, ranging from -0.18 to 0.36 (Table 4.8B). Thus, *T. brucei* observed and expected heterozygosity and F_{IS} values indicate moderate deviation from H-W expectations, and are similar to those reported in a previous study (Prugnolle, 2008), where F_{IS} ranged from -0.16 to 0.43. For *T. evansi* only isolates (Table 4.8C), within cluster allelic richness was intermediate to that found in *T. brucei*, indicating genetic diversity similar to that found in *T. brucei*. H_O ranged from 0.40 to 0.69, H_E ranged from 0.36 to 0.72, and F_{IS} values ranged from -0.30 to 0.19. Negative F_{IS} in some clusters in both *T. brucei* and *T. evansi* could result from clonal, non-sexual reproduction (as expected for the latter) because there is a well understood decrease in expected heterozygosity during clonal reproduction, which lowers F_{IS} (Prugnolle, 2008). The finding of relatively high allelic richness in all clusters and both positive and negative F_{IS} values in both *T. brucei* (Table 4.8B) and *T. evansi* (Table 4.8C) could be a reflection of different relative levels of sexual and clonal reproduction and recombination among *T. brucei* isolates in different clusters, and to the fact that for *T. evansi* isolates are strictly clonal.

To evaluate if levels of genetic differentiation among *T. evansi* isolates were different from the ones observed among *T. brucei* isolates, pairwise genetic distances was estimated, using Reynolds distances. First, a distance tree was estimated using all the 107 isolates (Figure 4.10).

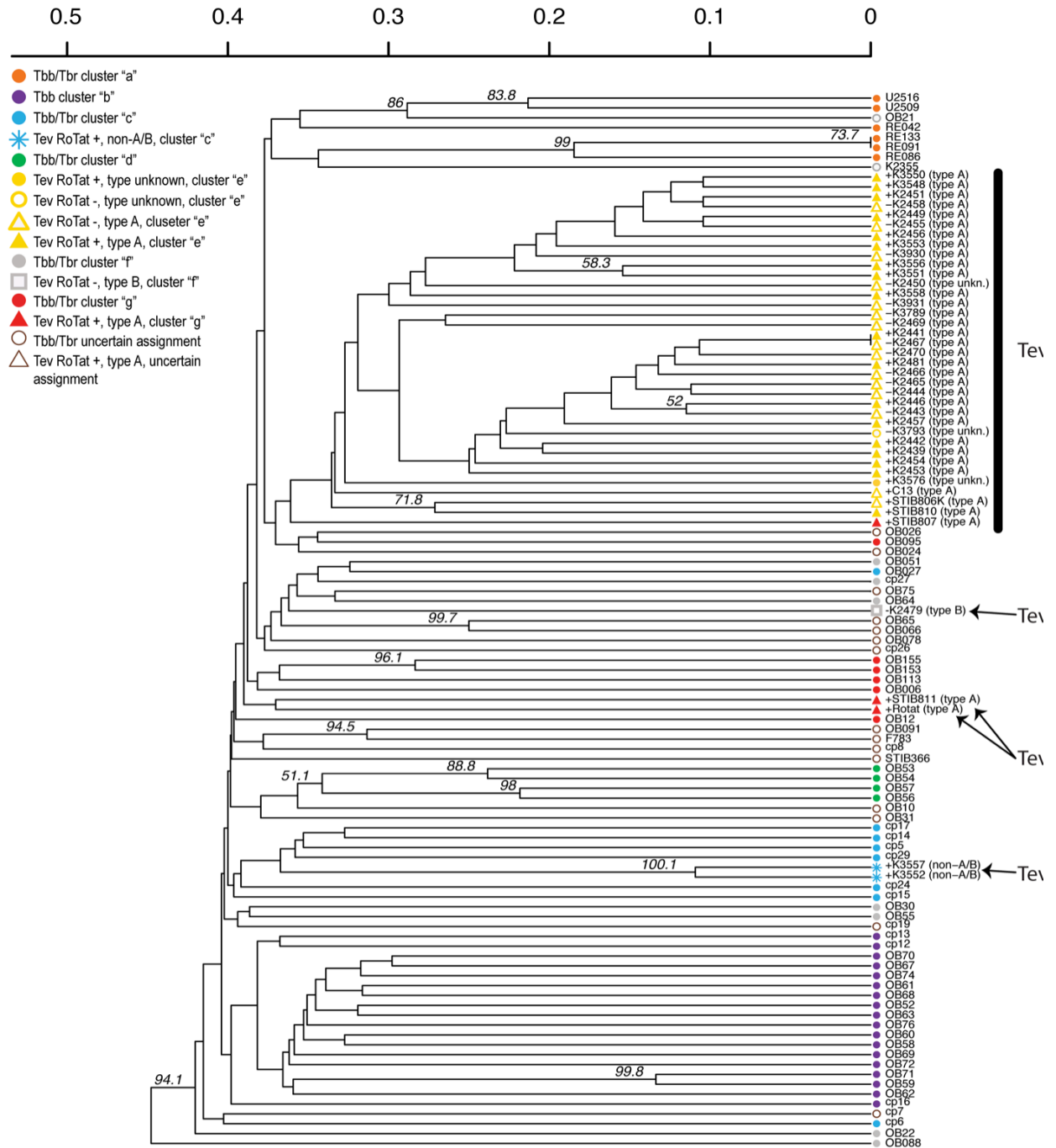


Figure 4. 10: Distance tree based on 15 microsatellite markers and Reynolds *et al* (1983) distances using the UPGMA method implemented in the R package, “PopPR” v2.3 (Goudet, 1995, 2005). Support values are shown on nodes only for values above 50% and are based on 1000 bootstrap replicates. Terminal tips identify the strains (Table 3.1 and Table 3.2) and are colour coded according to the upper left legend with respect to their STRUCTURE-defined cluster assignment and the results of the diagnostic PCR assays (Table 3.1). The major *T. evansi* cluster is shown with a black vertical bar, and the other *T. evansi* strains are marked with black arrows.

This tree clustered the *T. evansi* isolates in four different groups, confirming the results of both Bayesian and multivariate analyses (Figures 4.8 and 4.9), although bootstrap values among these groups are not high, thus limiting the strength of the inference that can be drawn from this analysis. Next, within-cluster distances was estimated using the STRUCTURE-defined clusters, including only the 84 isolates with $Q > 0.8$ (Table 4.7), as described for the estimates of basic diversity statistics (Table 4.8). Within-cluster mean distances among all isolates (Table 4.9A) averaged 0.70 and ranged from 0.57 in cluster “e” to 0.80 in cluster “f”, indicating that the lowest within-cluster distance occurs in the *T. evansi* only cluster, and the highest within-cluster distance occurs in a cluster that contains *T. b. brucei*, *T. b. rhodesiense* and *T. evansi* of type B.

Table 4. 9: Within-cluster distance using STRUCTURE-based genetic clusters including strains with Q values > 0.80

A.	N pairs	Mean distance	SD	Min	Max
“a” (orange)	28	0.67	0.15	0.37	0.82
“b” (purple)	240	0.73	0.06	0.27	0.84
“c” (blue)	90	0.74	0.09	0.22	0.85
“d” (green)	12	0.61	0.11	0.44	0.72
“e” (yellow)	1188	0.57	0.13	0.21	0.77
“f” (grey)	56	0.80	0.06	0.71	0.90
“g” (red)	72	0.78	0.05	0.57	0.85
Overall	1686	0.70	0.10	0.21	0.90
B.	N pairs	Mean distance	SD	Min	Max
Tb “a” (orange)	28	0.67	0.15	0.37	0.82
Tb “b” (purple)	240	0.73	0.06	0.27	0.84
Tb “c” (blue)	56	0.76	0.06	0.65	0.85
Tb “d” (green)	12	0.61	0.11	0.44	0.72
Tb “f” (grey)	42	0.81	0.06	0.71	0.90
Tb “g” (red)	30	0.76	0.06	0.57	0.82
Overall Tb	408	0.72	0.08	0.27	0.90

C.	N pairs	Mean distance	SD	Min	Max
Tev “c/f” (blue/grey)	6	0.60	0.29	0.22	0.78
Tev “e” (yellow)	1188	0.57	0.13	0.21	0.77
Tev “g” (red)	6	0.75	0.01	0.74	0.75
Overall Tev	1200	0.64	0.14	0.21	0.78

(A) all strains regardless of taxonomy, (B) *T. brucei* (Tb) strains, and (C) *T. evansi* (Tev) strains. Number of pairwise between-strain comparisons (N pairs), mean Reynolds (1983) (Kamvar *et al.*, 2015, 2014) distance (mean distance) estimated in the R package “PopPR” v2.3.0 (Goudet, 1995, 2005) standard deviation (SD), minimum distance (min), and maximum distance (max).

Within-cluster mean distances among *T. brucei* isolates averaged 0.72 and ranged from 0.61 in cluster “d” to 0.81 in cluster “f” (Table 4.9B). Finally, within-cluster mean distances among *T. evansi* isolates averaged 0.64 and ranged from 0.57 in cluster “e” to 0.75 in cluster “g” (Table 4.9C). The implications of these findings for evolutionary origins of *T. evansi* are discussed in detail below.

The analysis of variance (ANOVA) indicated that within-cluster distance was significantly dependent on cluster of assignment (p-value < 0.0001). The results of the Tukey-Kramer HSD test are reported in Table 4.10.

Table 4. 10: Summary of differences in within-cluster Reynolds (1983) distance of STRUCTURE-defined clusters

A.						
Cluster 1	Cluster 2	Dif	Std Err Dif	Lower CL	Upper CL	p-Value
within "f"	within "e"	0.24	0.02	0.18	0.29	<.0001
within "f"	within "d"	0.20	0.04	0.08	0.31	<.0001
within "g"	within "e"	0.19	0.02	0.13	0.25	<.0001
within "c"	within "e"	0.17	0.02	0.12	0.21	<.0001
within "b"	within "e"	0.16	0.01	0.13	0.18	<.0001
within "g"	within "d"	0.15	0.04	0.03	0.27	0.003
within "f"	within "a"	0.14	0.03	0.05	0.23	<.0001
within "c"	within "d"	0.13	0.04	0.02	0.24	0.010
within "b"	within "d"	0.12	0.04	0.02	0.22	0.010
within "a"	within "e"	0.10	0.02	0.03	0.16	0.001
within "g"	within "a"	0.09	0.03	0.00	0.18	0.038
within "f"	within "b"	0.08	0.02	0.02	0.14	0.002
within "c"	within "a"	0.07	0.03	-0.01	0.15	0.137
within "f"	within "c"	0.07	0.02	0.00	0.14	0.060
within "b"	within "a"	0.06	0.02	-0.01	0.13	0.133
within "a"	within "d"	0.06	0.04	-0.06	0.18	0.764
within "f"	within "g"	0.05	0.03	-0.03	0.13	0.550
within "d"	within "e"	0.04	0.03	-0.07	0.14	0.944
within "g"	within "b"	0.03	0.02	-0.03	0.09	0.794
within "g"	within "c"	0.02	0.03	-0.05	0.10	0.981
within "c"	within "b"	0.01	0.02	-0.04	0.06	0.999

B					
Cluster	Group "*" "	Group "•" "	Group "†" "	Group "§" "	Group "¥" "
within "a"			†	§	
within "b"		•	†		
within "c"	*	•	†		
within "d"				§	¥
within "e"					¥
within "f"	*				
within "g"	*	•			

Cluster based on analysis of variance (ANOVA, p-value < 0.0001), and the Tukey-Kramer HSD test performed in JMP v11.2 (SAS Institute Inc., Cary, NC, USA, 1989– 2012), using only the 86 strains with Q values >0.80 (Table 4.6): (A) Ordered difference report between clusters showing the clusters compared (cluster 1 and cluster 2), the difference in mean

Reynolds distance (Dif), the standard error of the difference (Std Err Dif), the lower confidence level (CL), the upper confidence level (CL), and the p-value of the pairwise comparison. (B) The connecting symbols report that summarizes the Tukey-Kramer HSD tests, where each symbol group (¥, §, †, •, *) contain significantly different within-cluster pairwise genetic distances (¥ joins clusters “d” and “e”; § joins clusters “a” and “d”; † joins clusters “a”, “b”, and “c”; • joins clusters “a”, “b”, “c”, and “g”; and * joins clusters “c”, “f”, and “g”).

and indicated that *T. evansi* cluster “e” and *T. brucei* cluster “d” had significantly lower within-cluster distance than any other cluster (Figure 4.11), suggesting that the most common *T. evansi* lineage (cluster “e”) is of recent origin and is made up of more closely related isolates than those included in most *T. brucei* clusters (except cluster “d”).

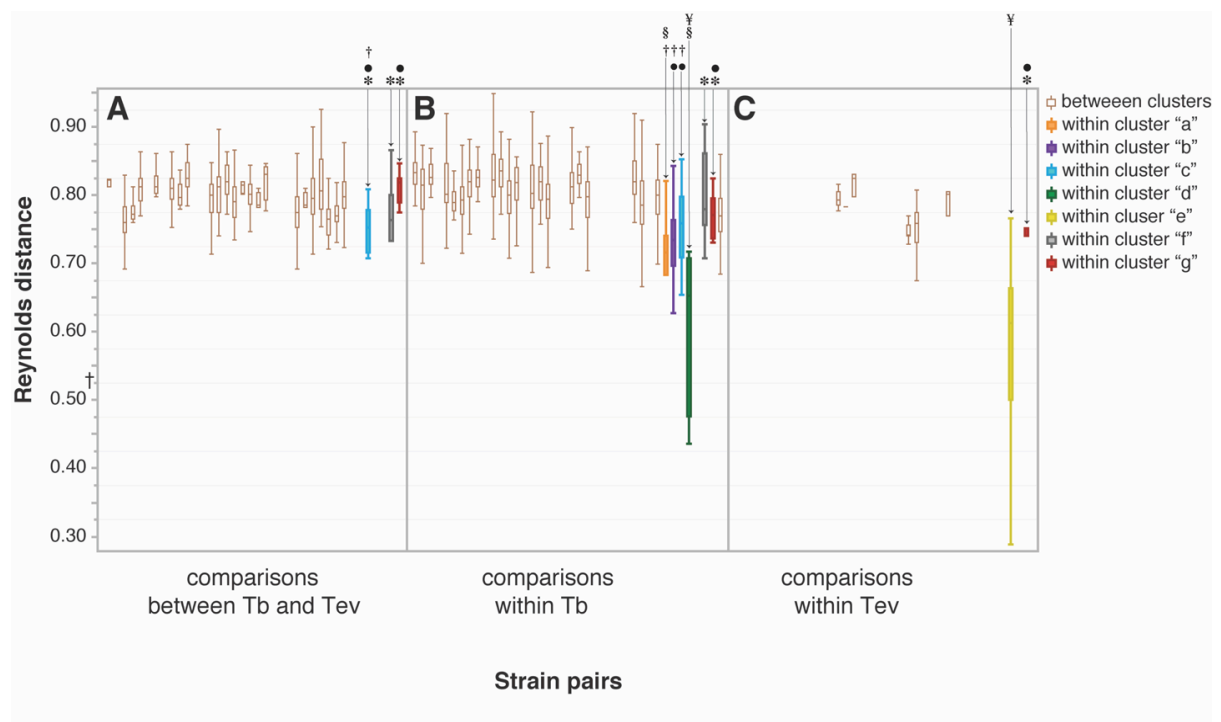


Figure 4. 11: Summary of pairwise Reynolds (1983) genetic distances computed in the R package “PopPR” v2.3.0 (Goudet, 1995, 2005) between strains belonging to the same or different STRUCTURE-defined clusters as outlier box-plots colour coded according to legend to the left. Boxes and whiskers on each box-plot represent the minimum, 1st quartile, 3rd quartile, and maximum distances. Panel (A) displays distances between a *T. brucei* strain and a *T. evansi* strain, panel (B) displays distances between two *T. brucei* strains, and panel (C) displays distances between two *T. evansi* strains. Each symbol (¥, §, †, •, and *) represents a group of statistically distinct within-cluster distance based on the analysis of variance (ANOVA, p-value < 0.0001), and the Tukey-Kramer HSD test performed in JMP v11.2 (SAS Institute Inc., Cary, NC, USA, 1989– 2012). Boxplots that are not connected with the same symbol contain significantly different levels of among-cluster genetic distances. For example, ¥ joins clusters “d” (green) and “e” (yellow), indicating significantly lower within-

cluster distance in these two clusters than any other cluster. See Table S5 for details of the Tukey-Kramer HSD test.

However, since this test could only be carried out for one of the *T. evansi* clusters, cluster “e”, because of low number of *T. evansi* isolates in the other clusters, the generalitiy of this finding remains uncertain without further sampling of a greater diversity of *T. evansi* isolates from non “e” clusters.

To compare among-cluster differentiation in *T. evansi* and *T. brucei*, among-cluster F_{ST} was estimated using the STRUCTURE-defined clusters and only including the 84 isolates with $Q > 0.8$ (Table 4.7), as described for the estimates of basic diversity statistics (Table 4.8). F_{ST} estimates are reported in Table 4.10. Among-cluster F_{ST} estimates between clusters regardless of taxonomy (Table 4.11A) ranged from 0.08 between clusters “g” and “e” to 0.31 between clusters “a” and “d” and showed significant differentiation between all clusters (p-value < 0.006), indicating that the lowest genetic differentiation was found between two clusters that contained *T. evansi* (“g” and “e”), and that the highest genetic differentiation was found between two clusters (“a” and “d”) made up of entirely *T. brucei* isolates.

Table 4. 11: Among-cluster genetic differentiation (F_{ST}) among each STRUCTURE-defined genetic cluster.

A.	"a"	"b"	"c"	"d"	"e"	"f"	"g"
"a"		0.000	0.000	0.006	0.000	0.000	0.000
"b"	0.21		0.000	0.000	0.000	0.000	0.000
"c"	0.17	0.16		0.001	0.000	0.000	0.000
"d"	0.31	0.18	0.18		0.000	0.002	0.001
"e"	0.11	0.23	0.15	0.14		0.000	0.000
"f"	0.15	0.15	0.10	0.16	0.12		0.000
"g"	0.13	0.17	0.13	0.20	0.08	0.11	

B.	Tb "a"	Tb "b"	Tb "c"	Tb "d"	Tb "f"	Tb "g"
Tb "a"		0.000	0.001	0.005	0.001	0.002
Tb "b"	0.21		0.000	0.000	0.000	0.000
Tb "c"	0.18	0.15		0.003	0.001	0.000
Tb "d"	0.31	0.18	0.19		0.004	0.005
Tb "f"	0.16	0.15	0.10	0.17		0.001
Tb "g"	0.15	0.17	0.15	0.27	0.14	

C.	Tev "c/f"	Tev "e"	Tev "g"
Tev "c/f"		0.000	0.105
Tev "e"	0.29		0.000
Tev "g"	0.06	0.09	

Using only strains with Q values >0.80 (Table. 4.6): (A) all strains, (B) *T. brucei* (Tb) strains only, and (C) *T. evansi* (Tev) strains only. Pairwise F_{ST} (below diagonal) was calculated in ARLEQUIN v.3.2 (Wright, 1951) with Wright's statistics (Wright, 1951), following the variance method developed by Weir and Cockerham (1984) (Weir and Cockerham, 1984) using 10,000 permutations to obtain exact p-values (above diagonal), with the only non-significant F_{ST} found (between *T. evansi* cluster "e" and "g") in bold.

Thus, the most common *T. evansi* cluster "e" is less differentiated from the *T. brucei*-only cluster "a" than both *T. brucei*-only clusters "a" and "d" are to one another. Among-cluster F_{ST} estimates in *T. brucei* (Table 4.11B) ranged from 0.10 to 0.31 (Table 4.11B), and showed significant differentiation between all clusters (p-value < 0.005), indicating high levels of genetic differentiation. Among-cluster F_{ST} in *T. evansi* (Table 4.11C) were similar to those in *T. brucei*, ranging from 0.06 to 0.29, and showed significant differentiation (p-value <

0.0001) between *T. evansi* in all clusters except the least differentiated clusters “e” and “g”, suggesting *T. evansi* cluster “e” and “g” are not significantly differentiated from each other. The low sample size of *T. evansi* in cluster “g” remains another possible reason for the non-significant p-value in F_{ST} estimates between “e” and “g”, and again highlight the need for further sampling of a greater diversity of *T. evansi* strains from non “e” clusters.

These results indicate that the genetic diversity across all *T. evansi* isolates (“overall” in Table 4.8C and 4.9C) represents a large amount of the genetic diversity found across *T. brucei* isolates (“overall” in Table 4.8B and 4.9B). However, within clusters including all isolates, the most common *T. evansi* cluster, cluster “e”, shows the least amount of genetic differentiation among isolates and the lowest amount of within-cluster genetic diversity compared to other clusters (Table 4.8A and 4.9A), with only the *T. brucei* cluster “d” showing similarly low levels (Table 4.8A and 4.9A). The Chi-square test showed that the time of isolation did not account for cluster assignment ($\chi^2=20.19$, degrees of freedom = 30, p-value = 0.9113).

4.2.4 Interpretation of evolutionary origins of *T. evansi*

Clustering and diversity analysis indicate that *T. evansi* strains likely originated from multiple genetic backgrounds (Figure 4.8 and 4.9) and that the genetic diversity harboured by the *T. evansi* isolates analyzed in this study encompass a large proportion of the total diversity found in the *T. brucei* isolates (Tables 4.8 and 4.9). The single type B and the two unclassified isolates fall into distinct clusters (“f” and “c”, respectively; Figure 4.8), while type A isolates separate into two clusters (“e” and “g”; Figure 4.8), that are closely associated in the multivariate analysis (yellow and red; Figure 4.9). Cluster “e” is made up entirely of *T. evansi* isolates (Figures 4.8 and 4.9), while cluster “g” includes a mix of *T. b. brucei*, *T. b. rhodesiense*, and *T. evansi* (Figures 4.8 and 4.9). Separation of type A into two closely related

clusters suggests that the *T. evansi* only cluster "e" has evolved from within cluster "g", and both have evolved from the same *T. brucei* ancestor. Nonetheless, these results could also indicate that traits that are common between *T. evansi* in clusters "e" and "g" have evolved twice, independently. Evidence for these alternative hypotheses remains inconclusive. Support for a single origin of type A from within cluster "g" comes from the non-significant differentiation (FST) found between the *T. evansi* isolates in clusters "e" and "g" (Fst = 0.06, p-value = 0.105; 4.11C Table), which indicates high similarity between these clusters. Furthermore, certain *T. evansi* isolates from China (STIB810, STIB811, and STIB806K) that were isolated within 3 years from each other and presumably are closely related can be found in both clusters "e" and "g": STIB810 assigns to cluster "e", STIB811 assigns to cluster "g", and STIB806K assigns about equally to both "e" and "g" (Figure 4.8), suggesting the "e" and "g" clusters are not the result of distinct geographic origins or outbreaks. Thus, distinct clustering of type B in cluster "f", distinct clustering of unclassified isolates in cluster "c", and nested clustering of type A isolates in the two closely related clusters "e" and "g" suggests independent origins of each *T. evansi* kDNA type from a diverse *T. brucei* background.

4.3 To determine the origin and dynamics of the *T. evansi* spatial expansion from Africa to multiple continents

STRUCTURE results indicated two major clusters (Figure 4.12). One cluster at $K=2$ was made up of *T. b. brucei*, *T. b. rhodesiense*, three *T. evansi* isolates and four *T. equiperdum* isolates (orange in Figure 4.13). The other cluster at $K=2$ contained the remaining *T. evansi* and *T. equiperdum* isolates (green in Figure 4.13). The next most likely number of clusters was nine (Figure 4.12).

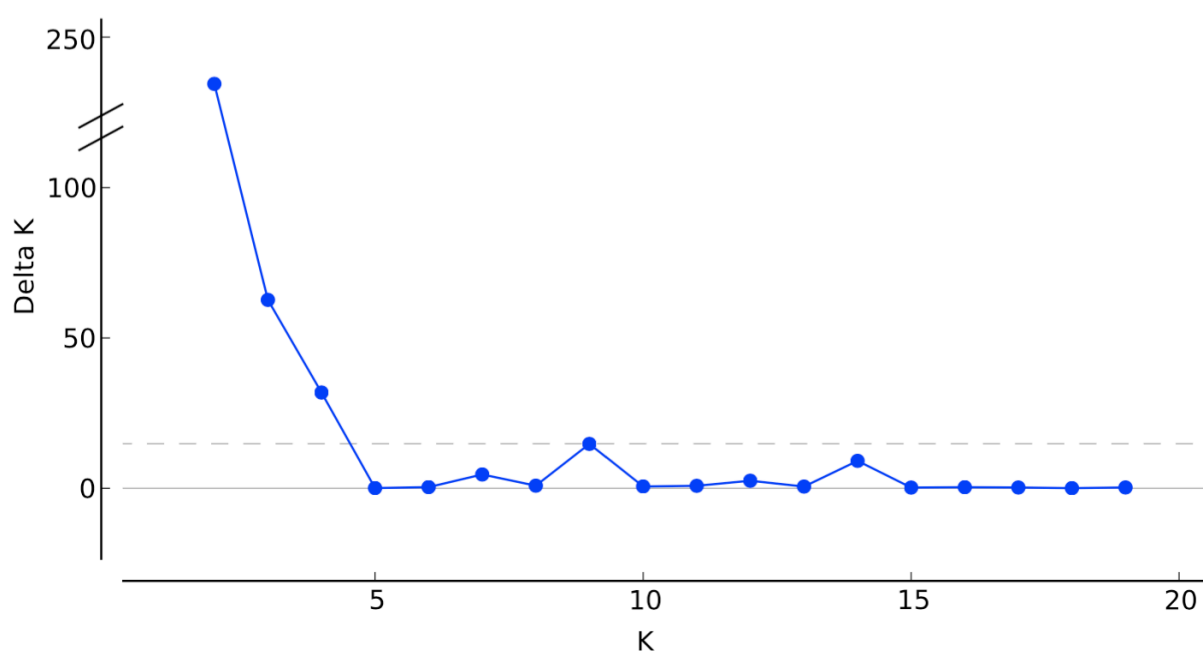


Figure 4. 12: STRUCTURE v2.3.4 plot of delta K (K=1 through 20) based on 20 runs each performed with a burn-in of 50,000 and a total of 250,000 iterations. Although $K=2$ had the highest delta K and thus explained the highest hierarchical level in the data, a K value of 9 was the next hierarchical level with a peak in delta K, and was able to distinguish structure within *Trypanosoma brucei brucei* and *T. b. rhodesiense*. See Figure S2 for display of $K=2$.

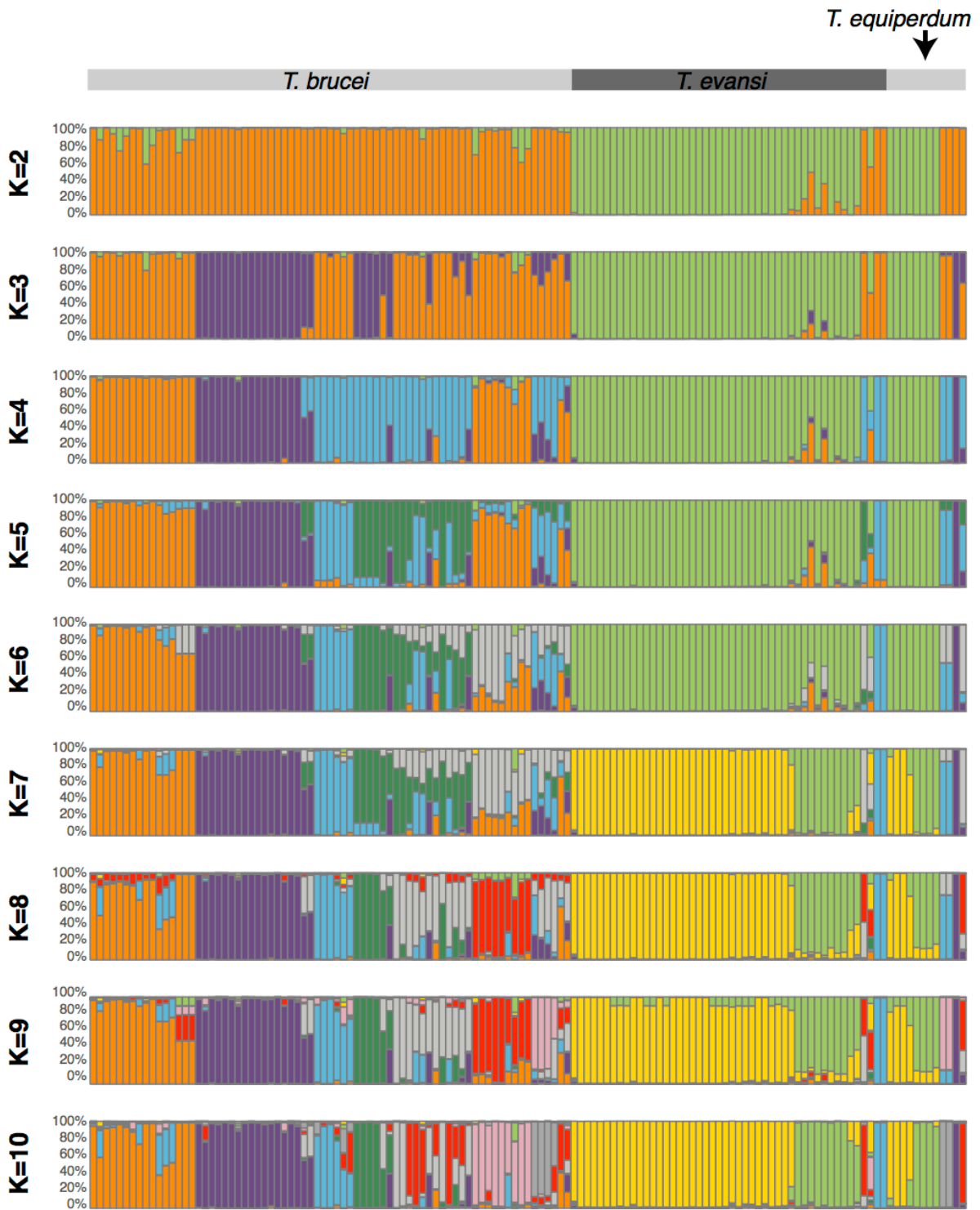
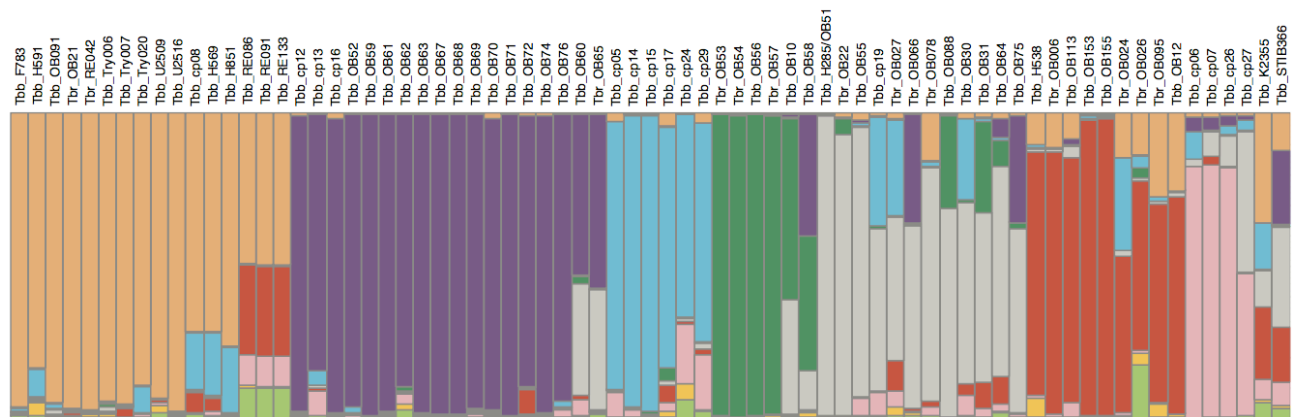


Figure 4. 13 : STRUCTURE (Pritchard *et al.*, 2000) results for K values 2-10 in the same order as 4.14. Each bar represents the composite genotype of one individual, the colours within the bar reflect the assignment probability (q-value) of that individual to one of K genetic clusters, and grey horizontal bars indicate the species of each isolate.

At this lower hierarchical level, a similar pattern emerged, with all but three *T. evansi* isolates and four *T. equiperdum* isolates clustered together in clusters “H” or “I” (yellow or green in Figure 4.14). The *T. evansi* and *T. equiperdum* isolates that were not included in clusters “H” or “I” either fell squarely within clusters “B”, “C” or “G” (purple, blue or pink in Figure 4.14), or were of mixed assignment to clusters “E”, “F” and “H” (grey, red or yellow in Figure 4.14). Besides these unusual *T. evansi* and *T. equiperdum* isolates, clusters “B”, “C”, and “G” contained only *T. b. brucei*, and clusters “A”, “D”, “E”, and “F” contained a mix of *T. b. brucei* and *T. b. rhodesiense*.

A.



B.

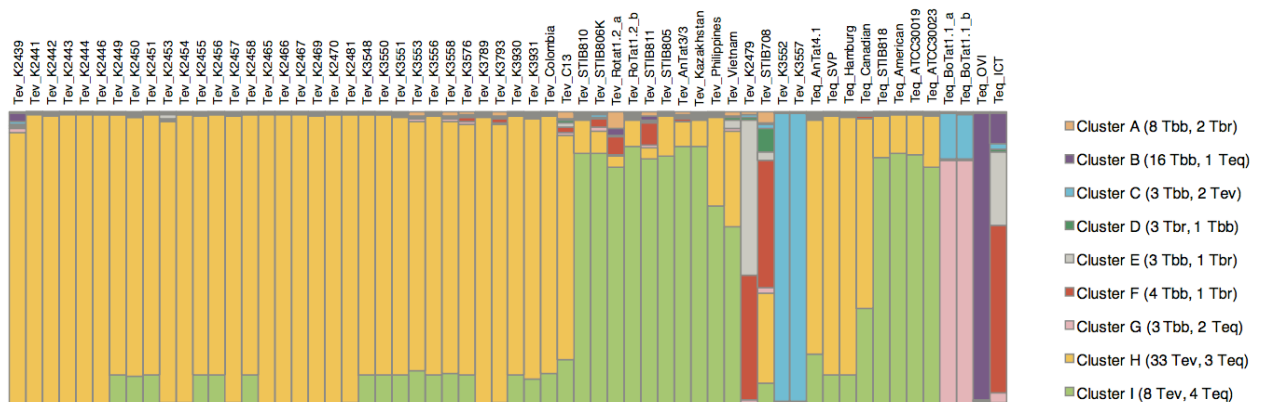
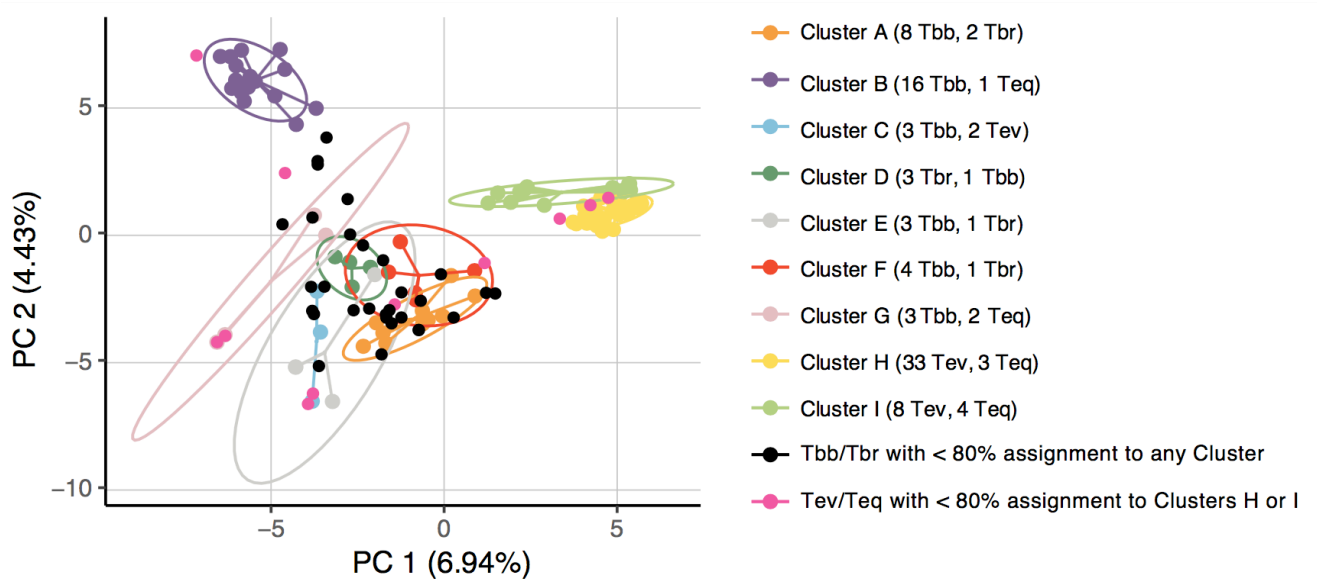


Figure 4. 14 : Plot of STRUSTRUCTURE v2.3.4 (Pritchard *et al.*, 2000) assignment scores with K=9 for (A) *Trypanosoma brucei brucei* (Tbb) and *T. b. rhodesiense* (Tbr) isolates, and (B) *T. evansi* (Tev) and *T. equiperdum* (Teq) isolates. Each vertical bar represents an isolate’s probability of assignment to one of nine genetic clusters "A" through "I", and grey horizontal bars indicate the species of each isolate.

In the PCA, *T. evansi* / *T. equiperdum* clusters “H” and “I” overlapped in the ellipses that circumscribed 80% of the variance, indicating close genetic similarity. Three *T. evansi* and four *T. equiperdum* isolates fell well outside of the 80% ellipses for clusters “H” and “I”, and either close to, or within, the 80% ellipses of *T. brucei* clusters (Figure 4.15).

A.



B.

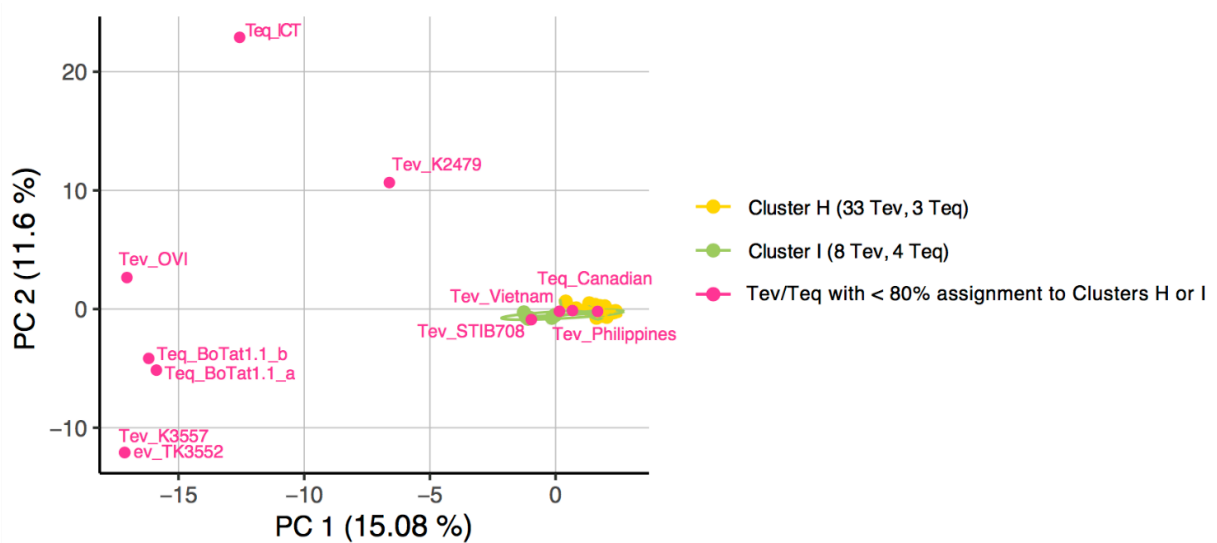


Figure 4. 15: Evaluation of the genetic differentiation between (A) all isolates, and (B) only *T. evansi* (Tev) and *T. equiperdum* (Teq) isolates, using principal components analysis (PCA) of microsatellite data. Points representing individual genotypes following the key. If an individual had > 80% STRUCTURE assignment probability, the point is connected by a line to the centroid of an ellipse, which circumscribes a region encompassing 80% of the variance observed within that STRUCTURE cluster. If an individual had < 80% STRUCTURE assignment probability (uncertain assignment), it is not included in any ellipse. PCA was performed in R using the package “adeigenet” (Jombart, 2008), and visualization was done using the package “ggplot2”.

Thus, the PCA analysis independently supported closer clustering of three *T. evansi* and four *T. equiperdum* isolates with *T. brucei* clusters than with the two main *T. evansi* / *T. equiperdum* clusters “H” and “I”. The NJ tree indicates close relationships between *T. evansi* isolates belonging to clusters “H” and “I” (yellow and green), but distant relationships among the three *T. evansi* and four *T. equiperdum* isolates with assignment to other clusters (Figure 4.16).

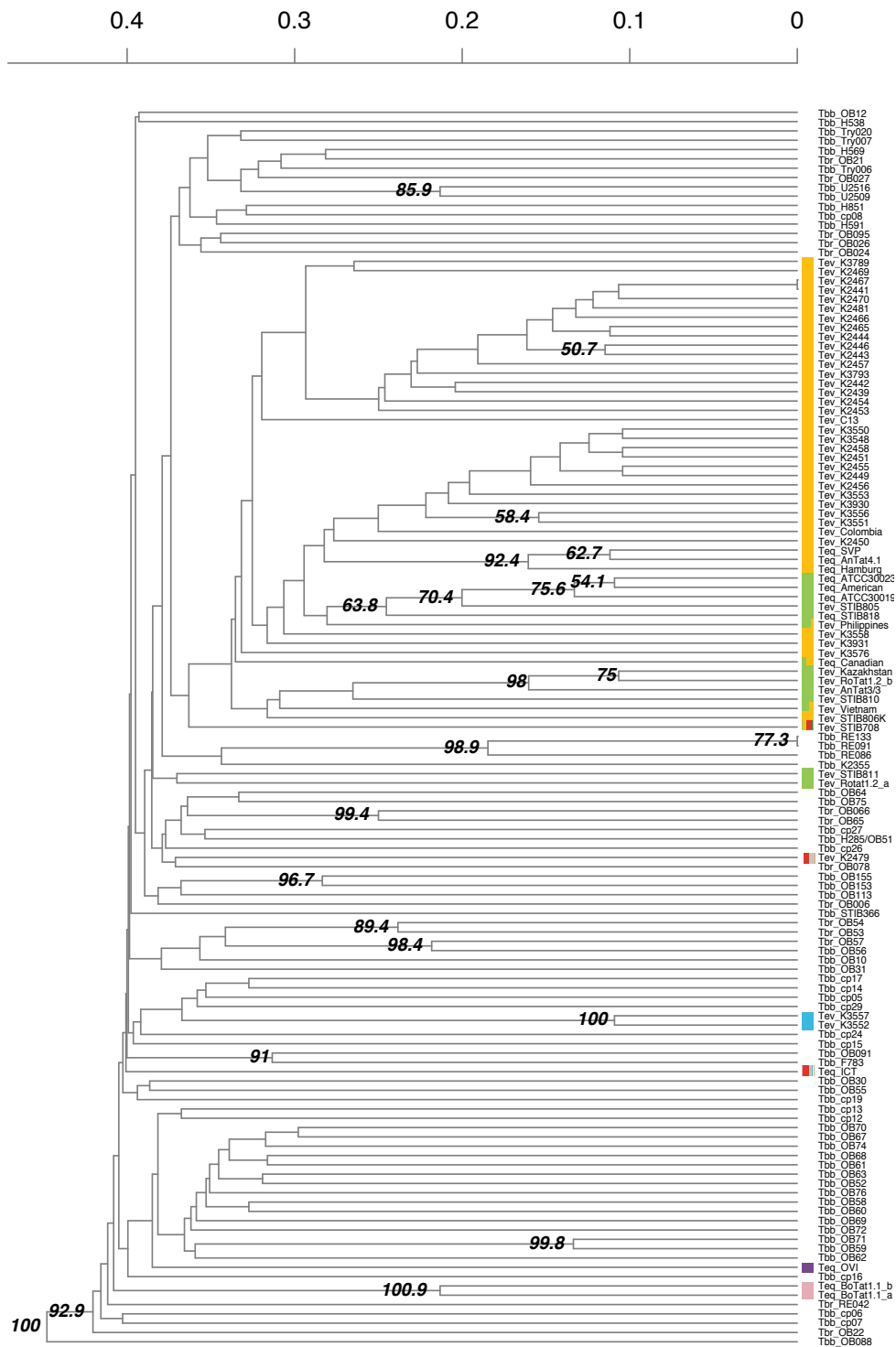


Figure 4. 16: Distance tree based on Reynolds *et al* (1983) distances using the UPGMA method implemented in the R package, “PopPR” v2.3. Support values are shown on nodes only for values above 50% and are based on 1000 bootstrap replicates. Terminal tips identify the isolates, and *T. evansi* isolates are colour coded according to their major cluster of assignment in STRUCTURE analysis.

Mean allelic richness was highest at 7.58 in *T. b. brucei*, lowest at 4.63 in *T. evansi*, and intermediate at 7.35 and 6.19 in *T. b. rhodesiense* and *T. equiperdum*, respectively (Table 4.12). Observed and expected heterozygosity levels, as well as F_{IS} estimates and significant deviations from Hardy-Weinberg indicate heterozygote deficits in *T. b. brucei*, *T. b. rhodesiense* and *T. equiperdum*, but not in *T. evansi* (Table 4.12).

Table 4. 12: Genetic diversity found within *Trypanosoma brucei brucei*, *T. b. rhodesiense*, *T. evansi*, and *T. equiperdum*.

	N	A _R	F _{IS}	p-value	H _O	H _E
<i>T. b. brucei</i>	59	7.58	0.30	0.0008*	0.59	0.84
<i>T. b. rhodesiense</i>	14	7.35	0.28	0.0008*	0.60	0.79
<i>T. evansi</i>	48	4.63	-0.07	0.0017	0.64	0.59
<i>T. equiperdum</i>	12	6.19	0.23	0.0008*	0.56	0.70
Overall	133	6.36	0.20	n/a	0.60	0.75

*significant after adjusting for multiple testing at a nominal level of 5% (below p-value of 0.00083).

The sample size (N), allelic richness (A_R), the inbreeding coefficient (F_{IS}) and the p-value for tests for deviations from Hardy-Weinberg equilibrium (p-value) calculated in *FSTAT v1.2* (Goudet, 2005), and observed and expected heterozygosity (H_O and H_E) calculated in the R package *HIERFSTAT v0.4-10* (Pritchard *et al.*, 2000).

Comparison of these results with Kamidi *et al*'s (2017) study supports the same grouping into two major clusters. However, in this analysis the next most likely clustering was K=9 rather than K=7 (Goudet, 1995). The data also showed more structure within the common *T. evansi* / *T. equiperdum* clusters (yellow and green in Figure 4.14), and an additional *T. brucei* cluster that contains two *T. equiperdum* isolates (pink in Figure 4.14).

All three analyses supported multiple origins of *T. evansi* and *T. equiperdum* from *T. brucei* ancestors. The STRUCTURE results grouped *T. evansi* / *T. equiperdum* within seven different clusters, the PCA indicated close relationships to at least four distinct clusters (Figure 4.15A), and the NJ tree placed *T. evansi* isolates in seven regions of the tree (Figure 4.16). Results suggest the most common *T. evansi* / *T. equiperdum* clusters (“H” and “I”) evolved either from a single origin with later divergence, or evolved independently from a *T. brucei* source similar to clusters “E” or “F”. Interestingly, in the

PCA, the three samples with mixed STRUCTURE assignments to clusters “H” and “I” fall almost exactly between the two clusters (Figure 4.15B), supporting a single origin of clusters “H” and “I” with later divergence rather than independent origins of clusters “H” and “I”. The origin of *T. evansi* isolates with mixed STRUCTURE assignment to clusters “E” and “F” may also be from the same source because PCA placed them intermediate to two extant *T. brucei* isolates and *T. evansi* / *T. equiperdum* clusters “H” and “I” (Figure 4.15A). In contrast, the origin of *T. evansi* and *T. equiperdum* assigned to cluster “B”, “C” and “G” are almost certainly from a different *T. brucei* origin because of their high STRUCTURE assignment probabilities to clusters distinct from the most common *T. evansi* / *T. equiperdum* clusters (Figures 4.13 and 4.14) and their distance from clusters “H” and “I” in the PCA (Figure 4.15) and the NJ tree (Figure 4.16).

CHAPTER FIVE

DISCUSSION

5.1 Differential virulence of *T. evansi* in mice

The present study demonstrated the existence of different levels of virulence in *T. evansi* isolates from Kenya. Virulence was measured using parasitaemia, mortality (survivorship data), levels of anaemia and weight loss experienced by the host during the infection: these are positive indicators of the probability of host death as described by various authors (De Menezes *et al.*, 2004; Mackinnon *et al.*, 2008; Mekata *et al.*, 2013). The observed virulence levels ranged from low, moderate to high. High and persistent parasitaemia was recorded in some animals whereas this appeared in waves in other groups infected with different trypanosome isolates. The high and persistent parasitaemia for over ten days was mainly associated with rapid decline in both packed cell volume and body weight, indicating disease severity. The results also demonstrated that low and intermittent parasitaemia was associated with maintenance and in some cases, weight gain when compared with uninfected animals ($p < 0.05$). The most pathogenic of the three categories was the moderate virulence category, which persisted in the host long enough, presenting the opportunity for horizontal transmission to new hosts to take place, with high density of parasites throughout the course of infection. The rapid death of the mice infected with the high virulent group of parasites suggested lack of trade-off between the host and pathogen as would occur in epidemics. The animals did not survive long enough to allow multiplication and transmission to new hosts.

Ability to control parasitaemia and remain productive is one of the main characteristics used in the determination of resistance to trypanosomiasis in animals (Noyes *et al.*, 2009); the other two being the ability to develop an effective immune response and to resist the development of anaemia (Noyes *et al.*, 2009). In the present study, the animals that were able

to control parasitaemia (low virulence) were also able to control PCV and generally maintain live body weights. Parasitaemia profiles were significantly different between low and high virulent groups as defined by survivorship. Under the trade-off hypothesis (Alizon *et al.*, 2009), it is assumed there are costs as well as fitness benefits to the host and parasite associated with virulence. The parasite maximizes transmissibility and length of infection while keeping the host alive and, in the present study, this was observed in the medium and low virulence groups where the parasites survived in the host between 15 - 60 dpi. Findings suggest that, where the majority of the infections (high virulence) lead to host death within 10 days, it is highly likely that transmission would cease immediately as in epidemics, concurring with observations of (Mackinnon *et al.*, 2008). Three *T. evansi* isolates showed intermittent parasitaemia in the low virulent group, suggesting possible development of new variants of the parasite in infected mice as the animals were able to control the infection and survived up to 60 days' observation period. Intermittent parasitaemia can be explained by the fact that parasites use different strategies to evade the mammalian hosts' immune system, one of which is population growth (Alizon *et al.*, 2009). This helps the parasite to avoid elimination by specific potent immune responses (Vincendeau and Bouteille, 2006). Parasites are challenged and killed by these specific responses, however, some yield variants that proliferate and produce a new population. This is repeated and is the basis of the antigenic variation (Maudlin and Holmes, 2004). The antigenic variation has posed challenges to vaccine development in trypanosomiasis (Magez *et al.*, 2010). Of 17 isolates investigated, with the exception of KETRI 3552, 3567, 3573 and 3576, the rest showed high and persistent parasitaemia, suggesting inability of the animals to mount defense to fight the infection caused by the highly virulent parasites. In a study using *E. coli*, (Berngruber *et al.*, 2013) tested the theory 'that predicts that selection for pathogen virulence and horizontal transmission is highest at the onset of an epidemic but decreases thereafter, as the epidemic

depletes the pool of susceptible hosts', providing proof that the virulent strain is strongly favoured in the early stage of the epidemic, but loses competition with the latent virus as prevalence increases. This could be the reason for high morbidity reported in camels in different parts of the world where the disease is endemic (Murray, 1979).

The ability to control parasitaemia enables the animals to develop an effective immune response (Murray, 1979). In their studies on parasitaemia in *Trypanosoma brucei* infected dogs, Nwosu and Ikeme, (1992) reported that some dogs showed acute disease and died in the first wave of parasitaemia on days 7 and 8 post-infection (PI) while the other two died from the sub-acute disease on days 24 and 28 PI corresponding to the second wave of parasitaemia (Nwosu and Ikeme, 1992). They also reported that the first wave of parasitaemia was associated with a sharp decrease in the packed cell volume. The fact that the animals that exhibited intermittent parasitaemia lived longer than those with persistent parasitaemia suggests that the antibodies produced by the mice were able to respond to the VSGs produced by the parasites (Vincendeau and Bouteille, 2006).

Anaemia is an inevitable consequence of trypanosome infection (Murray and Dexter 1988). According to Murray and Dexter (1988), the rapid drop of PCV is always correlated closely with the appearance of parasitaemia. Anaemia and weight loss are therefore two of several clinical signs of acute animal trypanosomiasis. Death is inevitable in the absence of intervention. In the field, the degree of anaemia is quantified easily by measuring % PCV; the measurement is usually very accurate, taking into consideration other possible pre-disposing factors such as parasite toxins e.g proteases making erythrocytes prone to phagocytosis (Mbaya *et al.*, 2010), and malnutrition of the host causes inadequate energy supply to erythrocytes which may alter the erythrocyte membrane surface therefore leading to weakening of the cell membrane, increased osmotic fragility and haemolysis (Mbaya *et al.*, 2010). In the present study, gradual decline in PCV was recorded in mice infected with

isolates that exhibited intermittent parasitaemia; the drop-in body weights were also gradual with weight gain recorded in others. However, there was a rapid drop in the PCV in the animals that exhibited high and persistent parasitaemia (moderate virulence) with rapid decline in bodyweights. This has been reported in studies on malaria where the virulent parasites that generated highest parasite densities exploited more of the host's resources, the red blood cells (Mackinnon *et al.*, 2008). The trypanosome species infecting the animals and the geographical location also influence the clinical picture of the disease.

Anaemia, poor productivity and infertility is a characteristic of chronic trypanosomiasis (Maudlin and Holmes, 2004). Our observations showed that intermittent parasitaemia was positively associated with low virulence, indicating that the mice were able to fight the infection, gain weight with gradual decline in PCV and survive for longer periods. This observation is consistent with previous reports (Eyob and Matios, 2013). Different nonexclusive mechanisms are thought to be involved in pathogenesis of anaemia this include: impaired erythropoiesis, increased erythro-phagocytosis, and direct alteration of red blood cells (Steverding, 2008).

In the current study, an increase in body weight in mice infected with parasites of low virulence was observed despite the effect of infection in majority of the animals during the early stages of infection. The increase could be related to the retention of body fluids in the form of oedema that accompanies trypanosomiasis (Steverding, 2008). It was shown that in rodent trypanosomiasis, there is a correlation between splenomegaly and parasitaemia. Increase in spleen size generally occurs between 7 to 10 days of infection with *Trypanosoma lewisi* and generally corresponds to the time of peak parasitaemia (Cherian and Dusanic, 1977). However, there was a marked drop in the body weight of infected mice at different points depending on the *T. evansi* isolate. Those mice infected with isolates from Asia and South America died before a decline in body weight was evident and the data on body weight

taken. The rapid death of the group of mice infected by the *T. evansi* isolates from Asia and South America can be attributed to the rapid propagation (less than 7 days) and high parasitemia levels that translate into energy requirements that exceed the capacity of the host (Perrone *et al.*, 2018). Since the isolates were maintained in culture this might have contributed to the high virulence observed.

5.2 Evolutionary origins of *T. evansi* in Kenya

The results from screening of 15 microsatellite loci largely aligns with previous phylogenetic and population genetic analyses, which indicated that *T. evansi* strains are nested phylogenetically within the more genetically diverse *T. brucei* (Carnes *et al.*, 2015; Claes *et al.*, 2002), likely originated from different *T. b. brucei* strains (Birhanu *et al.*, 2015; Claes *et al.*, 2002), and are highly variable (Birhanu *et al.*, 2015; Claes *et al.*, 2002). Some studies (Claes *et al.*, 2002; Salim *et al.*, 2011; Villareal *et al.*, 2013) found that the *T. evansi* strains sampled clustered closely with one another and separately from *T. b. brucei* and *T. b. rhodesiense* strains. It was suggested that this pattern of genetic similarity can be an artifact resulting from the limited number and type of isolates included in these studies. This is especially true for the *T. evansi* isolates that only included the common kDNA type A lineage (i.e. kDNA minicircle type A configuration and RoTat 1.2 positive). Indeed, other studies that have included both type A and type B *T. evansi* isolates have found similar results to what was found in this study, using a larger geographic and taxonomic diversity of isolates (Carnes *et al.*, 2015). Interestingly, these findings are also consistent with previous comparative genomic analysis (Carnes *et al.*, 2015) and with classical parasitological characterization, which indicates high similarity between *T. evansi* and *T. b. brucei* except for variable patterns of loss of part or all of their kDNA (Borst *et al.*, 1987; Carnes *et al.*, 2015; Lai *et al.*, 2008; Schnauffer *et al.*, 2002).

The level of population structure and grouping was observed for *T. brucei* is similar to results from previous microsatellite (Sistrom *et al.*, 2014, 2016) and genomic (Sistrom *et al.*, 2014, 2016) analyses, where *T. b. rhodesiense* isolates were consistently assigned to multiple clusters together with *T. b. brucei* isolates. This data confirms multiple independent origins of the human disease parasite, *T. b. rhodesiense*, from different non-human infective *T. b. brucei* strains and implies that the SRA gene has moved horizontally between strains, which is consistent with earlier studies and experimental evidence that this can occur in the field (Sistrom *et al.*, 2014, 2016). As pointed out previously, this finding has important practical implications for disease control and monitoring, as it provides further evidence that *T. b. brucei* strains can relatively easily transform into *T. b. rhodesiense* strains and pose a serious risk to human health (Sistrom *et al.*, 2014, 2016).

This work shows that *T. evansi* strains from Eastern Africa, the main region where both *T. evansi* and *T. b. brucei* strains co-occur, likely originated from multiple *T. b. brucei* strains and harbour a high degree of circulating genetic variation. This result is surprising because of the phenotypic similarities between all *T. evansi* strains, such as ability to sustained mechanical transmission outside the tsetse belt, variable loss of functional kDNA, and the common disease symptoms they cause in a variety of animals. Multiple origins of *T. evansi* phenotypes implies that complex traits such as ability for mechanical transmission have evolved multiple times, and that there is plenty of standing genetic diversity to provide opportunity for selection to generate novel strains.

5.3 Spatial expansion of *T. evansi*

From the results of the analyses, *T. evansi* and *T. equiperdum* largely originated from *T. brucei* ancestors which support multiple evolutionary origins. Using microsatellite and kDNA markers, the current study suggested that *T. evansi* / *T. equiperdum* evolved either from a single origin with later divergence or evolved independently from a *T. brucei* source. In some

of the previous studies (Carnes *et al.*, 2015; Lai *et al.*, 2008), certain isolates of *T. evansi* were most closely related to isolates that had been classified as *T. equiperdum* (Claes *et al.*, 2005). *T. evansi* from Asia and South America likely originated from different *T. b. brucei* strains and are highly variable (Birhanu *et al.*, 2015; Claes *et al.*, 2002). Some studies (Claes *et al.*, 2002; Salim *et al.*, 2011; Villareal *et al.*, 2013) found that the *T. evansi* and *T. equiperdum* strains sampled clustered closely with one another and separately from *T. brucei* and *T. b. rhodesiense* strains.

These findings challenge the taxonomic rank of a species for these parasites and have important implications for epidemiology, diagnostics and treatment. With the current state of knowledge about the evolution of *T. evansi* and *T. equiperdum* and their phylogenetic relationship to *T. brucei*, and, in this context, present a phylogenetic analysis of an isolate from the 2011 outbreak of dourine in Italy. The current study strongly suggests that the Italian *T. equiperdum* is genetically distinct from other *T. equiperdum* and *T. evansi* isolates; it thus represents an important addition to the emerging panel of new isolates from cases of dourine with unequivocal etiology.

CHAPTER SIX

SUMMARY OF FINDINGS, CONCLUSIONS AND RECOMMENDATIONS

6.1 Summary of findings

In conclusion isolates investigated for virulence studies were able to infect mice, multiply and cause disease. These findings suggest differential virulence between *T. evansi* isolates collected from the three endemic regions demonstrating low, moderate and high virulence. The different levels of virulence exhibited may be related to the host from which the parasites were isolated as well as the geographical location from where the isolates were obtained. For the evolutionary studies it shows that *T. evansi* strains from Eastern Africa, the main region where both *T. evansi* and *T. b. brucei* strains co-occur, likely originated from multiple *T. b. brucei* strains and harbour a high degree of circulating genetic variation. This result is surprising because of the phenotypic similarities between all *T. evansi* strains, such as ability to sustain mechanical transmission outside the tsetse belt, variable loss of functional kDNA, and the common disease symptoms they cause in a variety of animals. Multiple origins of *T. evansi* phenotypes implies that complex traits such as ability for mechanical transmission have evolved multiple times, and that there is plenty of standing genetic diversity to provide opportunity for selection to generate novel strains. Further research is needed to understand the mechanism of this evolutionary transition.

6.2 Conclusion

1. There was a single Type B strain (KETRI 2479) which was among the highly virulent strains. Detection of infections in animals infected with this particular Type B strain and other type B's which are yet to be identified will continue to pose a challenge in the absence of appropriate diagnostic tools. Non-RoTat *T. evansi* type A has been reported elsewhere with great implications on control of the surra in camels. Animals

infected with non-RoTat *T. evansi* Types A and B may remain a source of infection for a long time, resulting in high mortality and morbidity further complicating search for new diagnostics and vaccines to effectively control the disease in domestic animals.

2. On an evolutionary stand point of this study, it was concluded that *T. evansi* isolates originated from multiple *T. brucei* strains from different genetic backgrounds, implying independent origins of *T. evansi* from *T. brucei* strains. This surprising finding further suggested that the acquisition of the ability of *T. evansi* to be transmitted mechanically, and thus the ability to escape the obligate link with the African tsetse fly vector, has occurred repeatedly. These findings, if confirmed, have epidemiological implications, as *T. brucei* strains from different genetic backgrounds can become either causative agents of a dangerous, cosmopolitan livestock disease or of a lethal human disease, like for *T. b. rhodesiense*. Thus, risk of human infective *T. evansi* remains theoretical, but deserves consideration since this would allow human sleeping sickness to escape sub-Saharan Africa and take advantage of hosts worldwide.
3. The results provide further support for the idea that *T. evansi* and *T. equiperdum* are closely related and mechanical transmission and sexual transmission respectively have enabled them to infect other animals in the rest of the world (Asia and South America). New strains of these parasites are also emerging from the analysis. It is therefore important to monitor these parasites closely especially their genetic behavior to prevent and control new outbreaks of surra.

6.3 Recommendations from the current study

1. The virulence of *T. evansi* may be region-specific, this particular phenotype (virulence) of the different circulating parasites should be considered in the approaches to management and control of surra. New and appropriate diagnostic tools should be provided in the detection of infections in animals especially with Non-RotaT and *T. evansi* Type B since the only diagnostic test only picks Rotat 1.2 *T. evansi*. This will help in monitoring of surra.
2. Understanding the levels and patterns of inter-strains genetic diversity help in understanding the evolutionary origin of different *T. evansi* strains. This aid in control and monitoring of disease spread by providing data that inform on the rate and modality of novel genotypic combinations that exists in the circulating *T. evansi* strains. This study also provides a more comprehensive understanding of the epidemiology of surra, which indicates a need to consider the risk of horizontal transfer of epidemiologically relevant traits which is also a step towards the ultimate aim of trypanosomiasis prevention and/or elimination.
3. This study provide data that inform on the rate and modality of novel genotypic combinations that exists in the circulating *T. evansi* strains in the world.

6.4 Recommendations for future research

1. There is therefore need to collect more isolates from these and other surra endemic regions to confirm this virulence observation.
2. Adding genome-wide data will provide higher resolution of the phylogenetic relationships among these strains and insights on the genetic, functional and molecular basis of novel complex traits such as “mechanical transmission”.
3. Screening for genetic polymorphism in additional *T. evansi* isolates from across the world will help us understand the origin and timing of the *T. evansi* expansion,

evaluate if only a few genetically similar strains were responsible for the spread, and identify the *T. brucei* genetic background most likely to give rise to *T. evansi* strains.

REFERENCES

- Alizon, S., Hurford, A., Mideo, N., & Van Baalen, M. (2009). Virulence evolution and the trade-off hypothesis: History, current state of affairs and the future. *Journal of Evolutionary Biology*, 22(2), 245–259.
- Antoine-Moussiaux, N., Biischer, P., & Desmecht, D. (2009). Host-parasite interactions in trypanosomiasis: On the way to an antidisease strategy. *Infection and Immunity*, 77(4), 1276–1284.
- Balmer, O., Beadell, J. S., Gibson, W., & Caccone, A. (2011). Phylogeography and taxonomy of *Trypanosoma brucei*. *PLoS Neglected Tropical Diseases*, 5(2), e961.
- Balmer, O., Palma, C., Macleod, A., & Caccone, A. (2006). Characterization of di-, tri- and tetranucleotide microsatellite markers with perfect repeats for *Trypanosoma brucei* and related species. *Molecular Ecology Notes*, 6(2), 508–510.
- Berngruber, T. W., Froissart, R., Choisy, M., & Gandon, S. (2013). Evolution of Virulence in Emerging Epidemics. *PLoS Pathogens*, 9(3), e1003209.
- Birhanu, H., Gebrehiwot, T., Goddeeris, B. M., Büscher, P., & Van Reet, N. (2016). New *Trypanosoma evansi* Type B Isolates from Ethiopian Dromedary Camels. *PLoS Neglected Tropical Diseases*, 10(4), e0004556.
- Birhanu, H., Rog, S., Simon, T., Baelmans, R., Gebrehiwot, T., Goddeeris, B. M., & Buscher, P. (2015). Surra Sero K-SeT, a new immunochromatographic test for serodiagnosis of *Trypanosoma evansi* infection in domestic animals. *Veterinary Parasitology*, 211(3–4), 153–157.
- Borst, P., Fase-Fowler, F., & Gibson, W. C. (1987). Kinetoplast DNA of *Trypanosoma evansi*. *Molecular and Biochemical Parasitology* 23(1), 31–38.
- Brun, R. (2005). Human Asian trypanosomiasis, a new threat to human health? *American Journal of Tropical Medicine and Hygiene*, 73(3), 484.

- Brun, R., Blum, J., Chappuis, F., & Burri, C. (2010). Human African trypanosomiasis. *The Lancet*. [http://doi.org/10.1016/S0140-6736\(09\)60829-1](http://doi.org/10.1016/S0140-6736(09)60829-1).
- Brun, R., Hecker, H., & Lun, Z.-R. (1998). *Trypanosoma evansi* and *Trypanosoma equiperdum*: distribution, biology, treatment and phylogenetic relationship (a review). *Veterinary Parasitology*, 79(2), 95–107.
- Carnes, J., Anupama, A., Balmer, O., Jackson, A., Lewis, M., Brown, R., ... Schnauffer, A. (2015). Genome and Phylogenetic Analyses of *Trypanosoma evansi* Reveal Extensive Similarity to *Trypanosoma brucei* and Multiple Independent Origins for Dyskinetoplasty. *PLoS Neglected Tropical Diseases*, 9(1), e3404.
- Cherian, PV, Dusanic, D. (1977). *Trypanosoma lewisi*: immunoelectron microscopic studies on the surface antigens of bloodstream forms. *Experimental Parasitology*, 43(1), 128–42.
- Cibulskis, R. E. (1992). Genetic variation in *Trypanosoma brucei* and the epidemiology of sleeping sickness in the Lambwe Valley, Kenya. *Parasitology*, 104 Pt 1, 99–109.
- Claes, F., & Büscher, P. (2007). Molecular markers for the different (sub)-species of the Trypanozoon subgenus. In Developing methodologies for the use of polymerase chain reaction in the diagnosis and monitoring of trypanosomosis; final results of a coordinated research project. Vienna: International Atomic Energy Agency (IAEA), 2001–2005, 15–26.
- Claes, F., Büscher, P., Touratier, L., & Goddeeris, B. M. (2005). *Trypanosoma equiperdum*: Master of disguise or historical mistake? *Trends in Parasitology*. 21(7), 316-21.
- Claes, F., Verloo, D., De Waal, D. T., Urakawa, T., Majiwa, P., Goddeeris, B. M., & Buscher, P. (2002). Expression of RoTat 1.2 cross-reactive variable antigen type in *Trypanosoma evansi* and *Trypanosoma equiperdum*. *Annals of the New York Academy of Sciences*, 969, 174–179.

- De Menezes, V. T., Oliveira Queiroz, A., Gomes, M. A. M., Marques, M. A. P., & Jansen, A. M. (2004). Trypanosoma evansi in inbred and Swiss-Webster mice: Distinct aspects of pathogenesis. *Parasitology Research*, *94*(3), 193–200.
- Dean, S., Gould, M. K., Dewar, C. E., & Schnauffer, A. C. (2013). Single point mutations in ATP synthase compensate for mitochondrial genome loss in trypanosomes. *Proceedings of the National Academy of Sciences of the United States of America*, *110*(36), 14741–14746.
- Delespaux, V., & de Koning, H. P. (2007). Drugs and drug resistance in African trypanosomiasis. *Drug Resistance Updates*, *10*(1–2), 30–50. <http://doi.org/10.1016/j.drug.2007.02.004>.
- Desquesnes, M., Holzmüller, P., Lai, D. H., Dargantes, A., Lun, Z. R., & Jittaplapong, S. (2013). *Trypanosoma evansi* and surra: A review and perspectives on origin, history, distribution, taxonomy, morphology, hosts, and pathogenic effects. *BioMedical Research International*, 2013.
- Dijkshoorn, L. Ursing, B.M. Ursing, J. (2000). Strain, clone and species: comments on three basic concepts of bacteriology. *Journal of Medical Microbiology*, *49*(5), 397–401.
- Echodu, R., Siström, M., Bateta, R., Murilla, G., Okedi, L., Aksoy, S., Caccone, A. (2015). Genetic Diversity and Population Structure of *Trypanosoma brucei* in Uganda: Implications for the Epidemiology of Sleeping Sickness and Nagana. *PLoS Neglected Tropical Diseases*, *9*(2), 1–18.
- Evanno, G., Regnaut, S., & Goudet, J. (2005). Detecting the number of clusters of individuals using the software STRUCTURE: A simulation study. *Molecular Ecology*, *14*(8), 2611–2620.
- Excoffier, L., & Lischer, H. E. L. (2010). Arlequin suite ver 3.5: A new series of programs to perform population genetics analyses under Linux and Windows. *Molecular Ecology*

- Resources*, 10(3), 564–567.
- Eyob, E., & Matios, L. (2013). Review on camel trypanosomosis (surra) due to *Trypanosoma evansi*: Epidemiology and host response. *Journal of Veterinary Medicine and Animal Health*, 5(12), 334–343.
- Ezz El-Arab, A. M., Girgis, S. M., Hegazy, E. M., & Abd El-Khalek, A. B. (2006). Effect of dietary honey on intestinal microflora and toxicity of mycotoxins in mice. *BMC Complement Alternative Medicine*, 6(1), 6.
- Gibson, W. (2003). Species concepts for trypanosomes: from morphological to molecular definitions? *Kinetoplastid Biology and Disease*, 2(1), 10.
- Gibson, W. (2007). Resolution of the species problem in African trypanosomes. *International Journal for Parasitology*, 37(8), 29–38.
- Gibson, W. C., Wilson, A. J., & Moolo, S. K. (1983). Characterisation of *Trypanosoma* (Trypanozoon) *evansi* from camels in Kenya using isoenzyme electrophoresis. *Research in Veterinary Science*, 34(1), 114–8.
- Gichuki, C. and Brun, R. (1999). Animal models of CNS (second-stage) sleeping sickness. In Zak, O., Sande, M. Eds. *Handbook of Animal Models of Infection*, Academic Press: London, United Kingdom, 795–800.
- Goudet, J. (1995). FSTAT (Version 1.2): A Computer Program to Calculate F-Statistics. *J Hered*, 86(6), 485–486.
- Goudet, J. (2005). Hierfstat, a package for R to compute and test hierarchical F-statistics. *Molecular Ecology Notes*, 5, 184–186.
- Herbert, W. J., & Lumsden, W. H. R. (1976). *Trypanosoma brucei*: A rapid “matching” method for estimating the host’s parasitemia. *Experimental Parasitology*, 40(3), 427–431.
- Herrera, H. M., Davila, A. M. R., Norek, A., Abreu, U. G., Souza, S. S., D’Andrea, P. S., &

- Jansen, A. M. (2004). Enzootiology of *Trypanosoma evansi* in Pantanal, Brazil. *Veterinary Parasitology*, *125*(3–4), 263–275.
- Hoare, C. (1967). Evolutionary trends in mammalian trypanosomes. *Advances in Parasitology*, *5*, 41–91.
- Jakobsson, M., & Rosenberg, N. A. (2007). CLUMPP: A cluster matching and permutation program for dealing with label switching and multimodality in analysis of population structure. *Bioinformatics*, *23*(14), 1801–1806.
- Jensen, R. E., Simpson, L., & Englund, P. T. (2008). What happens when *Trypanosoma brucei* leaves Africa. *Trends in Parasitology*.
- Jombart, T. (2008). Adegnet: A R package for the multivariate analysis of genetic markers. *Bioinformatics*, *24*(11), 1403–1405.
- Kagira, J. M., Ngotho, M., & Thuita, J. (2007). Development of a rodent model for late stage rhodesian sleeping sickness. *Journal of Protozoology Research*, *17*, 48–56.
- Kamidi, C.M., Saarman, N.P., Dion, K., Mireji, P.O., Ouma, C., Murilla, G., Aksoy, S., Schnauffer, A. and Caccone, A. (2017). Multiple evolutionary origins of *Trypanosoma evansi* in Kenya. *PLoS Neglected Tropical Diseases*, *11*(9), e0005895. <http://doi.org/10.1371/journal.pntd.0005895>
- Kamvar, Z. N., Brooks, J. C., & Grünwald, N. J. (2015). Novel R tools for analysis of genome-wide population genetic data with emphasis on clonality. *Frontiers in Genetics*, *6*, 1–10.
- Kamvar, Z. N., Tabima, J. F., & Grünwald, N. J. (2014). Poppr: an R package for genetic analysis of populations with clonal, partially clonal, and/or sexual reproduction. *Peer Journal*, *2*, e281.
- Koffi, M., De Meeûs, T., Séré, M., Bucheton, B., Simo, G., Njiokou, F., Salim, B., Kaboré, J., MacLeod, A., Camara, M. and Solano, P. Population Genetics and Reproductive

- Strategies of African Trypanosomes: Revisiting Available Published Data. *PLoS Neglected Tropical Diseases*, 9(10), 1–21.
- Lai, D.-H., Hashimi, H., Lun, Z.-R., Ayala, F. J., & Lukes, J. (2008). Adaptations of *Trypanosoma brucei* to gradual loss of kinetoplast DNA: *Trypanosoma equiperdum* and *Trypanosoma evansi* are petite mutants of *Trypanosoma brucei*. *Proceedings of the National Academy of Sciences of the United States of America*, 105(6), 1999–2004.
- Lalmanach G, Boulange A, Serveau C, Lecaille F, Scharfstein J, G. F. and A. E. (2002). Congopain from *Trypanosoma congolense*: drug target and vaccine candidate. *Biological Chemistry*, 383, 739–749.
- Little, T. J., Chadwick, W., & Watt, K. (2008). Parasite variation and the evolution of virulence in a Daphnia-microparasite system. *Parasitology*, 135(3), 303–308.
- Luckins, A. G. (1988). *Trypanosoma evansi* in Asia. *Parasitology Today*.
- Lun, Z. R., Lai, D. H., Li, F. J., Lukeš, J., & Ayala, F. J. (2010). *Trypanosoma brucei*: Two steps to spread out from Africa. *Trends in Parasitology*, 26(9), 424–427.
- Lun ZR1, Brun R, G. W. (1992). Kinetoplast DNA and molecular karyotypes of *Trypanosoma evansi* and *Trypanosoma equiperdum* from China. *Molecular and Biochemical Parasitology*, 50(2), 189–96.
- Mackinnon, M. J., Gandon, S., & Read, A. F. (2008). Virulence evolution in response to vaccination: The case of malaria. *Vaccine*, 26, C42–C52.
- MacLeod, A., Tait, A., & Turner, C. M. (2001). The population genetics of *Trypanosoma brucei* and the origin of human infectivity. *Philosophical Transactions of the Royal Society of London. Series B, Biological Sciences*, 356(1411), 1035–44.
- Magez, S., Caljon, G., Tran, T., Stijlemans, B., & Radwanska, M. (2010). Current status of vaccination against African trypanosomiasis. *Parasitology*, 137(14), 2017–27.
- Martinez-gutierrez, M., A Correa-london, L., Castellanos, J. E., Gallego-Gomez, J. C., &

- Osorio, J. E. (2014). Lovastatin Delays Infection and Increases Survival Rates in AG129 Mice Infected with Dengue Virus Serotype 2. *PLoS ONE*, 9(2), e87412. <http://doi.org/10.1371/journal.pone.0087412>
- Masiga, D. K., Ndung'u, K., Tweedie, A., Tait, A., & Turner, C. M. R. (2006). *Trypanosoma evansi*: Genetic variability detected using amplified restriction fragment length polymorphism (AFLP) and random amplified polymorphic DNA (RAPD) analysis of Kenyan isolates. *Experimental Parasitology*, 114(3), 147–153.
- Matovu, E., Seebeck, T., Enyaru, J. C. K., & Kaminsky, R. (2001). Drug resistance in *Trypanosoma brucei* species., the causative agents of sleeping sickness in man and nagana in cattle. *Microbes and Infection*. 3(9), .763-770.
- Maudlin, & P H Holmes, M. A. M. (2004). The Trypanosomiases. *CABI Publishing*.
- Mbaya, A., Kumshe, H., & Nwosu, C. O. (2010). The Mechanisms of Anaemia in Trypanosomosis : A Review. *InTech Open Access*, 269–282. <http://doi.org/10.5772/29530>
- Mekata, H., Konnai, S., Mingala, C.N., Abes, N.S., Gutierrez, C.A., Dargantes, A.P., Witola, W.H., Inoue, N., Onuma, M., Murata, S. and Ohashi, K. (2013). Isolation, cloning, and pathologic analysis of *Trypanosoma evansi* field isolates. *Parasitology Research*, 112(4), 1513–1521.
- Morrison, W. I., Roelants, G. E., Mayor-Withey, K. S., & Murray, M. (1978). Susceptibility of inbred strains of mice to *Trypanosoma congolense*: correlation with changes in spleen lymphocyte populations. *Clinical and Experimental Immunology*, 32(1), 25–40.
- Muchiri, M.W., Ndung'u, K., Kibugu, J.K., Thuita, J.K., Gitonga, P.K., Ngae, G.N., Mdachi, R.E. and Kagira, J.M. (2015). Comparative pathogenicity of *Trypanosoma brucei rhodesiense* strains in Swiss white mice and *Mastomys natalensis* rats. *Acta Tropica*, 150, 23–28. <http://doi.org/10.1016/j.actatropica.2015.06.010>

- Murilla, G. A., Ndung'u, K., Thuita, J. K., Gitonga, P. K., Kahiga, D. T., Auma, J. E., ... Ndung'u, J. M. (2014). Kenya Trypanosomiasis Research Institute Cryobank for Human and Animal Trypanosome Isolates to Support Research: Opportunities and Challenges. *PLoS Neglected Tropical Diseases*, 8(5), e2747. <http://doi.org/10.1371/journal.pntd.0002747>
- Murilla, G., Ndung'u, K., & Auma, J. (2016). Isolation and Cryopreservation of Trypanosomes and their Vectors for Research and Development in Resource-Constrained Settings. In *Cryopreservation in eukaryotes*. p. 10.
- Murray, M., D. T. (1988). Anaemia in bovine African trypanosomiasis. A review. *Acta Tropica*, 45(4), 389–432.
- Murray, M. (1979). Anaemia of bovine African trypanosomiasis: An overview. In: Pathogenicity of Trypanosomes. *proceedings of a workshop, IDRC, Ottawa*. 132, 121–127.
- Naessens, J., Kitani, H., & Nakamura, Y. (2005). TNF- α mediates the development of anaemia in a murine *Trypanosoma brucei* rhodesiense infection, but not the anaemia associated with a murine *Trypanosoma congolense* infection. *Clinical and Experimental Immunology*. 139(3), 405–410.
- Ndung'u, K., Ngotho, M., Kinyua, J., Kagira, J., Guya, S., Ndung'u, J., & Murilla, G. (2008). Pathogenicity of bloodstream and cerebrospinal fluid forms of *Trypanosoma brucei* rhodesiense in Swiss White Mice. *African Journal of Health Sciences*, 15(1), 34–41.
- Nelder, J., & R. J. Baker. (1972). Generalized linear models. In *Encyclopaedia of statistical sciences*. 4.
- Ngaira, J. M., Bett, B., Karanja, S. M., & Njagi, E. N. M. (2003). Evaluation of antigen and antibody rapid detection tests for *Trypanosoma evansi* infection in camels in Kenya. *Veterinary Parasitology*, 114, 131–141.

- Ngaira, J. M., Njagi, E. N. M., Ngeranwa, J. J. N., & Olembo, N. K. (2004). PCR amplification of RoTat 1.2 VSG gene in *Trypanosoma evansi* isolates in Kenya. *Veterinary Parasitology*, *120*(1–2), 23–33.
- Ngaira, J. M., Olembo, N. K., Njagi, E. N. M., & Ngeranwa, J. J. N. (2005). The detection of non-RoTat 1.2 *Trypanosoma evansi*. *Experimental Parasitology*, *110*(1), 30–38.
- Njiru, Z. K., & Constantine, C. C. (2007). Population sub-structuring among *Trypanosoma evansi* stocks. *Parasitology Research*, *101*(5), 1215–1224.
- Njiru, Z. K., Constantine, C. C., Guya, S., Crowther, J., Kiragu, J. M., Thompson, R. C. A., & Dávila, A. M. R. (2005). The use of ITS1 rDNA PCR in detecting pathogenic African trypanosomes. *Parasitology Research*, *95*(3), 186–192.
- Njiru, Z. K., Constantine, C. C., Masiga, D. K., Reid, S. A., Thompson, R. C. A., & Gibson, W. C. (2006). Characterization of *Trypanosoma evansi* type B. *Infection, Genetics and Evolution*, *6*(4), 292–300.
- Nneka Chizoba Enwezor, F., & Kojo Bedu Sackey, A. (2005). Camel trypanosomosis - a review. *Veterinary Archives*, *75*(5), 439–452. <http://doi.org/10.1177/0146167205282740>
- Noyes, H. A., Alimohammadian, M. H., Agaba, M., Brass, A., Fuchs, H., Gailus-Durner, V., ... Naessens, J. (2009). Mechanisms controlling anaemia in *Trypanosoma congolense* infected mice. *PLoS ONE*, *4*(4), e5170.
- Nwosu, C. O., & Ikeme, M. M. (1992). Parasitaemia and clinical manifestations in *Trypanosoma brucei* infected dogs. *Revue d'élevage et de Médecine Vétérinaire Des Pays Tropicaux*, *45*(3–4), 273–7.
- O'brien, P. C. (1998). Comparing two samples: extensions of the t, rank-sum, and log-rank tests. *Journal of the American Statistical Association*, *83*(401), 52–61.
- Perrone, T., Aso, P. M., Mijares, A., Holzmuller, P., Gonzatti, M., & Parra, N. (2018). Comparison of infectivity and virulence of clones of *Trypanosoma evansi* and

- Trypanosoma equiperdum* Venezuelan strains in mice. *Veterinary Parasitology*, 253(July 2017), 60–64. <http://doi.org/10.1016/j.vetpar.2018.02.024>
- Pritchard, J., Stephens, M., & Donnelly, P. (2000). Inference of population structure using multilocus genotype data. *Genetics*, 155(2), 945–959.
- Prugnolle, F. (2008). Clonality and deviation from hardy-weinberg expectations. *Parasite Journal*. 15(3)455–457.
- Radwanska, M., Chamekh, M., Vanhamme, L., Claes, F., Magez, S., Magnus, E., Pays, E. (2002). The serum resistance-associated gene as a diagnostic tool for the detection of *Trypanosoma brucei rhodesiense*. *American Journal of Tropical Medicine and Hygiene*, 67(6), 684–690.
- Reid, S. A. (2002). *Trypanosoma evansi* control and containment in Australasia. *Trends in Parasitology*. 18(5), 219-224.
- Reynolds, J., Weir, B. S., & Cockerham, C. C. (1983). Estimation of the coancestry coefficient: Basis for a short-term genetic distance. *Genetics*, 105(3), 767–779.
- Robson, J., Rickman, L. R., Allsopp, R., & Scott, D. (1972). The composition of the *Trypanosoma brucei* subgroup in nonhuman reservoirs in the Lambwe Valley, Kenya, with particular reference to the distribution of *Trypanosoma rhodesiense*. *Bulletin of the World Health Organization*, 46(6), 765–770.
- Salim, B., de Meeûs, T., Bakheit, M. A., Kamau, J., Nakamura, I., & Sugimoto, C. (2011). Population genetics of *Trypanosoma evansi* from Camel in the Sudan. *PLoS Neglected Tropical Diseases*, 5(6), e1196.
- Schnauffer, A., Domingo, G. J., & Stuart, K. (2002). Natural and induced dyskinetoplastic trypanosomatids: how to live without mitochondrial DNA. *International Journal for Parasitology*, 32(9), 1071–1084.
- Seamer, J., Southee, J., Thompson, A., Trussell, B., West, C., & Jennings, M. (1993).

- Removal of blood from laboratory mammals and birds. *Laboratory Animals*, 27(1), 1–22.
- Sistrom, M., Echodu, R., Hyseni, C., Enyaru, J., Aksoy, S., & Caccone, A. (2013). Taking advantage of genomic data to develop reliable microsatellite loci in *Trypanosoma brucei*. *Molecular Ecology Resources*, 13(2), 341–343.
- Sistrom, M., Evans, B., Benoit, J., Balmer, O., Aksoy, S., & Caccone, A. (2016). De novo genome assembly shows genome wide similarity between *Trypanosoma brucei brucei* and *Trypanosoma brucei rhodesiense*. *PLoS ONE*, 11(2), e01447660.
- Sistrom, M., Evans, B., Bjornson, R., Gibson, W., Balmer, O., Mäser, P., Caccone, A. (2014). Comparative genomics reveals multiple genetic backgrounds of human pathogenicity in the *Trypanosoma brucei* complex. *Genome Biology and Evolution*, 6(10), 2811–9.
- Steinert, M., & Van Assel, S. (1980). Sequence heterogeneity in kinetoplast DNA: Reassociation kinetics. *Plasmid*, 3(1), 7–17.
- Steverding, D. (2008). The history of African trypanosomiasis. *Parasites & Vectors*, 1(1), 3.
- Urakawa, T., Verloo, D., Moens, L., Büscher, P., & Majiwa, P. a. (2001). *Trypanosoma evansi*: cloning and expression in *Spodoptera frugiperda* insect cells of the diagnostic antigen RoTat1.2. *Experimental Parasitology*, 99, 181–9.
- Villareal, M. V, Mingala, C. N., & Rivera, W. L. (2013). Molecular characterization of *Trypanosoma evansi* isolates from water buffaloes (*Bubalus bubalis*) in the Philippines. *Acta Parasitologica*. 58(1), 6–12.
- Vincendeau, P., & Bouteille, B. (2006). Immunology and immunopathology of African trypanosomiasis. *Anais Da Academia Brasileira de Ciencias*, 78(4), 645–665.
- Weir, C., & Cockerham, c. (1984). Estimating F-Statistics for the Analysis of Population Structure. *Evolution (NY)*, 38, 1358.
- Weir, W., Capewell, P., Foth, B., Clucas, C., Pountain, A., Steketee, P., Berriman, M. (2015).

- Population genomics reveals the origin and asexual evolution of human infective trypanosomes, 5, e11473. <http://doi.org/10.7554/eLife.11473>
- Welburn, S. C., Maudlin, I., & Simarro, P. P. (2009). Controlling sleeping sickness - a review. *Parasitology*, 136(14), 1943–9.
- Wen, Y.-Z., Lun, Z.-R., Zhu, X.-Q., Hide, G., & Lai, D.-H. (2016). Further evidence from SSCP and ITS DNA sequencing support *Trypanosoma evansi* and *Trypanosoma equiperdum* as subspecies or even strains of *Trypanosoma brucei*. *Infection, Genetics and Evolution*, 41, 56–62.
- WHO, 2017. Human African Trypanosomiasis. WHO factsheets.
- WHO 2014 *Trypanosomiasis, human African (sleeping sickness)*; Fact sheet N°259; 14.
- Wright, S. (1951). The genetical structure of populations. *Annals Eugenics*, 15, 323 – 354.
- Zíková, A., Panigrahi, A. K., Dalley, R. a, Acestor, N., Anupama, A., Ogata, Y., Stuart, K. (2008). *Trypanosoma brucei* mitochondrial ribosomes: affinity purification and component identification by mass spectrometry. *Molecular & Cellular Proteomics* : 7(7), 1286–1296.

APPENDICES

Appendix 1: Ethical approval



KENYA AGRICULTURAL & LIVESTOCK RESEARCH ORGANIZATION
Biotechnology Research Institute, MUGUGA
P. O. BOX 362, Kikuyu, 00902

Our Ref: C/BioRi/4/325/II/1

2nd February 2016

M/S Kamidi Christine Muhonja,
Principal Investigator (PI).

Dear Christine

RE: IACUC Approval

The Institutional Animal Care and Use Committee (IACUC) of the Kenya Agricultural and Livestock Research Organization-Biotechnology Research Institute (KALRO-BioRi) has reviewed your proposal entitled “**Molecular and phenotypic characterization of *Trypanosoma evansi* types A and B: development and evaluation of genetically attenuated parasites as vaccine.** The committee is agreement that that the proposed study addresses an important subject with potential benefits for the control of African animal trypanosomiasis. The study methods are appropriate and are consistent with IACUC recommendations as well as National (KVA) standards of animal welfare. The committee has therefore resolved to support your study (the PI) personally responsible to ensure that high standards of animal welfare are observed. The committee may make impromptu visits to ensure compliance with its regulations.

Yours Sincerely



Dr John Thuita

Ag Chairman, Institutional Animal Care and Use Committee (IACUC)
KALRO-Biotechnology Research Institute

Appendix 2: DNA extraction protocol

Protocol: Purification of Total DNA from Animal Blood or Cells (Spin-Column Protocol)

This protocol is designed for purification of total DNA from animal blood (with nucleated or nonnucleated erythrocytes) or from cultured animal or human cells.

Important points before starting

- If using the DNeasy Blood & Tissue Kit for the first time, read "Important Notes" (page 15).
- All centrifugation steps are carried out at room temperature (15–25°C) in a microcentrifuge.
- Vortexing should be performed by pulse-vortexing for 5–10 s.
- PBS is required for use in step 1 (see page 14 for composition). Buffer ATL is not required in this protocol.
- Optional: RNase A may be used to digest RNA during the procedure. RNase A is not provided in the DNeasy Blood & Tissue Kit (see "Copurification of RNA", page 19).

Things to do before starting

- Buffer AL may form a precipitate upon storage. If necessary, warm to 56°C until the precipitate has fully dissolved.
- Buffer AW1 and Buffer AW2 are supplied as concentrates. Before using for the first time, add the appropriate amount of ethanol (96–100%) as indicated on the bottle to obtain a working solution.
- Preheat a thermomixer, shaking water bath, or rocking platform to 56°C for use in step 2.

Procedure

1. For blood with nonnucleated erythrocytes, follow step 1a; for blood with nucleated erythrocytes, follow step 1b; for cultured cells, follow step 1c.

Blood from mammals contains nonnucleated erythrocytes. Blood from animals such as birds, fish, or frogs contains nucleated erythrocytes.

- 1a. **Nonnucleated:** Pipet 20 µl proteinase K into a 1.5 ml or 2 ml microcentrifuge tube (not provided). Add 50–100 µl anticoagulated blood. Adjust the volume to 220 µl with PBS. Continue with step 2.

Optional: If RNA-free genomic DNA is required, add 4 µl RNase A (100 mg/ml) and incubate for 2 min at room temperature before continuing with step 2.

- 1b. Nucleated:** Pipet 20 μ l proteinase K into a 1.5 ml or 2 ml microcentrifuge tube (not provided). Add 5–10 μ l anticoagulated blood. Adjust the volume to 220 μ l with PBS. Continue with step 2.

Optional: If RNA-free genomic DNA is required, add 4 μ l RNase A (100 mg/ml) and incubate for 2 min at room temperature before continuing with step 2.

- 1c. Cultured cells:** Centrifuge the appropriate number of cells (maximum 5×10^6) for 5 min at 300 x g. Resuspend the pellet in 200 μ l PBS. Add 20 μ l proteinase K. Continue with step 2.

When using a frozen cell pellet, allow cells to thaw before adding PBS until the pellet can be dislodged by gently flicking the tube.

Ensure that an appropriate number of cells is used in the procedure. For cell lines with a high degree of ploidy (e.g., HeLa cells), it is recommended to use less than the maximum number of cells listed in Table 1, page 16.

Optional: If RNA-free genomic DNA is required, add 4 μ l RNase A (100 mg/ml), mix by vortexing, and incubate for 2 min at room temperature before continuing with step 2.

- 2. Add 200 μ l Buffer AL (without added ethanol). Mix thoroughly by vortexing, and incubate at 56°C for 10 min.**

Ensure that ethanol has not been added to Buffer AL (see "Buffer AL", page 18). Buffer AL can be purchased separately (see page 56 for ordering information).

It is essential that the sample and Buffer AL are mixed immediately and thoroughly by vortexing or pipetting to yield a homogeneous solution.

- 3. Add 200 μ l ethanol (96–100%) to the sample, and mix thoroughly by vortexing.**

It is important that the sample and the ethanol are mixed thoroughly to yield a homogeneous solution.

- 4. Pipet the mixture from step 3 into the DNeasy Mini spin column placed in a 2 ml collection tube (provided). Centrifuge at $\geq 6000 \times g$ (8000 rpm) for 1 min. Discard flow-through and collection tube.***

- 5. Place the DNeasy Mini spin column in a new 2 ml collection tube (provided), add 500 μ l Buffer AW1, and centrifuge for 1 min at $\geq 6000 \times g$ (8000 rpm). Discard flow-through and collection tube.***

- 6. Place the DNeasy Mini spin column in a new 2 ml collection tube (provided), add 500 μ l Buffer AW2, and centrifuge for 3 min at 20,000 x g (14,000 rpm) to dry the DNeasy membrane. Discard flow-through and collection tube.**

It is important to dry the membrane of the DNeasy Mini spin column, since residual ethanol may interfere with subsequent reactions. This centrifugation step ensures that no residual ethanol will be carried over during the following elution.

* Flow-through contains Buffer AL or Buffer AW1 and is therefore not compatible with bleach. See page 8 for safety information.

Following the centrifugation step, remove the DNeasy Mini spin column carefully so that the column does not come into contact with the flow-through, since this will result in carryover of ethanol. If carryover of ethanol occurs, empty the collection tube, then reuse it in another centrifugation for 1 min at 20,000 x g (14,000 rpm).

7. **Place the DNeasy Mini spin column in a clean 1.5 ml or 2 ml microcentrifuge tube (not provided), and pipet 200 μ l Buffer AE directly onto the DNeasy membrane. Incubate at room temperature for 1 min, and then centrifuge for 1 min at ≥ 6000 x g (8000 rpm) to elute.**

Elution with 100 μ l (instead of 200 μ l) increases the final DNA concentration in the eluate, but also decreases the overall DNA yield (see Figure 2, page 21).

8. **Recommended: For maximum DNA yield, repeat elution once as described in step 7.**

This step leads to increased overall DNA yield.

A new microcentrifuge tube can be used for the second elution step to prevent dilution of the first eluate. Alternatively, to combine the eluates, the microcentrifuge tube from step 7 can be reused for the second elution step.

Note: Do not elute more than 200 μ l into a 1.5 ml microcentrifuge tube because the DNeasy Mini spin column will come into contact with the eluate.

Appendix 3: Manuscripts generated from current work

Parasitology

cambridge.org/par

Research Article

Cite this article: Kamidi CM, Auma J, Mireji PO, Ndungu K, Bateta R, Kurgat R, Ouma C, Aksoy S, Murilla G (2018). Differential virulence of camel *Trypanosoma evansi* isolates in mice. *Parasitology* 0, 1–8. <https://doi.org/10.1017/S0031182017002359>

Received: 10 July 2017

Revised: 4 December 2017

Accepted: 5 December 2017

Key words:

Packed cell volume; survival; *Trypanosoma evansi*; virulence.

Author for correspondence:

Christine M. Kamidi and Grace Murilla,
E-mail: tmuhonja@gmail.com, gmurilla@yahoo.co.uk

Differential virulence of camel *Trypanosoma evansi* isolates in mice

Christine M. Kamidi^{1,2,3}, Joanna Auma², Paul O. Mireji^{2,4}, Kariuki Ndungu², Rosemary Bateta², Richard Kurgat², Collins Ouma¹, Serap Aksoy³ and Grace Murilla^{2,3}

¹Department of Biomedical Sciences and Technology, School of Public Health and Community Development, Maseno University, Maseno, Kenya; ²Biotechnology Research Institute (BioRI) – Kenya Agricultural and Livestock Research Organization (KALRO), P.O. Box 362, Kikuyu 00902, Kenya; ³Department of Epidemiology of Microbial Diseases, Yale School of Public Health, New Haven, CT, USA and ⁴Centre for Geographic Medicine Research Coast, Kenya Medical Research Institute, P.O. Box 428, Kilifi, Kenya

Abstract

This study assessed the virulence of *Trypanosoma evansi*, the causative agent of camel trypanosomiasis (surra), affecting mainly camels among other hosts in Africa, Asia and South America, with high mortality and morbidity. Using Swiss white mice, we assessed virulence of 17 *T. evansi* isolates collected from surra endemic countries. We determined parasitaemia, live body weight, packed cell volume (PCV) and survivorship in mice, for a period of 60 days' post infection. Based on survivorship, the 17 isolates were classified into three virulence categories; low (31–60 days), moderate (11–30 days) and high (0–10 days). Differences in survivorship, PCV and bodyweights between categories were significant and correlated ($P < 0.05$). Of the 10 Kenyan isolates, four were of low, five moderate and one (Type B) of high virulence. These findings suggest differential virulence between *T. evansi* isolates. In conclusion, these results show that the virulence of *T. evansi* may be region specific, the phenotype of the circulating parasite should be considered in the management of surra. There is also need to collect more isolates from other surra endemic regions to confirm this observation.

RESEARCH ARTICLE

Multiple evolutionary origins of *Trypanosoma evansi* in Kenya

Christine M. Kamidi^{1,2,3*}, Norah P. Saarman^{4*}, Kirstin Dion⁴, Paul O. Mireji^{1,3,5}, Collins Ouma², Grace Murilla¹, Serap Aksoy³, Achim Schnauffer⁶, Adalgisa Caccone^{3,4}

1 Biotechnology Research Institute, Kenya Agricultural and Livestock Research Organization, Kikuyu, Kenya, **2** Department of Biomedical Sciences and Technology, School of Public Health and Community Development, Maseno University, Maseno, Kenya, **3** Yale School of Public Health, Department of Epidemiology of Microbial Diseases, New Haven, CT, United States of America, **4** Department of Ecology & Evolutionary Biology, Yale University, New Haven, CT, United States of America, **5** Centre for Geographic Medicine Research Coast, Kenya Medical Research Institute, Kilifi, Kenya, **6** Centre for Immunity, Infection & Evolution, and Institute of Immunology & Infection Research, University of Edinburgh, Edinburgh, Scotland, United Kingdom

© These authors contributed equally to this work.

* tmuhonja@gmail.com (CMK); norah.saarman@yale.edu, nosaaman@gmail.com (NPS)



OPEN ACCESS

Citation: Kamidi CM, Saarman NP, Dion K, Mireji PO, Ouma C, Murilla G, et al. (2017) Multiple evolutionary origins of *Trypanosoma evansi* in Kenya. *PLoS Negl Trop Dis* 11(9): e0005895. <https://doi.org/10.1371/journal.pntd.0005895>

Editor: Daniel K. Masiga, International Centre of Insect Physiology and Ecology, KENYA

Received: April 17, 2017

Accepted: August 22, 2017

Published: September 7, 2017

Copyright: © 2017 Kamidi et al. This is an open access article distributed under the terms of the [Creative Commons Attribution License](https://creativecommons.org/licenses/by/4.0/), which permits unrestricted use, distribution, and reproduction in any medium, provided the original author and source are credited.

Data Availability Statement: All data files are available from the dryad database doi:[10.5061/dryad.8q678](https://doi.org/10.5061/dryad.8q678).

Funding: This work received financial support from National Institute of Health Fogarty Center D43TW007391 and from IAEA contract number 16181/RO. AS was supported by MRC Senior Research Fellowship MR/L019701/1 to AS and NS by parasitology training grant fellowship to NPS (5T32AI007404-24). The research was accomplished while CMK was a Fogarty Research Fellow at Yale University. The funders had no role

Abstract

Trypanosoma evansi is the parasite causing surra, a form of trypanosomiasis in camels and other livestock, and a serious economic burden in Kenya and many other parts of the world. *Trypanosoma evansi* transmission can be sustained mechanically by tabanid and Stomoxys biting flies, whereas the closely related African trypanosomes *T. brucei brucei* and *T. b. rhodesiense* require cyclical development in tsetse flies (genus *Glossina*) for transmission. In this study, we investigated the evolutionary origins of *T. evansi*. We used 15 polymorphic microsatellites to quantify levels and patterns of genetic diversity among 41 *T. evansi* isolates and 66 isolates of *T. b. brucei* ($n = 51$) and *T. b. rhodesiense* ($n = 15$), including many from Kenya, a region where *T. evansi* may have evolved from *T. brucei*. We found that *T. evansi* strains belong to at least two distinct *T. brucei* genetic units and contain genetic diversity that is similar to that in *T. brucei* strains. Results indicated that the 41 *T. evansi* isolates originated from multiple *T. brucei* strains from different genetic backgrounds, implying independent origins of *T. evansi* from *T. brucei* strains. This surprising finding further suggested that the acquisition of the ability of *T. evansi* to be transmitted mechanically, and thus the ability to escape the obligate link with the African tsetse fly vector, has occurred repeatedly. These findings, if confirmed, have epidemiological implications, as *T. brucei* strains from different genetic backgrounds can become either causative agents of a dangerous, cosmopolitan livestock disease or of a lethal human disease, like for *T. b. rhodesiense*.

Author summary

Trypanosoma evansi is an important pathogen of the camel and other livestock where it is a causative agent of surra (an economically burdensome disease). The *T. evansi* is found in Kenya and the rest of the world. This study indicates that *T. evansi* originated recently

Appendix 4: Abstracts presented in meetings from the current work

1. 34th International Scientific Council for Trypanosomiasis Research Conference (ISCTRC) in Zambia.



Kenindia Business Park Building, Museum Hill, Westlands Road
P. O. Box 30786, 00100-Nairobi, Kenya, Telephone: 254-20-3674000, Fax: 254-20-3674341
Email: ibar.office@au-ibar.org, www.au-ibar.org

Ref: DIR/DIS/P7/E/0817

August 09, 2017

Ms. Christine Muhonja Kamidi
PhD Student
KALRO-BioRI
P.O. Box 362
Kikuyu
Kenya
Tel: +254 721 244 021
Email: tmuhonja@gmail.com

Dear Ms. Muhonja,

SUBJECT: ACCEPTANCE OF YOUR ABSTRACT AND INVITATION TO ATTEND THE 34TH INTERNATIONAL SCIENTIFIC COUNCIL FOR TRYPANOSOMIASIS RESEARCH AND CONTROL (ISCTRC) CONFERENCE IN LIVINGSTONE ZAMBIA 11TH – 15TH SEPTEMBER 2017

Following submission of the abstract entitled “Multiple evolutionary origins of *Trypanosoma evansi* in Kenya” we are pleased to inform you that after the review of the abstract, it has been accepted for oral presentation during the 34th ISCTRC Conference that will be held from 11th – 15th September, 2017 in Livingstone, Zambia.

Oral presentations will be made using Microsoft PowerPoint slides, with appropriate text spacing and font. The time allocated for oral presentation will be strictly 15 minutes. Presenters are requested to submit the Microsoft PowerPoint presentations, and the full manuscript if available, to the Secretariat in advance of the presentation to be uploaded in the computer.

We invite you to participate in the conference and request you to confirm your participation by August 18th, 2017, if we do not receive your confirmation by then your slot will be allocated to another available presenter.

Information note on the conference venue, accommodation and other logistical requirements is herewith attached. Meanwhile, please feel free to contact us should you require any more clarifications or information.

We are looking forward to seeing you at the conference.

Yours sincerely,

Prof. Ahmed Elsawalhy
Director/Head of Mission



2. The 3rd Africa International Biotechnology and Biomedical Conference
(AIBBC 2017) 12 – 16th September 2017, Nairobi Kenya.

Dear Participant

Thank you for submitting your abstract to the upcoming AIBBC 2017 (Sep. 12-16, Nairobi, Kenya).
<https://www.aibbc-society.org/>

This is to inform you that your abstract has been received and your talk or poster is being scheduled. Please wait for further communication regarding your presentation date and time. We will avail this information immediately we finalize the conference program.

A tentative outline of the program is as follows.

Keynote talk: 30 minutes (Q&A inclusive)

Session talk: 20 min (Q&A inclusive)

Poster presentations 1h 30 min (both on Day1 and Day 2)

Once again thank you for choosing to participate at the AIBBC 2017.

We look forward to a great meeting with over 130 people expected to attend.

Kind regards,
Kennedy

.....